Mechanistic Studies of the Photochemistry of 4-Nitrobiphenyls and 1-Acyl-7-Nitroindolines

By

James Patrick Morrison
B.Sc., University of Victoria, 1999

A Thesis Submitted in Partial Fulfillment of the
Requirements for the Degree of

Master of Science

In the Department of Chemistry

We accept this thesis as conforming
to the required standard

[redacted]

Dr. P. C. Wan, Supervisor (Department of Chemistry)

[redacted]

Dr. W. J. Balfour, Department Member (Department of Chemistry)

[redacted]

Dr. D. J. Berg, Department Member (Department of Chemistry)

[redacted]

Dr. R. W. Olafson, Outside Member (Department of Biochemistry and Microbiology)

[redacted]

Dr. E. Krogh, External Examiner (Malaspina University-College)

University of Victoria

Supervisor: Dr. P.C. Wan

Abstract

The photochemistry of three *p*-nitrobiphenyl derivatives has been investigated to explore the ability of photoexcited nitro groups to induce chemistry through the biphenyl ring system. Previous work has shown that the nitro group is highly electron withdrawing at both *meta* and *para* positions (on the benzene ring) in the excited triplet state, inducing decarboxylations and retro-Aldol type reactions, as well as a novel intramolecular redox-type reaction. The mechanisms of all of these reactions are believed to involve a crucial photogenerated nitrobenzyl carbanion intermediate. Analogous reactions with enhanced quantum efficiencies were observed in the nitrobiphenyls studied in this work. This is further evidence that twisted ground state biaryls (and possibly higher order oligophenylenes) may be thought as highly polarizable electronically conjugated π-systems in the excited state with the ability to induce efficient photochemistry. Moreover, a charge transfer triplet state is believed to be responsible for inducing highly efficient novel acid-catalyzed pathways observed for the photodecarboxylation of 4'-nitro-[1,1'-biphenyl]-4-acetic acid (**58**) and the photoredox reaction of 4'-nitro-[1,1'-biphenyl]-4-β-ethanol (**59**), neither of which have been observed in the corresponding nitrophenyl (parent) system.

1-Acyl-7-nitroindolines have recently been shown to be efficient photoactivated protecting groups in aqueous solution. Of particular interest is the change in mechanism of photochemical release that depends on the water content in solution. In wet (1% water) dioxane-CH_2Cl_2 mixture, photolysis yields the released carboxylic acid and the nitroindoline, via a formal hydrolysis of the amide. In wholly aqueous solution,

photolysis yields the released carboxylic acid and the nitrosoindole, via a formal intramolecular redox mechanism. Studied in this work are the mechanistic details of photorelease in solutions of varying H_2O-CH_3CN composition, using several model substrates, via product studies, deuterium isotope effects, kinetic studies (UV-Vis), and nanosecond laser flash photolysis. The data support two competing mechanisms operating via T_1. The two mechanisms differ in how the acyl group is "hydrolyzed" from the substrate. Both mechanisms have in common the photochemical transfer of the acyl group from the amide nitrogen to one of the oxygen atoms of the nitro group (in a fast step, within the 20 ns laser pulse), to give the critical nitro-linked ester intermediate. In solutions of higher water content, the predominant pathway for reaction of this ester is via a net S_N1 solvolysis reaction involving loss of the acyl group *with* one of the oxygens of the nitro group. This results in a formal intramolecular redox reaction of the aromatic ring system, to give the nitroso*iso*indole, which tautomerizes to give the final nitrosoindole product (tautomerization rates have been measured in this work). In solutions of lower water content, the major pathway is hydrolysis via the standard addition-elimination mechanism (via a tetrahedral intermediate) with water as the nucleophile. This releases the carboxylic acid and the nitroindoline product. The photochemistry in wholly aqueous medium is of more interest for potential applications of this system. Therefore, laser flash photolysis studies were carried out primarily in this medium. The first formed transient (within the 20 ns laser pulse) at λ_{max} = 450 nm is assignable to the critical intermediate in which the acyl group has migrated to the nitro oxygen (the nitro-linked ester intermediate above). The first order decay of this species in water has an observed rate constant of $\approx 5 \times 10^6$ s^{-1} and this is assigned to the release of

protected acetic acid (for the parent system) and formation of the nitroso*iso*indole. Therefore, these 1-acyl-7-nitroindolines photorelease their protected functionalities at very fast rates, in the submicrosecond time scale, significantly faster than the time scales for standard *o*-nitrobenzyl systems that have been measured, further demonstrating their potential utility.

Examiners:

[redacted]

Dr. P. C. Wan, Supervisor (Department of Chemistry)

[redacted]

Dr. W. J. Balfour, Department Member (Department of Chemistry)

[redacted]

Dr. D. J. Berg, Department Member (Department of Chemistry)

[redacted]

Dr. R. W. Olafson, Outside Member (Department of Biochemistry and Microbiology)

[redacted]

Dr. E. Krogh, External Examiner (Malaspina University-College)

Table of Contents

Abstract.....ii

Table of Contents.....v

List of Tables.....ix

List of Figures.....x

List of Important Abbreviations.....xiv

Acknowledgements.....xv

Chapter 1

Introduction

1.1 Overview of Nitroaromatic Photochemistry.....1

1.1.1 Electronic Nature of the Excited State.....3

1.1.2 Photoaddition.....3

1.1.3 Photoreduction.....4

1.1.4 Photosubstitution.....6

1.1.5 Intramolecular Photoredox Reactions.....8

1.1.5.1 Long Distance Intramolecular Photoredox Reactions.....8

1.1.5.2 *ortho*-Substituted Nitroaromatic Systems.....10

1.1.5.3 Water-Mediated Intramolecular Photoredox Chemistry of *para*- and *meta*-Substituted Nitroaromatic Systems.....13

1.1.5.3.1 Photoredox Chemistry of *para*-Nitrobenzyls.....13

1.1.5.3.2 Photoredox Chemistry of *meta*-Nitrobenzyls.....15

1.1.6 Water-Mediated Carbon-Carbon Bond Cleavage Generating *meta*- and *para*-Nitrobenzyl Anions.....18

1.1.6.1 Decarboxylation.....18

1.1.6.2 Photo-retro-Aldol Reaction.....22

1.1.7 Photochemistry of 1-Acyl-7-Nitroindolines.....25

1.1.7.1 Amide Bond Hydrolysis in an Organic Solvent.....25

1.1.7.2 Water-Mediated Photoredox Chemistry with Amide Bond Cleavage.....27

1.2 Biphenyl Chromophore.....29

1.3 Research Proposal.....32

Chapter 2

Photoredox, Photodecarboxylation, and Photo-retro-Aldol Chemistry of 4-Nitrobiphenyls

2.1 Introduction.....35

2.2 Synthesis.....38

2.3 UV-Vis Studies.....42

2.3.1 UV-Vis Studies in Neutral Aqueous Solution.....42

2.3.2 UV-Vis Studies in Basic Aqueous Solution.....43

2.3.3 UV-Vis Studies in Acidic Aqueous Solution.....45

2.4 Product Studies.....47

2.4.1 Photolysis of **57** in Neutral Aqueous Solution.....47

2.4.2 Photolysis of **57** in Acidic Aqueous Solution.....50

2.4.3 Photolysis of **58** in Neutral Aqueous Solution.....50

2.4.4 Photolysis of **58** in Acidic Aqueous Solution.....51

2.4.5 Photolysis of **59** in Basic Aqueous Solution.....51

2.4.6 Photolysis of **65** in Neutral Aqueous Solution.....52

2.4.7 Photolysis of Non-Nitro Analogs **76**, **77** and **78**.....53

2.4.8 Deuterium Isotope Studies.....54

2.4.9 Quantum Yields and pH Trends.....55

2.4.10 Triplet Sensitization and Quenching.....58

2.5 Laser Flash Photolysis and Mechanisms of Reaction.....60

2.6 Summary.....72

Chapter 3

Mechanisms of Photorelease of Carboxylic Acids from 1-Acyl-7-Nitroindolines in Aqueous Acetonitrile

3.1 Introduction.....73

3.2 Materials.....74

3.3 UV-Vis Studies.....75

3.4 Product Studies.....77

3.5 Triplet Sensitization.....81

3.6 Quantum Yields.....82

3.7 Laser Flash Photolysis (LFP).....83

3.8 Mechanisms of Reaction.....89

Chapter 4

Experimental

4.1 General Procedures and Instrumentation.....92

4.2 Materials.....92

4.2.1 Common Laboratory Reagents and Solvents.....92

4.2.2 Synthesis.....93

4.3 UV-Vis Studies....98

4.4 Product Studies....99

4.4.1 Preparative Photolysis....99

4.4.2 Analytical Photolysis in NMR tubes....104

4.4.3 Dark Reactions....106

4.4.4 Deuterium Isotope Effects by Preparative Photolysis....106

4.4.5 Quantum Yields and pH Effects....107

4.4.6 Triplet Sensitization....108

4.4.7 Triplet Quenching....109

4.5 Laser Flash Photolysis (LFP) Studies....110

4.6 X-Ray Crystallography....113

References....115

List of Tables

Table 2.1 Comparison of Quantum Efficiencies of Reaction of Nitrobiphenyl and Nitrophenyl Systems.....56

Table 2.2 Summary of Observed Triplet Transients for **57**, **58**, **64**, **67**, and **68** in 1:1 H_2O-CH_3CN.....62

Table 2.3 Summary of LFP Data for Compounds **57**, **58** and **68**.....69

Table 4.1 Crystal data for **59** (Figure 2.1).....114

List of Figures

Figure 2.1 X-ray crystal structure of the asymmetric unit of **59** (ORTEP). Torsional angles about the central biphenyl bond: C(3), C(4), C(7), C(8) = 3.2°; C(17), C(18),C(21), C(22) = 6°; C(33), C(32), C(35), C(40) = 25°.....41

Figure 2.2 UV-Vis traces observed on photolysis of **57** in 1:1 H_2O-CH_3CN (pH 7). Each trace represents about 1 min photolysis at 300 nm.....43

Figure 2.3 UV-Vis traces observed on photolysis of **58** in 1:1 H_2O-CH_3CN (pH 7). Each trace represents about 15 s photolysis at 300 nm.....43

Figure 2.4 UV-Vis traces observed on photolysis of **59** in 1:1 H_2O-CH_3CN (pH 13, solid lines). Each trace represents about 1 min photolysis at 300 nm. Dashed line represents spectrum upon acidification.....44

Figure 2.5 UV-Vis traces observed on photolysis of **57** in 1:1 H_2O-CH_3CN (pH 2). Each trace represents about 30 s photolysis at 300 nm.....46

Figure 2.6 UV-Vis traces observed on photolysis of **58** in 1:1 H_2O-CH_3CN (pH 2). Each trace represents about 30 s photolysis at 300 nm.....46

Figure 2.7 Plot of quantum yield for photoredox reaction of **57** vs pH (in 1:1 H_2O-CH_3CN, pH is of the aqueous portion). The filled circles show formation of **73**, filled squares formation of **64** and **71**.....57

Figure 2.8 Plot of quantum yield for photodecarboxylation reaction of **58** vs pH (in 1:1 H_2O-CH_3CN, pH is of the aqueous portion). The filled circles show formation of **75**, filled squares formation of **68** and **74**. Open square represents mixture of 60% **75** and 40% **68** (and trace **74**)...58

Figure 2.9 Stern-Volmer plot of the quenching of the photo-redox reaction

of **57** by sorbic acid at pH 2 in 1:1 CH_3CN-H_2O.....59

Figure 2.10 LFP traces for **67** in 1:1 CH_3CN-H_2O, pH 7, N_2 purged. Circles represent CT triplet state of **67** taken immediately after the laser pulse, diamonds and triangles represent spectra sampled during the decay to form substrate, squares represent decay back to baseline. Inset: Decay of CT triplet state of **67** ($k_{obs} \approx 5.9 \times 10^5\ s^{-1}$) at 620 nm.....61

Figure 2.11 LFP traces for **58** in 1:1 CH_3CN-H_2O, pH 7, N_2 purged. Circles represent spectrum taken immediately after the laser pulse, which includes carbanion **82** at 470 nm and the CT triplet state of **58** at 620 nm. Squares and triangles represent the decay of the CT triplet state to background, represented by diamonds.....63

Figure 2.12 Decay traces of **82**, generated from **58** neutral 1:1 $H_2O(D_2O)$-CH_3CN (N_2 purged). Bottom trace is the decay of **82** in H_2O, which follows first order kinetics ($k_{obs} \approx 6.2 \times 10^2\ s^{-1}$). Top trace is the decay of **82** in D_2O, which cannot be fit to a simple first order decay (but which decays to baseline).....65

Figure 2.13 LFP traces for **58** in 1:1 CH_3CN-H_2O, pH 2, N_2 purged. Squares represent the spectrum of the CT triplet state of **58** at 620 nm, taken immediately after the laser pulse. Diamonds and triangles represent the decay of the CT triplet state to form *aci*-nitro **84** at 440 nm, which is fully represented by the diamonds. Left inset: Decay trace represents disappearance of the CT triplet state of **58** at 620 nm, which coincides with the growth trace of *aci*-nitro

84 at 440 nm ($k_{obs} \approx 2.7 \times 10^6\ s^{-1}$). Right inset: Decay of *aci*-nitro **84** at 440 nm ($k_{obs} \approx 4.2 \times 10^3\ s^{-1}$).....70

Figure 3.1 UV-Vis traces for the conversion of **60** to **54** on photolysis at 350 nm in 100% H_2O (solid traces, estimated 100% conversion). Each trace represents 8 min irradiation time. Exhaustive photolysis in 99% CH_3CN-1% H_2O gave a product with λ_{max} = 434 nm (**86**, dashed trace)..76

Figure 3.2 Plot of relative yields of photoproducts **54** and **86** from photolysis of **60** and **62** as a function of water content (in CH_3CN). Squares and circles denote products formed from photolysis of **60** and **62** respectively. Solid markers represent **54** and open markers represent **86**.....78

Figure 3.3 UV-Vis traces of tautomerization of photogenerated **87** to **54** at pH 6. Dashed line is the spectrum observed about 5 s after photolysis of **60**. Solid line is the spectrum observed after 90 min. Note that conversion < 30% and therefore, the absorption spectrum is dominated by that of starting material **60**. Inset shows decay of **87** to form **54** ($k_{obs} \approx 7.8 \times 10^{-2}\ min^{-1}$) at 307 nm.....80

Figure 3.4 LFP traces for **60** in 99% CH_3CN-1% H_2O. Squares represent spectrum of **90** taken immediately after the laser pulse, diamonds and circles represent spectra sampled during the decay to form **92**, represented by the triangles. Inset: Decay of **90** to form **92** ($k_{obs} \approx 1.4 \times 10^5\ s^{-1}$) at 410 nm.....84

Figure 3.5 LFP traces for **60** in 100% water. Squares represent spectrum of **90** taken immediately after the laser pulse, circles and diamonds represent spectra sampled during the decay to form **87**, represented by the triangles. Inset: Decay trace of **90** to form **87** ($k_{obs} \approx 5 \times 10^6\ s^{-1}$) at 450 nm.....85

Figure 3.6 LFP traces for **62** in 100% water. Squares represent spectrum of **93** taken immediately after the laser pulse, which releases α-methoxyacetate to generate the observed **94,** represented by circles, which on deprotonation gives **87** (represented by diamonds). Left inset: initial decay of **93** to **94** ($k_{obs} \approx 2 \times 10^7\ s^{-1}$) at 450 nm. Right inset: slower decay of **94** to **87** ($k_{obs} \approx 1.5 \times 10^6\ s^{-1}$) at 420 nm.....87

List of Important Abbreviations

CT	Charge Transfer
HOMO	Highest Occupied Molecular Orbital
LFP	Laser Flash Photolysis
LUMO	Lowest Unoccupied Molecular Orbital
PMT	Photomultiplier Tube
S_1	Lowest Energy Singlet Excited State
T_1	Lowest Energy Triplet Excited State
TLC	Thin Layer Chromatography
Φ	Quantum Yield
YAG	Yttrium Aluminum Garnet

Acknowledgements

I would like to thank Dr. Peter Wan for taking the time to sort through the endless details that have been examined in this work, for listening to my account of events and taking the time to steer me in the right direction. Thanks also for the thought provoking conversations and novel points of view. Thank you Darryl Brousmiche, John Cole, Musheng Xu, Matt Lukeman, Sierra Rayne, Ryan Sasaki, Kaya Forest, Devin Mitchell, Charlotte Norris and Hans Osthoff for your friendship and support, both in and out of the lab. I would like to express my thanks to Dr. Cornelia Bohne and Luis Netter for their helpful discussions and technical support with the laser system. I am also grateful to Dr. John Corrie for providing the nitroindoline project and for his advice, and to George Papageorgiou for his synthetic contributions. Thanks is also extended to David McGillivray for his valiant efforts with the mass spectroscopy. Thanks also to everyone in the Chemistry Department and at UVic who has aided me in this undertaking.

Dedication

To my Family

Chapter 1

Introduction

1.1 Overview of Nitroaromatic Photochemistry

The study of nitroaromatic photochemistry dates back a century. In fact, the photoreactivity of *o*-nitrobenzaldehyde (**1**) by Ciamician and Silber in 1901 (Equation 1), was one of the first photochemical reactions reported.[1] In the original publication **1** was found to generate *o*-nitrosobenzoic acid (**2**) upon photolysis, the first reported nitroaromatic photochemical reaction, which was to be followed by many more. While a multitude of different structures have been explored in this field, there remains a fascination with such seemingly simple molecules as *o*-substituted nitrobenzenes, which continue to be a topic of current photochemical study one hundred years later.[2] The longevity in research in *o*-nitrobenzene photochemistry is testimonial of the interesting chemistries that nitroaromatics can undergo.

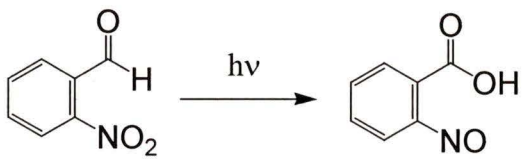

1 **2** (1)

While the study of nitroaromatic photochemistry has spanned a long period of time much still remains to be discovered. This field is often compared with carbonyl photochemistry, partly because the two functional groups are structurally similar, but also because of the contrast in relative understanding in the two fields. Nitroaromatic photochemistry has not been as easy to classify as carbonyl photochemistry, due to the

greater variety of photoreactions that nitroaromatics exhibit. There are also some impracticalities with nitroaromatic photochemistry which give rise to difficulties in mechanistic studies. A valuable tool in mechanistic organic photochemistry is measurement of luminescence, which yields insight into the disposition of the excited state. Unfortunately the fluorescent and phosphorescent efficiencies of nitroaromatics are generally quite low, such that luminescent studies are often unachievable, impeding chemists from studying the excited state in the most direct manner possible.[3] Also, the nitro group has a variety of possible functional groups to which it can be transformed, each functional group displaying its own distinct thermal and excited state chemistry, rendering some photoreactions intractable.[1] Carbonyls, comparatively, generally fluoresce and phosphoresce more strongly and have relatively fewer functional groups that can be generated, and those products generated usually have more predictable behaviour.[1] Despite these complications nitroaromatic photochemistry has received increased attention, because, as this work hopefully demonstrates, there is a wide range of interesting chemistry possible.

As there are several more thorough reviews available,[1,3,4] the intention of this introduction is to briefly outline the breadth of nitroaromatic photochemistry, with emphasis on specific topics relevant to the body of work presented in the following chapters. A short section covering biphenyls is also included, as demanded by the nature of the material to be presented in Chapter 2.

1.1.1 Electronic Nature of the Excited State

Nitroaromatics generally have low lying triplet states in comparison to the singlet state energy.[1,3,4] As such, intersystem crossing from the singlet state to the triplet state is highly efficient in most cases. However, although many reactions do occur via the triplet state,[1,3] some reactions occur via the singlet state.[1,2] Attempts have been made to categorize the triplet excited states of nitroaromatics into three general categories: n,π*, π, π* and charge transfer (CT). The n,π* state is characterized by its facility to be reduced by a hydrogen atom or an electron, the π,π* state is more susceptible to substitution, but will reluctantly be reduced, and the CT state has been described as being relatively less reactive.[1] Nevertheless, it is often difficult to categorize the lowest energy excited state (from which chemistry, if possible, generally occurs) as the nature of the reactive excited state can change dramatically by varying substituents or solvent systems. For these reasons the field is more anecdotal, and it is important to be wary of categorizations of nitroaromatic compounds.

1.1.2 Photoaddition

There have been several reported examples of the nitro group in nitrobenzene photochemically adding across a double bond.[1,3,4] The first reported isolation of a cyclo adduct was by de Mayo and coworkers, who discovered that at -70 °C nitrobenzene adds across the double bond of cyclohexene to give cycloadduct **3** upon photolysis (Equation 2).[5] Although **3** was found to be stable at –20 °C, it decomposed over the course of a few minutes at room temperature. This reaction has been shown to proceed via the n,π* triplet state of nitrobenzene.

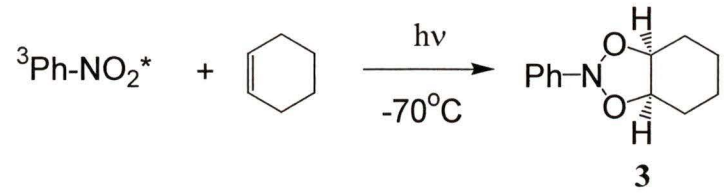

3 (2)

A more stable cyclo adduct was prepared by photolysis of 1,3-dinitrobenzene, **4a**, in dichloromethane in the presence of adamantylideneadamantane, **5**, to give dioxazolidine, **6a** (Equation 3).[6] Nitrobenzenes **4b** and **4c** also added to **5** upon photolysis to give **6b** and **6c**, respectively. In contrast to **3**, compounds **6a-c** were stable at room temperature. In fact **6c** was found to be stable in refluxing benzene (but was found to decompose in refluxing toluene).

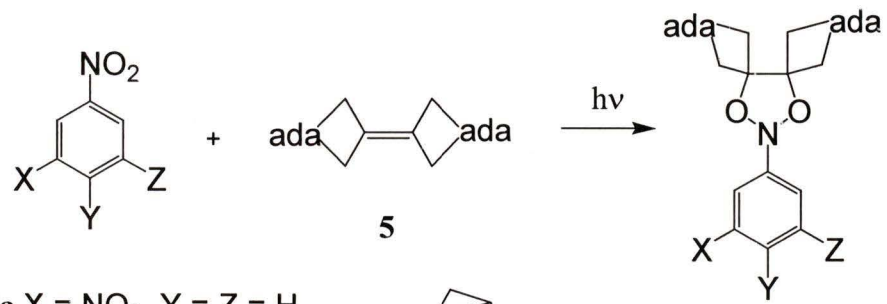

5 (3)

4a X = NO$_2$, Y = Z = H
4b X = H, Y = NO$_2$, Z = H
4c X = Y = Z = NO$_2$

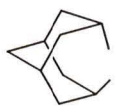

= ada

6a-c

1.1.3 Photoreduction

Photoreduction of nitroaromatics in neutral solution is generally agreed to occur via initial H-abstraction involving the triplet state.[1] The simplest example of nitroaromatic photoreduction is the photolysis of nitrobenzene in degassed 2-propanol, which results in the production of phenylhydroxylamine and acetone.[7] H-abstraction occurs from the n,π* triplet state to form the radical pair shown below (Equation 4).

$$^3(ArNO_2)^* + (CH_3)_2CHOH \longrightarrow Ar\dot{N}O_2H + (CH_3)_2\dot{C}OH \qquad (4)$$

$$Ar\dot{N}O_2H + (CH_3)_2\dot{C}OH \longrightarrow ArN(OH)_2 + (CH_3)_2CO \qquad (5)$$

The mechanism of subsequent steps to form product remain open to speculation. A second H-abstraction by the initially formed radical is an attractive partial explanation (Equation 5), however the actual second steps must be more complex than this, as significant amounts of secondary reduction products of nitrobenzene, namely nitrosobenzene and aniline, are formed upon photolysis.[8] Although there have been several attempts to explain the observed photochemistry, a fully satisfactory explanation has not been reported.[1] Overall, the quantum yield of the reduction of nitrobenzene (measured by the disappearance of starting material) is $\Phi_d \approx 0.011$.[7]

The efficiency of the reduction of nitrobenzene in 2-propanol is enhanced by the presence of HCl.[9] The reduction products in this case are chlorinated anilines,[9] which are also the observed reduction products in 12 **M** HCl.[10] The quantum yield for disappearance of nitrobenzene is 0.11 in 12 **M** HCl.[10] HCl is believed to enhance the reduction efficiency of nitrobenzene by acting as a source of electrons, rather than as an acid. Transfer of an electron from the chloride ion to the n,π* triplet state of nitrobenzene is proposed as the initial step, which is supported by the observation that electron donating substituents on nitrobenzene decrease the efficiency of the reduction.

Electron transfer is also proposed to explain enhanced photoreduction of nitrobenzenes in basic alcoholic solution versus neutral alcoholic solution.[1] In this case, the electron donor is proposed to be alkoxide ion. The reduction products of nitrobenzene are anilines, azo and azoxy compounds.

1.1.4 Photosubstitution

In nitroaromatic photosubstitutions the effect of the nitro group is dominated by its ability as an electron withdrawing group. In contrast to the ground state, where the activated site is *ortho* or *para* to the nitro group, in the excited state the activated site is often *meta* to the nitro group.[1,3,4] This is known as the *meta* effect, exemplified by the photosubstitution of 3,4-dimethoxy-1-nitrobenzene with methyl amine to give **7**, where methyl amine preferentially substitutes the methoxy at the *meta* position over the *para* position (Equation 6).

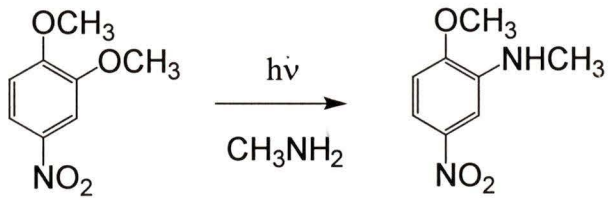

(6)

7

Further evidence of the *meta* effect is the photosubstitution (and overall oxidation) of 4-methoxy-1-nitrobenzene with cyanide to form **8** (Equation 7).[12]

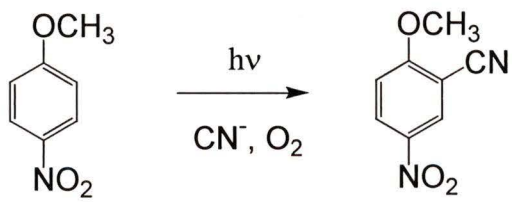

(7)

8

Exceptions to *meta* activation in nucleophilic photosubstitution of nitroaromatics have been reported, some of which are rationalized using Frontier Molecular Orbital (FMO) arguments.[13] Using FMO arguments two rules have been proposed:

1. Nucleophilic photosubstitutions that involve a one-step formation of a σ-complex via direct interaction between an excited aromatic substrate and a nucleophile are (substrate) HOMO controlled:

$$ArH^* + Nu: \rightarrow \sigma\text{-complex} \quad (S_N2Ar^* \text{ mechanism})$$

2. Nucleophilic photosubstitutions that involve electron transfer from a nucleophile to a nitroaromatic substrate and subsequent recombination of the resultant radical ions are (substrate) LUMO controlled:

$$ArH^* + Nu: \rightarrow ArH^{-\bullet} + Nu^{\bullet} \rightarrow \sigma\text{-complex}$$

While equations 6 and 7 describe substitution reactions following the S_N2Ar^* mechanism, the following intramolecular rearrangement of **9** proceeds via LUMO control. Nitro-substituted aromatic rings are known to have high electron affinity, thus the determining factor which allows electron transfer to occur as the preliminary step is the electron donating ability of the phenyl substituted amine (Equation 8).[14] Note that LUMO control leads to *para* substitution.

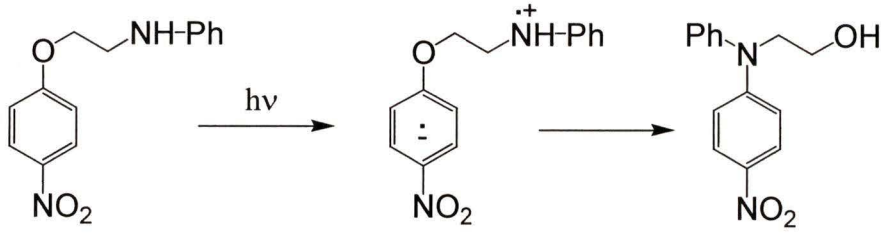

9 (8)

The reaction described in Equation 8 is also an example of a photo-Smiles rearrangement. It should be clarified that the LUMO controlled mechanism is not the exclusive mechanism of photo-Smiles rearrangements, other nitro-substituted photo-Smiles rearrangements have been reported which proceed via the S_N2Ar^* mechanism.[15] The (S_N2Ar^*) *meta*-directed photo-Smiles rearrangements involve amines with weaker electron donating ability.

1.1.5 Intramolecular Photoredox Reactions

1.1.5.1 Long Distance Intramolecular Photoredox Reactions

In intramolecular nitroaromatic photoredox reactions the nitro group is specifically involved in the reaction. In the numerous examples of this type of reaction the oxidant is consistently the nitro group, whereas the reducing group varies. The interaction of the nitro group with the reducing group can occur via a variety of mechanisms. In the most obvious mechanism, the nitro group interacts directly through space with the reducing group. In cases where this is spatially impossible, interaction through conjugation or via solvent necessarily occurs. Of course, the route actually used may also be a combination of the above, but in some cases certain interactions can be ruled out.

In a clear example where conjugation of nitro with the reducing group is impossible, photolysis of **10** was found to generate **13** in an intramolecular photoredox reaction which includes photorelease of phenylamine (Equation 9).[16] The mechanism of redox reaction of **10** was proposed to involve the triplet biradical **11** which forms the

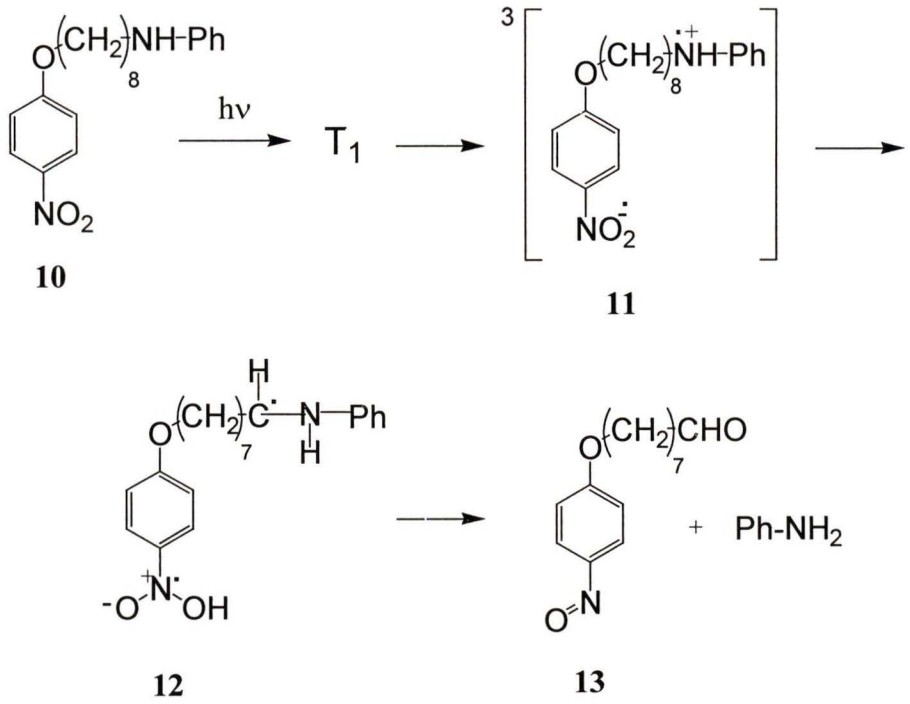

(9)

singlet biradical intermediate **12**. Formation of redox product **13** from **12** requires a second electron transfer to occur intramolecularly, followed by conventional ground state chemistry. This mechanism is supported by the observed strong influence of magnetic fields.[16c] In the presence of a magnetic field (< 1 T) the triplet state intermediate **11** is stabilized such that the yield for intersystem crossing from **11** to **12** decreases. This lengthens the lifetime of **11**, allowing an otherwise minor side reaction (no added magnetic field) to become competitive, resulting in the observation of another product (comprising up to 50 % of product yield at 1 T). It is interesting to note the structural similarities of **10** with **9**, which undergoes photo-Smiles rearrangement upon irradiation (*vide supra*). The obvious difference is the length of the methylene chain. Analogous compounds of **9** and **10**, which differ in chain length, have been systematically studied. Results of photolysis in benzene indicate that where methylene chains are < 7 carbons

long the photo-Smiles rearrangement occurs, and where chains are ≥ 8 methylene units redox reaction dominates.[16]

1.1.5.2 *ortho*-Substituted Nitroaromatic Systems

Intramolecular photoredox reactions have been more extensively documented when the nitro group is in close proximity to the reducing group, as in *o*-nitrobenzyl systems. Due to the close proximity of nitro to the reducing group, direct (through space) interaction is spatially allowed. Generally the nitro group in *o*-nitrobenzyls abstracts a hydrogen atom from the adjacent (*ortho*) benzylic position as the first step in these redox reactions.[1,3,4] Thus there is a general rule, known as Sach's rule, which states that compounds with benzylic hydrogen atoms *ortho* to a nitro group are photochemically reactive. This is true even in the solid state, as the close proximity of the nitro group to the benzylic hydrogens allows for solvent independent abstraction. Once hydrogen abstraction has occurred, the resultant *aci*-nitro species can either transfer the hydrogen back to the benzylic position, regenerating substrate, or subsequent irreversible steps can occur, which will lead to a redox reaction.

The classic example of this type of photoreaction is the formation of *o*-nitrosobenzoic acid (**2**) from *o*-nitrobenzaldehyde (**1**), which (see Introduction to Section 1.1) is the first reported example a nitroaromatic photoreaction.[1] Since the initial report by Ciamician and Silber, subsequent publications have revealed additional mechanistic details of this reaction. Pertinent details and their mechanistic interpretation are reported here and in Equation 10.[17] Within picoseconds of excitation of **1** a transient is formed with λ_{max} = 440 nm. This transient, which is assigned to *aci*-nitro **14** (also a ketene), is

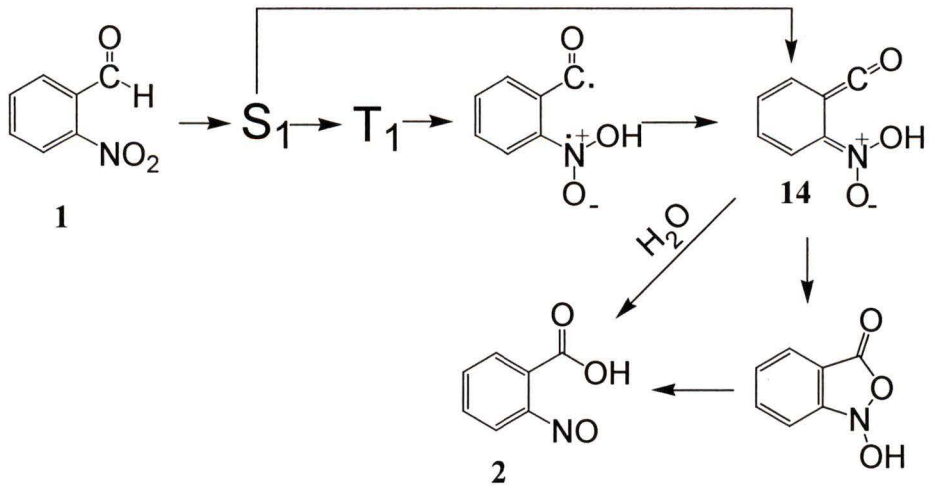

(10)

observed to decay over the course of nanoseconds. Evidence supports formation of **14** from both the singlet and triplet states.[17] Transient **14** has been observed to decay faster in aqueous or alcoholic acetonitrile than in dry acetonitrile, which reveals its sensitivity towards hydroxylic molecules, consistent with the enol character of **14**. The transient was also observed in benzene and THF, which is consistent with the known reactivity of **1** in these solvents. Formation of **2** from **14** in the absence of water is believed to occur via transfer of an oxygen atom from the nitrogen to the benzylic position (as shown), whereas in the presence of water the process can occur via attack at the ketene carbon by water to form a hydrated nitroso, followed by dehydration to give **2**.[17a] The quantum yield for formation of **2** is ≈ 0.5 in a variety of solvents.[17]

Analogous redox chemistry (to the above) occurs for all *o*-nitrobenzyls containing benzylic hydrogen atoms. This general reactivity of *o*-nitrobenzyls has been applied extensively for use as photo-removable protecting groups. This is achieved by bonding the desired removable group to the benzylic position of the *o*-nitrobenzyl via an N or O linkage (in the manner that **X** is bonded in Equation 11).[18] Prior to photolysis these

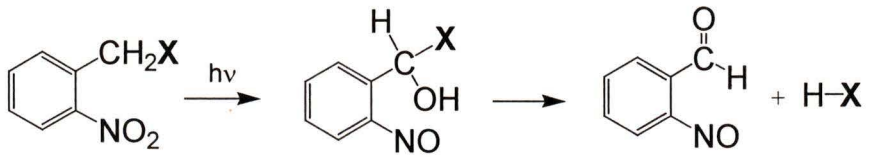

(11)

X = -OOCNHR, -OR, -NHCOR, -$OOCHNH_2R$, sugars, phosphates

compounds are stable in a variety of conditions, including acid catalyzed hydrolysis. Upon photolysis however, intramolecular photoredox reaction gives an *o*-nitrosobenzaldehyde derivative, which itself is easily hydrolyzable. It is the hydrolysis of this compound which releases a variety of functional groups such as amines, amides, alcohols, carboxyls, aldehydes and ketones among others.

Applications of *o*-nitrobenzyl photoremovable protecting groups include protecting functional groups in synthesis, binding substrate to polystyrene resin in solid phase synthesis, photoresists, and liberation of fluorophores and phosphates, among other applications.[1,18] For certain purposes it is important that the release time be as fast as possible. One such application is the use of photorelease groups in biological settings, because photolysis of a "caged" molecule allows one to induce a concentration jump of the uncaged molecule. For example, free ATP has many interesting biological effects. Affecting a concentration jump of ATP in a biological setting makes it possible to study the effect of ATP in a controlled manner. Of course, the ability to kinetically resolve the effects of a molecule are limited by the rate of release of the molecule. While the formation of the *o*-nitrosobenzaldehyde derivative is quite fast, the rate of release is equal to the rate of hydrolysis of that *o*-nitrosobenzaldehyde derivative.[19] For ATP releasing *o*-nitrosobenzaldehyde derivatives, this rate constant is 86 s^{-1} at pH 7, which limits time resolved examination of the effects of ATP release to processes slower than this.

1.1.5.3 Water-Mediated Intramolecular Photoredox Chemistry of *para*- and *meta*-Substituted Nitroaromatic Systems

When the nitro group is *meta*- or *para*-substituted, direct (through space) intramolecular interaction with the benzylic position is spatially impossible. However, interaction through conjugation and solvent can occur, and intramolecular photoredox chemistry is possible. In contrast to the *o*-nitrobenzyl system, photoredox reactions of *m*- and *p*-nitrobenzyl systems are solvent dependent, occurring only in aqueous solution. [1,3,4] In absence of water these molecules are relatively photoinert, or exhibit other photochemistry.

1.1.5.3.1 Photoredox Chemistry of *para*-Nitrobenzyls

The first reported example of a *p*-nitrobenzyl intramolecular photoredox reaction was the conversion of *p*-nitrobenzaldehyde (**15**) to *p*-nitrosobenzoic acid (**16**, Equation 12), which has been extensively studied by Wubbels and coworkers.[20] In deducing the mechanism for this reaction it was observed that the quantum yield for product formation is directly proportional to water content, and in 99:1 H_2O-CH_3CN, it was nearly optimized at 0.034. Quantum efficiency for product formation exhibited no dependence on pH between pH 0 and 10, nor was it affected by radical trapping reagents such as dioxane, methanol or oxygen. Photolysis of **15** in aqueous ammonia gave vital mechanistic information, as it resulted in the formation of *p*-nitrosobenzamide, which suggested the ketene intermediate **17**. Formation of **17** was also consistent with the observed independence of pH and lack of an observable radical. Further investigation using Laser Flash Photolysis (LFP) revealed a transient absorption spectrum with λ_{max} =

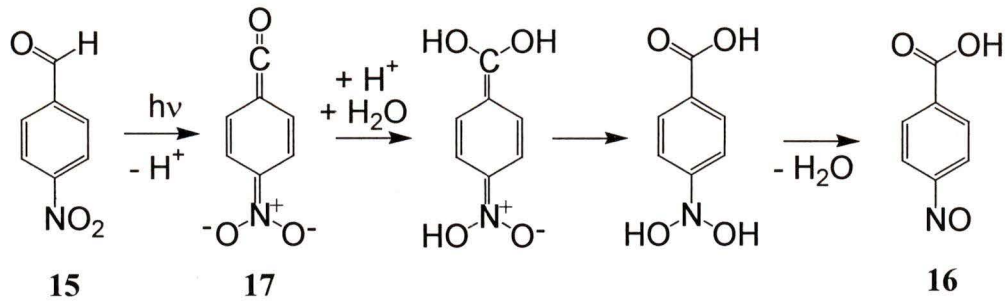

15 **17** **16** (12)

350 nm and its lifetime (τ) was in the order of 1.3 to 1.6 μs between pH 5 and 12 (100% H_2O).[21] This was assigned to transient **17**. LFP experiments were consistent with formation of **17** from the triplet state of **15**, presumably by deprotonation at the formyl carbon. Subsequent reaction of **17** to form product is believed to occur by conventional ground state steps as shown. This includes net addition of water to **17**, protonation, and subsequent dehydration to yield **16**.

p-Nitrobenzyl alcohol (**18**) also undergoes intramolecular photoredox reaction, forming *p*-nitrosobenzaldehyde (**19**) as was shown by Wan and Yates (Equation 13).[23] This requires a basic aqueous medium (pH > 11), otherwise **18** is photoinert. It is reasoned that hydroxide ion is required to assist formation of the reactive intermediate, suggesting that specific base catalyzed deprotonation at the benzylic position of **18** occurs in the excited state. This is believed to occur concertedly with protonation of the nitro group by water, allowing formation of the crucial *aci*-nitro intermediate **20**. Evidence supporting benzylic deprotonation also comes from deuterium isotope studies, which involved replacement of protons at the benzylic position with deuterons in the substrate (e.g. **21**). This markedly inhibited product formation. For example, α-deuterated **21** was observed to react 6 times less efficiently than **18** at pH 14 ($\Phi_H/\Phi_D = 6.1 \pm 0.6$). This

primary kinetic isotope effect is strong evidence of deprotonation occurring at the benzylic site in the product determining step. This implies that **20** does not return to substrate, rather it tautomerizes to yield the hydrated form of **19**, which upon dehydration gives **19**.

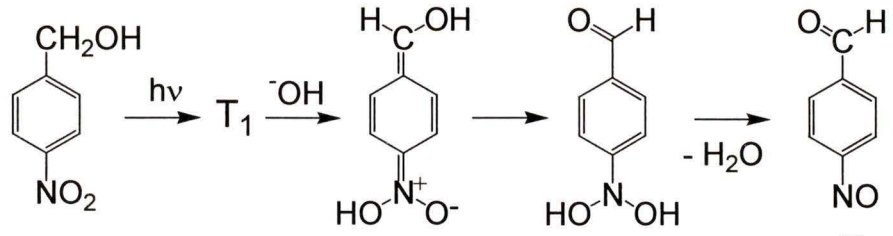

(13)

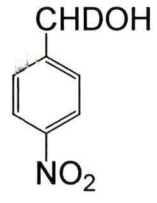

21

1.1.5.3.2 Photoredox Chemistry of *meta*-Nitrobenzyls

Photoredox activity of the *meta* isomer is more complicated. While *m*-nitrobenzaldehyde is photoinert at any pH (in contrast to *p*-nitrobenzaldehyde (**15**)),[20a] *m*-nitrobenzyl alcohol (**22**) shows enhanced reactivity in comparison to its *para* analog **18** (consistent with a normal *meta* effect).[23b] As shown by Wan and Yates, **22** is photoreactive across the entire pH scale to form **23** and **24** (Equation 14), in contrast to **18** which reacts only at pH > 11.[23] The quantum efficiency of product formation for **22** is 0.055 at pH 7, more than five times that of **18** at pH 14. While **22** exhibits enhanced reactivity, the redox reaction is complicated. In contrast to the simple 2 electron reduction

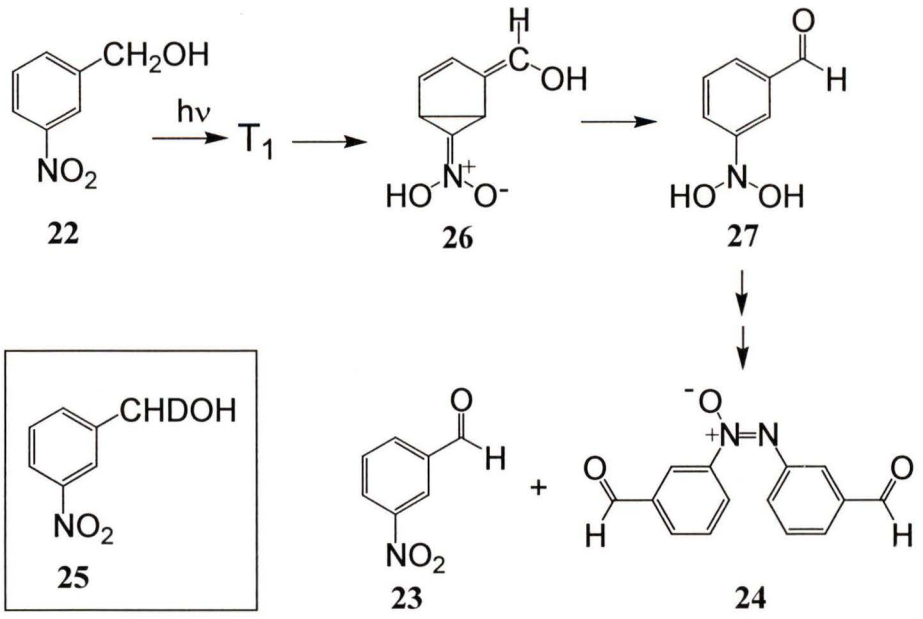

(14)

(of the nitro group) / 2 electron oxidation (of the alcohol) observed for **18**, photolysis of **22** gives an apparently unbalanced redox product mixture. This includes *m*-nitrobenzaldehyde (**23**) as the major product (≈ 75 %) and azoxy compound **24** as the minor product (≈ 25 %). Nonetheless, evidence suggests that the initial photochemical steps for **22** appear to be analogous to those of **18**. In particular, deuterium isotope studies of α-monodeuterated analog **25** suggest that benzylic deprotonation of the triplet state of **22** occurs at the product determining step. The quantum efficiency of product formation for **25** was observed to be more than two times less than **22**, such that Φ_H/Φ_D = 2.4 ± 0.2, at pH 7. While this deprotonation has been shown to be specific base catalyzed, observed reactivity of **22** at pH 7 implies that water is sufficiently basic enough to allow deprotonation. Thus there is reason to believe that **26** is formed along the reaction pathway, but the subsequent steps to generate *m*-nitrobenzaldehyde (**23**) and

azoxy product **24** are not as clearly understood. Note that **26** represents a non-Kekulé formula showing interaction of the *meta* position in the excited state.

A common direct pathway to form an azoxy group is to condense hydroxyl amine (H(HO)N-R) with a nitroso group. Azoxy **24** could be formed from such a pathway, which would imply that hydrated nitroso **27** and hydroxylamine **28** are formed upon photolysis (Equations 15 and 16). The mechanism proposed by Wan and Yates involves formation of **27** as the primary product, followed by disproportionation of **27** to give **25** and hydroxylamine **28** (Equation 15).[23] Condensation of **27** and **28** would form azoxy **24** (Equations 16). However, this mechanism predicts a 1 to 1 ratio of **23** and **24**, in discord of the observed 3 to 1 ratio (of **23** to **24**, respectively). Thus there appears to be some reduction product missing from the product mixture. As these reactions were run under argon purged conditions, reaction with oxygen cannot explain such a large discrepancy. Secondary photochemistry of **24**, resulting in its decomposition, was reported to account for its low yield.

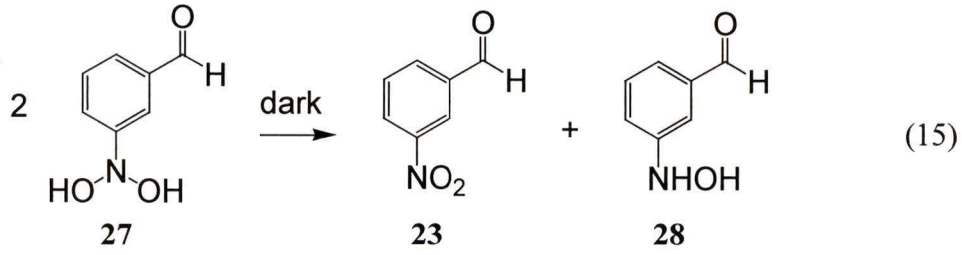

(15)

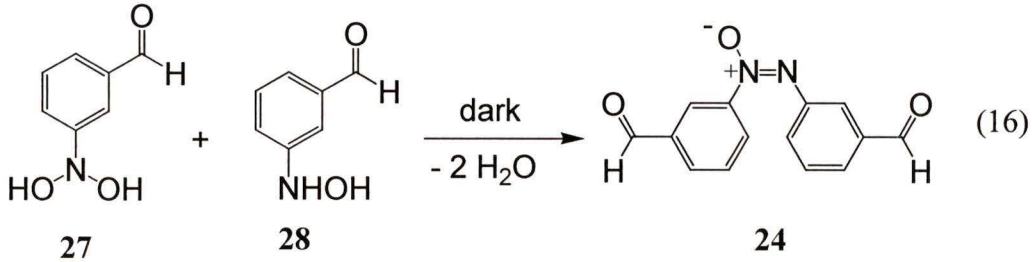

(16)

1.1.6 Water-Mediated Carbon-Carbon Bond Cleavage Generating *meta* and *para*–Nitrobenzyl Anions

1.1.6.1 Decarboxylation

Heterolytic carbon-carbon bond cleavage has been found to occur at the benzylic positions of several nitrobenzyls upon photolysis in aqueous media.[1,3,4] The first such reaction reported was the decarboxylation of *m*- and *p*-nitrophenyl acetate (**29** and **30**, respectively) by Margerum and Petrusis (Equations 17 and 18).[24] The *ortho* analog was also reported to decarboxylate, however with far lower efficiency than **29** and **30** ($\Phi_m = \Phi_p = 0.6$, $\Phi_o = 0.04$). A competing reversible intramolecular hydrogen transfer explains the reduced decarboxylation efficiency of the *ortho* compound.

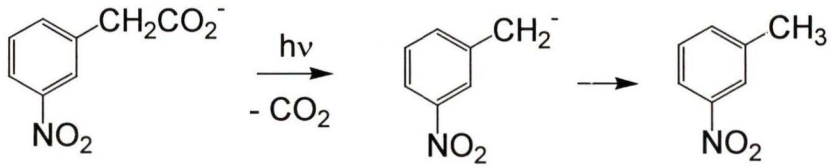

29 **32** **33** (17)

These reactions were observed to be water mediated, as photolysis of **29** and **30** in other common solvents did not result in decarboxylation.[24] Decarboxylation from protonated **29** and **30** (at pH < 2, *m*- and *p*-nitrophenyl acetic acids) also does not occur, thus the quantum yields of formation of products **32** and **33** across the pH scale reflect the concentration of the acetate present. In neutral and basic media the quantum yields are 0.6, but below pH 6 the quantum yields gradually decrease such that they approach zero by pH 2.

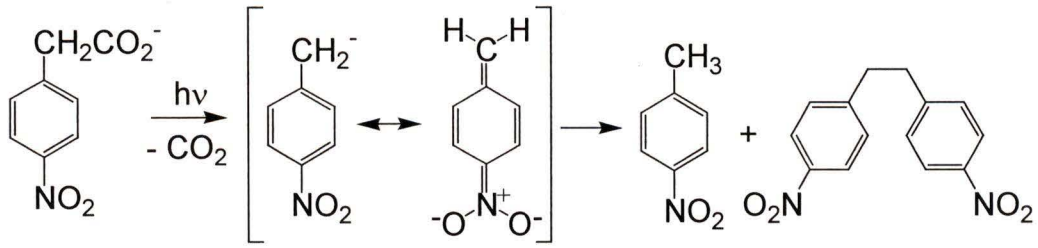

(18)

30 **31** **35** **34**

(Ratio of **35** to **34** dependent on pH, substrate concentration and photolysis rate)

Upon photolysis of *para* isomer **30** a long lived intermediate (λ_{max} = 356 nm, decaying over the course of tens of seconds at pH 13) was observed using standard UV-Vis spectrophotometry and microsecond flash photolysis. At lower pH (< 7) this transient was shorter lived, suitable behavior for a transient assigned to carbanion **31**. The long lifetime of this carbanion is explained by an important resonance contributor, the *aci*-nitro anion form, where the negative charge is on the nitro group (Equation 18). Final products for photolysis of **30** were found to be 4,4'-dinitrobibenzyl **34** and *p*-nitrotoluene **35** (ratio dependent on pH, concentration and photolysis rate). The mechanism for formation of **34** remained unclear at the time of publication.

Photolysis of *meta* isomer **29** generates carbanion **32**, however the lack of its observation by microsecond flash photolysis indicates a short lifetime, stemming from the inability of **32** to be resonance stabilized as the *para* isomer is (Equation 17). The primary product of photolysis of **29** is *m*-nitrotoluene, **33**. As this product comprises > 98% of the product mixture between pH 2 and 14, protonation of **32** by water must occur.

A more in depth analysis of transient **31**, and an investigation of possible mechanisms to form **34**, were undertaken using nano and picosecond laser flash

photolysis by Craig and coworkers.[25] Therein it was reported that **31** is formed from a precursor transient which absorbs with λ_{max} = 290 nm, assigned as **36**, the triplet state of carbanion **31** (Scheme 1.1).[24a] The triplet state carbanion **36** itself is formed on the picosecond time scale by adiabatic decarboxylation of the triplet state of substrate **30**, which itself is formed within 5 picoseconds of excitation of **30**. At pH > 3 decay of **36** occurs simultaneously with growth of **31** (at 356 nm) on the nanosecond time scale. At pH < 3 decay of **36** gives **37**, the *aci*-nitro species (the protonated form of **31**). *aci*-Nitro **37** has a distinct absorption band with λ_{max} = 330 nm, approximately 30 nm blue shifter with respect to *aci*-nitro anion (or carbanion) **31**.

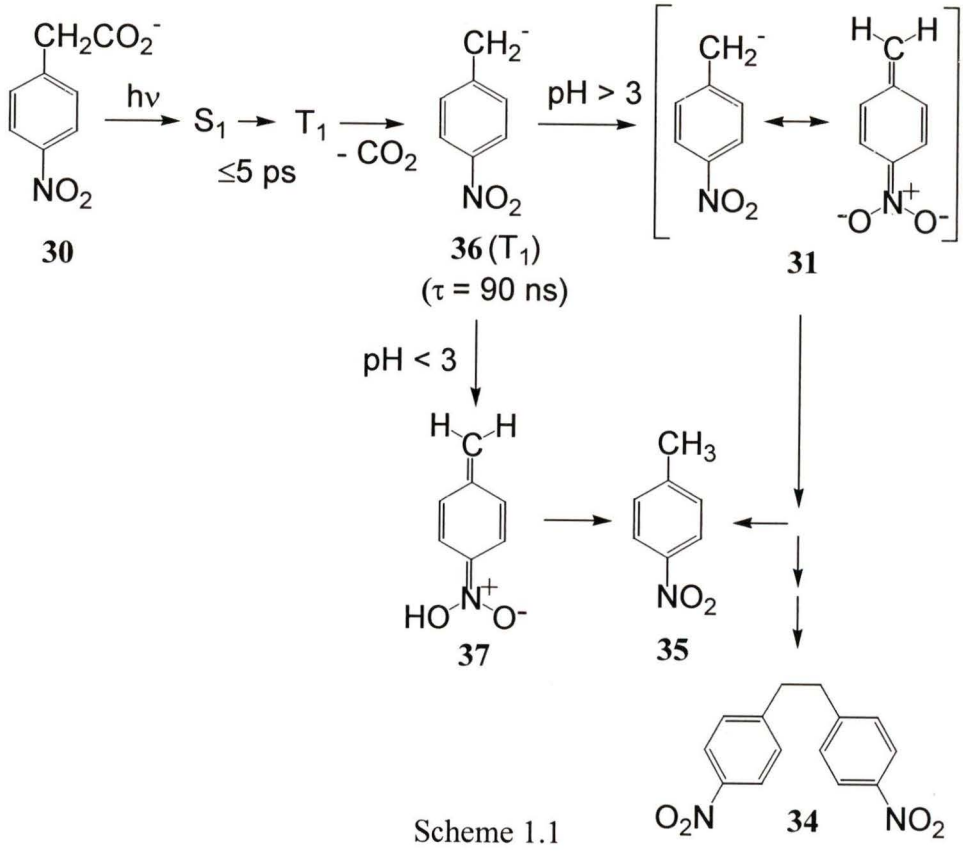

Scheme 1.1

Disappearance of **31** was found to occur with mixed first and second order characteristics.[24b] This complex decay behavior was explained as two competing decay pathways available for **31**, one pseudo first order and the other second order. The first order pathway is solvent protonation of **31** at the benzylic carbon to form *p*-nitrotoluene (**35**, Equation 19). The second order pathway is coupling of two *aci*-nitro anions **31**, to form 4,4'-dinitrobibenzyl dianion **38** (Equation 20). Considerable charge transfer of the negative charge to the nitro group is believed to have occurred to allow coupling of these two negatively charged species. Dianion **38** is short lived; it quickly transfers two electrons to the most abundant electron acceptor in the system, substrate **30**, forming

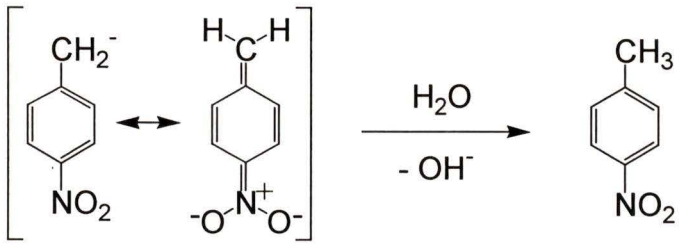

31 **35** (19)

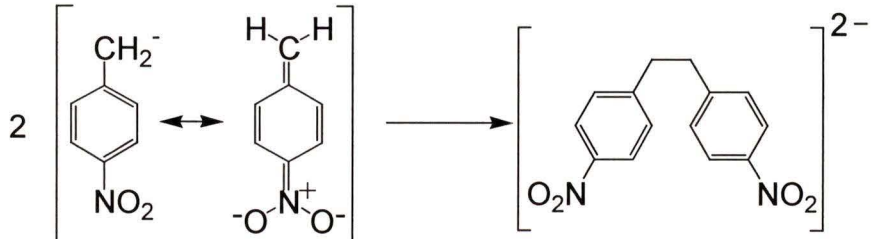

31 **38** (20)

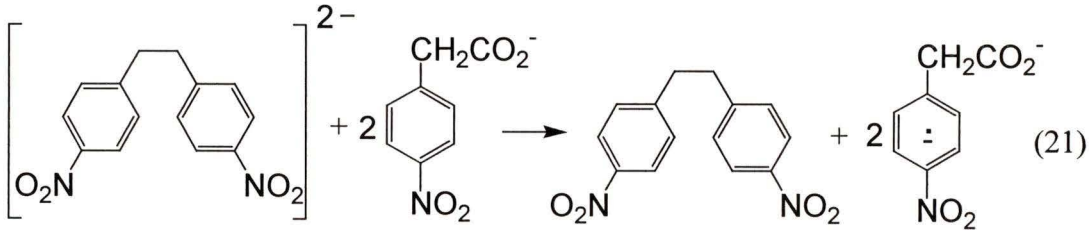

38 **30** **34** **39** (21)

radical anion **39** which is claimed to have been detected by ESR (Equation 21).[24b] Electron transfer from **39** to oxygen ultimately occurs in the work up of the reaction.

1.1.6.2 Photo-retro-Aldol Reaction

A second photochemical method to invoke heterolytic carbon-carbon bond cleavage producing nitrobenzyl anions was developed by Wan and Muralidharan.[26] Photolysis of appropriate β(3- or 4-nitrobiphenyl)ethanol derivatives in alkaline aqueous solution was found to result in a photo-retro-Aldol reaction from the triplet state, giving the appropriate aldehyde and carbanion. For example, photolysis of **40** at pH > 11 results in the formation of **34**, **35** and formaldehyde (Equation 22). Observation of the characteristic absorption band of **31**, its characteristic behaviour, and formation of products **34** and **35** implied formation of transient **31**. The observed hydroxide ion catalysis of these reactions was explained to be due to the role of hydroxide ion in assisting deprotonation of the alcohol of triplet excited **40**. The quantum yield of product formation for **40** was found to be 0.021 at pH 13.

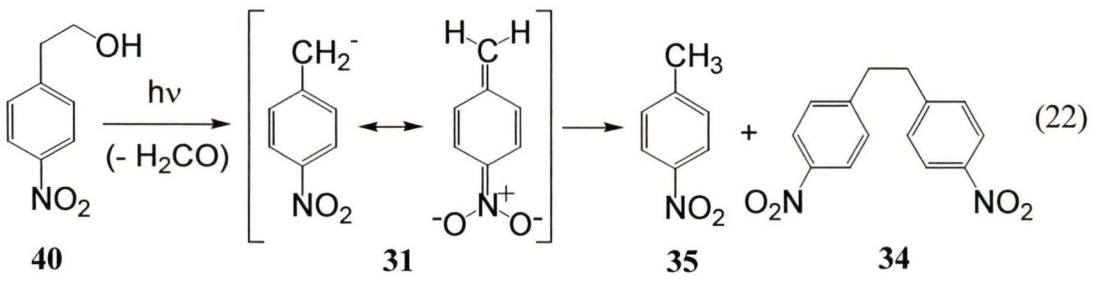

40 **31** **35** **34** (22)

Meta isomer **41** reacts in a manner similar to **40** to generate mostly **33** and trace **42**, with a quantum yield of 0.039 (Equation 23).[26] This enhanced reactivity in comparison to the *para* isomer demonstrates a normal *meta* effect, and is thus consistent

with the same mechanism being operative. The relative yield of **33** and **42** was 95% and 5% respectively, consistent with carbanion **32** being the reactive intermediate in this reaction.

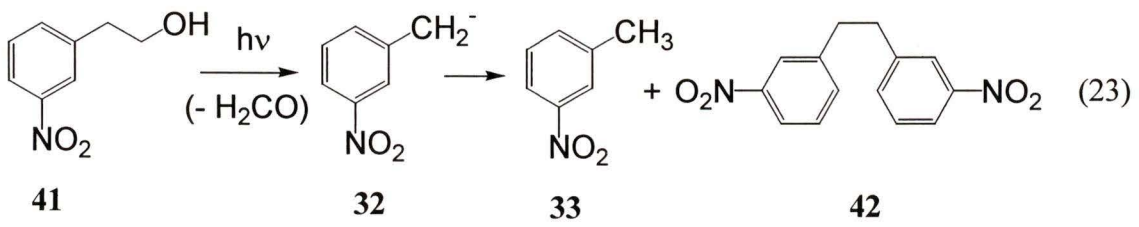

(23)

In an interesting study, modification of the leaving groups of *m*- and *p*-nitrobenzyls allowed the photogeneration of carbocations.[26] Photolysis of acetals **43** and **44** in aqueous media generates oxocarbocation **45**. As would be expected, this photoreaction was observed to be independent of pH, substantiating the assigned role of hydroxide ion (to deprotonate the hydroxide proton) in the above retro-Aldol reactions. Water was found to trap **45** to give hydroxy ester **46**, presumably via the intermediate hemi-orthoester **47** (Equation 24).

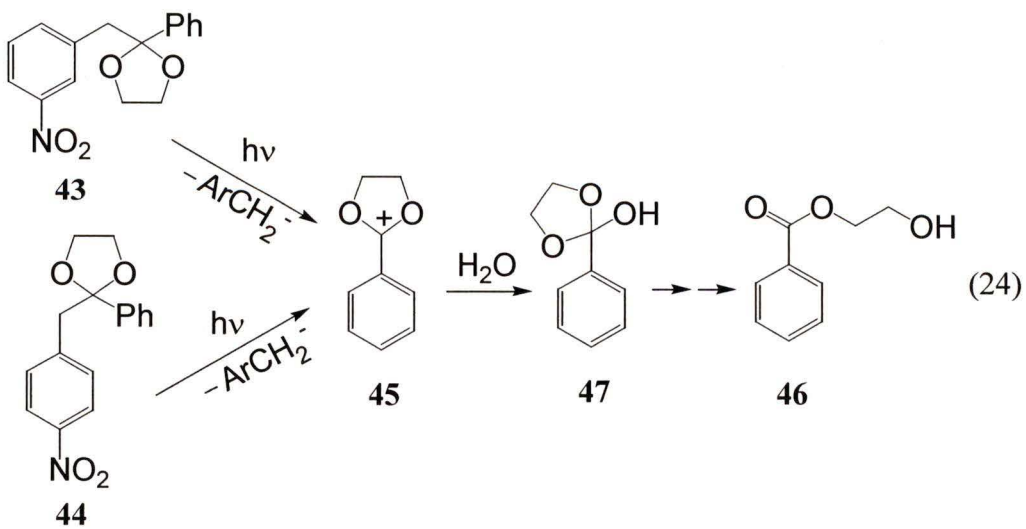

(24)

Further evidence of the generation of transients **31** and **32** during photolysis of β(3- or 4-nitrobiphenyl)ethanol derivatives was the observed oxygen trapping to yield oxygenated products.[26] While photolysis in oxygen saturated solution did not affect the quantum yields of substrate loss, > 60% of the observed product was comprised of the appropriate hydroperoxide **48** or **49** (< 15% of the product mixture was the corresponding nitrotoluene and bibenzyl, the remainder of the product mixture was recovered starting material).

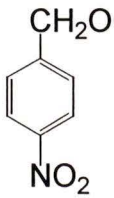

48

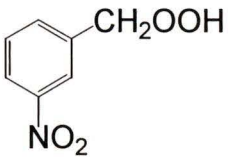

49

In support of the anion coupling mechanism proposed by Craig and coworkers, which explained the apparent lack of redox balance to the generation of radical anions of starting material,[25b] Muraldiharan and Wan provided ESR spectra of substrate radical anions generated from photo-retro-Aldol reaction.[27] It was also demonstrated that in the presence of a better electron acceptor than the substrate, electron trasfer to that electron acceptor will occur to produce the correponding radical anion (as observed by ESR). For example, addition of *m*-nitrobenzaldehyde to a photolysis mixture of β(3- or 4-

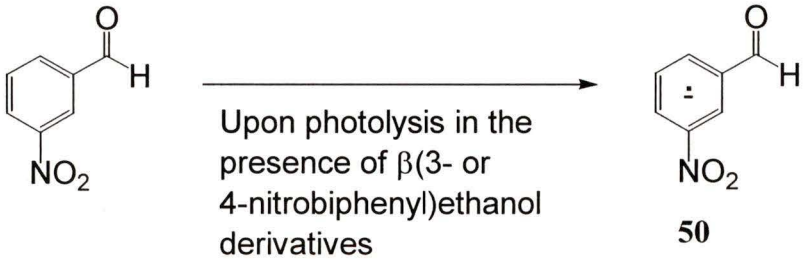

50

(25)

nitrobiphenyl)ethanol derivatives resulted in the generation of the radical anion **50** (Equation 25).

1.1.7 Photochemistry of 1-Acyl-7-Nitroindolines

As described above (in Section 1.1.5.2), photoremovable protecting groups have several practical applications. As such, there is considerable interest in developing improved photoremovable groups, with emphasis on chemical robustness, high quantum efficiency, stereoselectivity, and speed of release. Generally there is a need to be able to release a variety of functional groups, and to do so with less harmful longer wavelength light. One such group which releases a variety of carboxyl functional groups upon photolysis with long wavelength photolysis (> 400 nm) is 1-acyl-7-nitroindoline, which was first reported to exhibit such activity in 1976.[28] While the original publication was not a mechanistic publication, it certainly revealed some interesting mechanistic details of the reactivity of 1-acyl-7-nitroindolines.

1.1.7.1 Amide Bond Hydrolysis in an Organic Solvent

Like *o*-nitrobenzyls, the photochemistry of 1-acyl-7-nitroindolines is influenced by the ability of the nitro group to interact directly with its *ortho* substituent. The special features of *ortho* substitution were acknowledged by Patchornik and coworkers in their original study of 5-bromo-7-nitroindoline (Bni group, **51**) wherein they report the enhanced susceptibility of the amide bond of 1-acyl derivatives (**52**) to nucleophilic cleavage upon photolysis in organic solvents with trace amounts of hydroxylic nucleophiles (Equation 26).[28] It was observed that similar compounds with the nitro

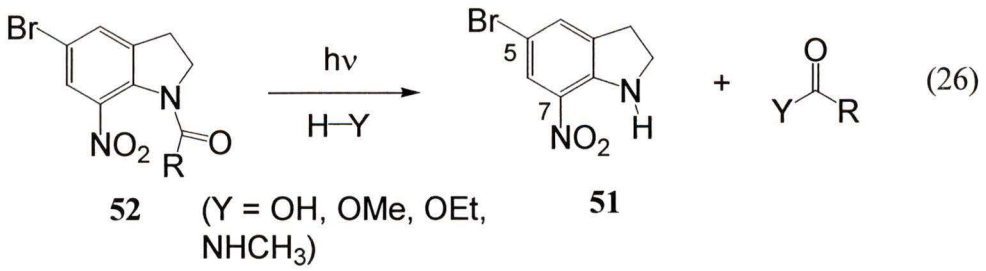

group in the 5 or 6 position did not give amide bond cleavage, consistent with a special reactivity being available only to the *ortho* nitro compound. In contrast to the 7-nitro group, the 5-bromine of **52** was found to be non-essential, as replacement of this group with a phenyl did not affect the dominant reactive pathway. Photorelease was also determined to be possible with a variety of R groups.

The photoproducts of **52** are the free Bni group (**51**) and the corresponding carboxyl group.[28] Several nucleophiles were found to be effective in amide bond cleavage of 1-acyl-7-nitroindolines upon photolysis in organic solvent. Photolysis of **52** in a mixture containing water (for example 2:3:0.05 CH_2Cl_2-dioxane-H_20), resulted in hydrolysis of the amide bond to generate free carboxylic acid. Photolysis in the presence of methanol gave free methyl ester, and photolysis in the presence of ammonia gave free amide.

The characteristics of the Bni group make it suitable as a protecting group in synthetic applications. Indeed the practicalities of its use in the synthesis of peptides was subject of a subsequent publication by Patchornik and coworkers.[29] The advantage of Bni group is its dual ability to both block the C-terminus of the peptide during chain elongation and its ability to controllably activate the C-terminus to nucleophilic attack, allowing attachment of a second peptide to the C-terminus photochemically. Using a

peptide synthetic method devised by the authors, several peptides were prepared and the degree of racemization induced during the preparation was measured using several racemization tests. In comparison to the same peptides prepared using two other methods (a method involving azide, and a method involving dicyclohexylcarbodiimide) the peptides prepared using the Bni group exhibited high optical purity, in some cases exceeding that of the peptides synthesized using conventional synthetic methods.

More recently Nicolaou and coworkers have examined 1-acyl-7-nitroindolines for use as a photolabile linker for the purpose of solid phase combinatorial synthesis.[30] Therein a method for the linking of 7-nitroindoline to aminomethylated polystyrene resin, and its use to orchestrate inter and intra molecular photoreactions with amines was described.

1.1.7.2 Water-Mediated Photoredox Chemistry with Amide Bond Cleavage

In the interest of developing a photorelease tool for the study of biological processes, Corrie and coworkers have examined the photoreactivity of 1-acyl-7-nitroindolines in 100% water.[31] In this study fundamental differences in the reactivity of the 1-acyl-7-nitroindoline chromophore in organic solvent and in 100% water were observed. While photolysis of **53** in 100% water did result in hydrolysis of the amide bond and release of the appropriate carboxylic acid, it was observed that the fate of the nitroindoline moiety was not the expected nitroindoline, but nitrosoindole **54** (Equation 27).

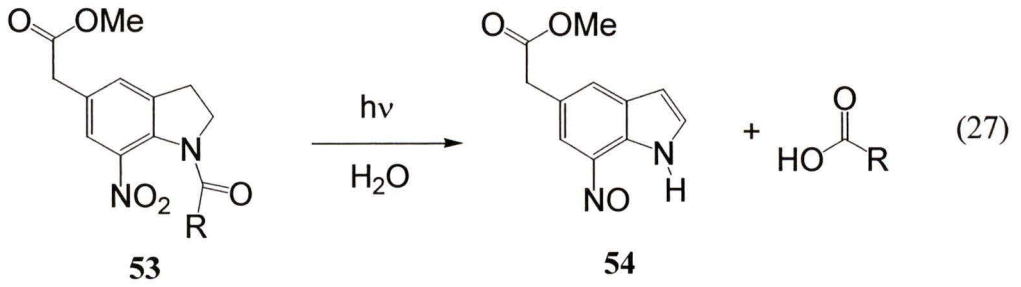

53 **54** (27)

Formation of a different product implies a new mechanism in 100% water. With an interest in probing this dichotomy, Corrie and coworkers carried out a preliminary mechanistic investigation of the water mediated reaction.[31] Using **53** (R = $(CH_2)_4OPO_3^{2-}$), which does not contain a free carboxylate, flash photolysis in isotopically enriched ^{18}O water was followed by IR. Using these means it was possible to detect carboxylate within microseconds of its release, and compare carboxylate stretching frequencies with those generated upon photolysis in unenriched water. These experiments indicated that the new oxygen atom in the released carboxylate does not come from the solvent, necessitating that it be introduced from the nitro group. This implies formation of a nitro-linked acyl group, such as **55**, is involved in the reaction pathway. Similar nitro-linked acyl groups have been reported in the photorelease pathway of carboxylic acids from N-acyl-8-nitrotetrahydroquinolines.[32]

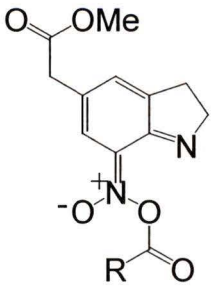

55

A study of the kinetics of proton release upon photolysis of **53** was undertaken using flash photolysis in which the color change of pH indicator bromothymol blue was monitored.[31] These experiments revealed that the time scale for the major signal (≈ 85 %) exceeds the time scale of the instrument ($k > 10^5$),[31] suggesting that the chemical events are fast.

The quantum yield of product formation from **53** was measured by Corrie and coworkers for the water mediated mechanism, and determined to be 0.043.[31] Photolysis experiments in both 100% water and organic solvent (2:3:0.05 CH_2Cl_2-dioxane-H_2O) allowed for the observation that the reaction in organic solvent was approximately twice as efficient as the reaction in 100% water.

From these studies some understanding of the mechanistic details of the water mediated mechanism was gained. However, a complete understanding was not attained. For the purpose of photorelease in biological experiments, it is especially pertinent to understand the time scale at which photorelease occurs, to determine the limits of these compounds for use in time resolved photorelease experiments. It is also of interest to understand the limitations on product quantum yields. Evidently there is considerable room for improvement, as a recent publication has reported that the product quantum yield of the water mediated reaction can be doubled through simple aromatic substituent manipulations.[33]

1.2 Biphenyl Chromophore

While most of the nitroaromatic photochemistry reviewed in this introduction can be viewed as confined to substituted nitrobenzene photochemistry, there is considerable

interesting work involving the nitro group attached to other aromatic chromophores, such as naphthalene, anthracene, acetophenone, pyridine, and biphenyl, to name a few.[1,3,4,18] While some chromophores have received more attention than others, the photochemistry of nitrobiphenyls, for reasons outlined in this section, deserves more attention than it has hitherto received.

A basic understanding of the photophysical properties of biphenyls is an essential prerequisite to understanding photochemistry of a molecule containing this unit. As with most biphenyls, the parent unsubstituted biphenyl is twisted in the ground state at the central carbon-carbon bond such that the dihedral angle is between 15° and 40°. This conformation is energetically favoured in the ground state despite the apparent benefits that extended conjugation of a planar structure may yield. This preference of a twisted conformation is in part due to steric effects that the *ortho* hydrogens of each ring have on one another (Equation 28).[34] Upon excitation electronic factors outweigh steric factors, and biphenyl relaxes toward planarity, allowing increased conjugation between adjacent phenyl rings. Effects of this conformational change can be seen in the absorption and fluorescence spectra of biphenyl. In the ground state, the twisted molecular structure is more flexible giving rise to a broad, featureless absorption spectrum, while in the excited state the molecular structure is more rigid, thus the fluorescence spectrum is sharp with distinct features.

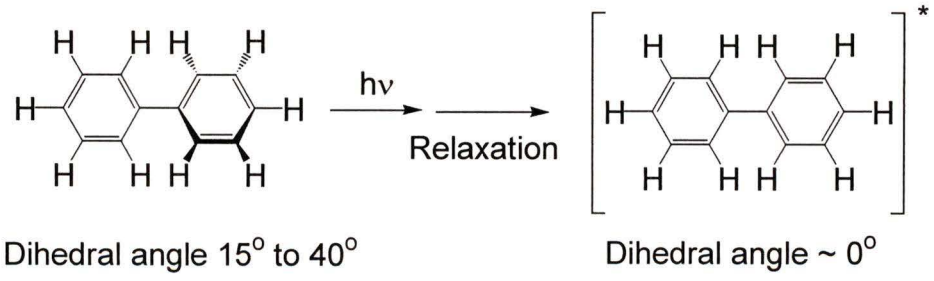

(28)

Biphenyls substituted with a donating and a withdrawing group on either ring (each *para* to the central carbon-carbon bond) have received particular interest due to their interesting excited state properties.[35] In particular, such biphenyls undergo a large change in dipole moments upon excitation due to a shift in the electron density from the

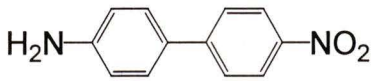

56

donor substituted ring to the acceptor substituted ring. For example, in the ground state the dipole moment of *p*-amino-*p'*-nitrobiphenyl (**56**) is about 7-8 D, while in the excited triplet charge transfer state its dipole moment is approximately 50 D, as determined from a combination of calculated and experimental data.[36] In comparison to the excited state of *p*-aminonitrobenzene (which contains only one phenyl ring), the dipole moment of the excited state of **56** is larger, a feature reflecting the higher polarizability of biphenyl over benzene.

While there has been considerable interest in the use of such donor-acceptor biphenyls for various purposes, systematic investigations of nitrobiphenyl photochemistry where charge transfer excited states have been proposed are unreported. However, given the strong charge transfer properties of the excited state, it seems logical that this chromophore could be used to invoke new photochemistry.

1.3 Research Proposal

Previous work with *m*- and *p*-nitrobenzyls has demonstrated that the strongly electron withdrawing nitro group can enhance photoredox, photodecarboxylation and photo-retro-Aldol chemistry through charge transfer mechanisms mediated by water. Enhanced polarizability of biphenyls (compared to the benzene ring) suggests that such photochemistry could not only be possible, but enhanced for nitrobiphenyl systems. In this study three such molecules were investigated. These compounds are 4'-nitro-[1,1'-biphenyl]-4-methanol (**57**), which is designed to probe photoredox reaction ability, 4'-nitro-[1,1'-biphenyl]-4-acetic acid (**58**), which was anticipated to decarboxylate from the acetate form, and 4'-nitro-[1,1'-biphenyl]-4-(β)-ethanol (**59**), which was included to study the anticipated photo-retro-Aldol reaction.

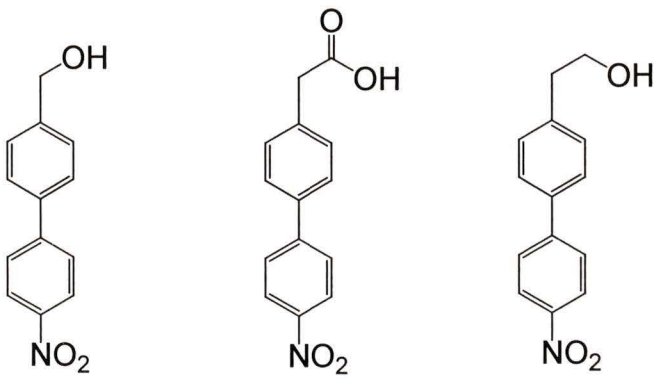

57 **58** **59**

Product studies in 50% water (50% CH_3CN as cosolvent) allowed determination of the viability of the expected reactions. The effect of pH was found to have significant impact on the reactivity of *m*- and *p*-nitrobenzyls, and thus pH studies were also probed. LFP was expected to allow observations of transients, the identity and behaviour of

which provided key information concerning reaction mechanisms, which was supported by product studies. This investigation of 4-nitrobiphenyls is reported in Chapter 2.

Lack of a detailed mechanistic study of the reactivity of 1-acyl-7-nitroindolines was rectified with the second project described herein. Mechanistic data uncovered previously, together with product and LFP studies in the present work are incorporated into a detailed mechanism explaining the observed reactivity in mostly organic (99:1 CH_3CN-H_2O) and in wholly aqueous solution. In particular, the time frame for photorelease of acetate in 100% aqueous solution was determined. For this study the following nitroindolines were included: methyl 1-acetyl-7-nitroindoline-5-acetate (**60**), methyl 1-acetyl-2,2-dideutero-7-nitroindoline-5-acetate (**61**), methyl 1-α-methoxy acetyl-7-nitroindoline-5-acetate (**62**), methyl 1-α-methoxy acetyl-2,2-dideutero-7-nitroindoline-5-acetate (**63**).

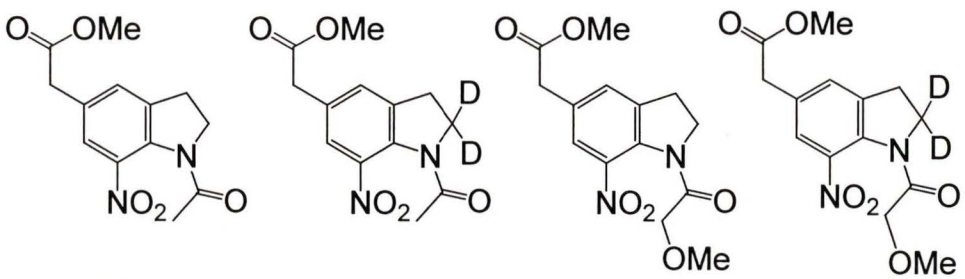

60 **61** **62** **63**

The simplest molecule containing all the essential functionalities, **60**, served as the primary model of the photorelease reaction. Effects of an electron withdrawing group on the leaving group were investigated using **62**, to probe this effect on the mechanism.

In anticipation of deuterium isotope effects, **61** and **63** were included. The effect of water content in CH_3CN was investigated for **60** and **62** by product study to yield insight into the mechanistic dichotomy. LFP provided vital information allowing determination of the time frame of acetate release. This investigation of 1-acyl-7-nitroindoline photochemistry is reported in Chapter 3.

Chapter 2

Photoredox, Photodecarboxylation, and Photo-Retro-Aldol Chemistry of 4-Nitrobiphenyls

2.1 Introduction

As discussed in Chapter 1, a water mediated charge transfer mechanism has been found to be operative in *m*- and *p*-nitrobenzyl photoredox, photodecarboxylation and photo-retro-Aldol chemistry. Due to the enhanced polarizability of biphenyl in the excited state over benzene, exploration of similar nitrobiphenyl photochemistry seems a logical progression. The enhanced polarizability of biphenyl has been the motivation in photochemical studies of other systems,[37] however to our knowledge a systematic investigation of charge transfer photochemistry of nitrobiphenyls has not been explored.

Photoredox reaction of *p*-nitrobenzyl alcohol (**18**) was found to occur upon photolysis in highly basic aqueous solution to generate *p*-nitrosobenzaldehyde (**19**), as was shown by Wan and Yates (Equation 29, *m*-nitrobenzyl alcohol reacts similarly at pH 7).[23] To probe analogous nitrobiphenyl photochemistry **57**, which is modeled after **18**, was synthesized and studied.

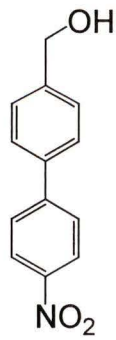

57

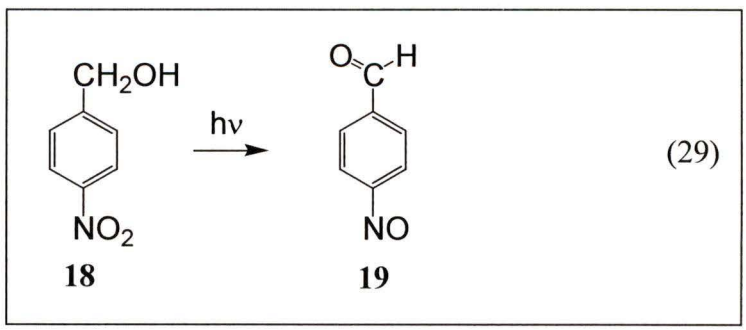

18 **19**

(29)

It was shown by Wubbels and coworkers that *p*-nitrobenzaldehyde (**15**) undergoes photoredox reaction to give *p*-nitrosobenzoic acid (**16**), upon photolysis in water (Equation 30), however *m*-nitrobenzaldehyde was found to be photoinert under the same conditions.[20] This study probes the analogous aldehyde, namely 4'-nitro-[1,1'-biphenyl]-4-aldehyde (**64**) which was synthesized and investigated for possible photoredox activity.

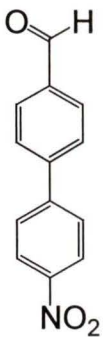

64

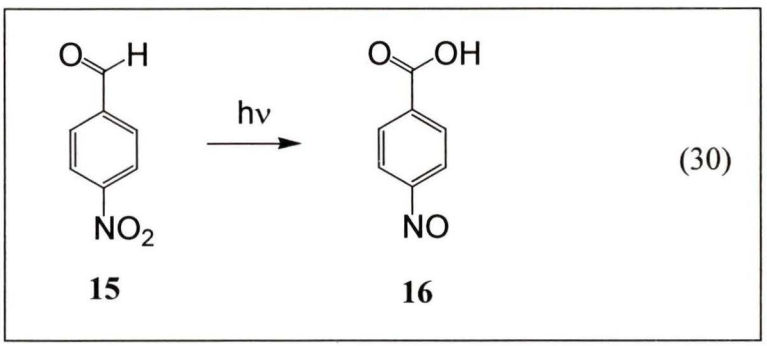

15 **16** (30)

Wan and Yates[23] demonstrated that α-deuterated *m*- and *p*-nitrobenzyl alcohols (α-monodeuterated *p*-nitrobenzyl alcohol **21** shown below) have markedly lower product forming quantum efficiencies than the non deuterated analogs. These deuterium isotope effects are consistent with benzylic deprotonation occurring at the product determining step, thus instrumental in deducing the mechanism of the observed photoreactivity. In anticipation of a similar deuterium isotope effect in the photoredox reaction of the biphenyl system, α-deuterated alcohol **64** was also synthesized and included in this study.

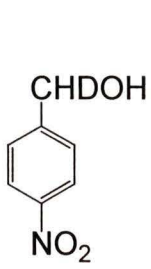

21

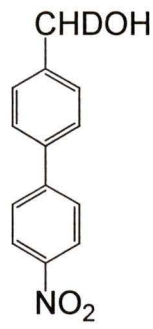

65

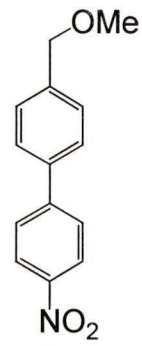

66

Generality of redox reactivity for the 4-nitro-4'-substituted-biphenyl chromophore will be demonstrated in the examination of the photoredox reactivity reactivity of the α-methoxy derivative **66**. Analogous to *o*-nitrobenzyl photorelease groups, which form hemi-acetals upon photolysis and subsequently hydrolyze to release the protected compound,[18] it will be shown that photoredox chemistry of **66** induces release of "protected" methanol.

Heterolytic carbon-carbon bond cleavage was demonstrated by Margerum and Petrusis[24] to occur during the photodecarboxylation of the acetate form of *p*-nitrophenyl acetic acid (**30**) upon photolysis in water (pH > 2)(Equation 31)(*m*-Nitrophenyl acetic acid is similarly reactive). This investigation reports on photodecarboxylation of the

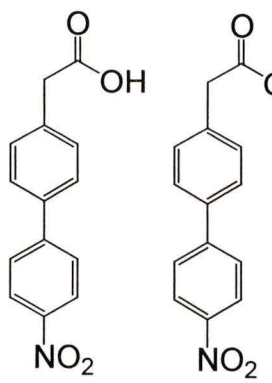

58

67

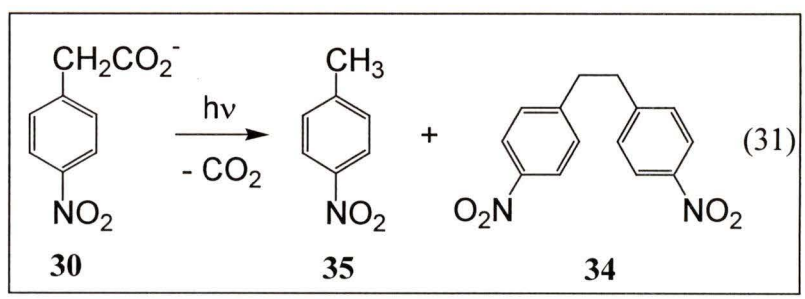

30 **35** **34**

corresponding nitrobiphenyl **58**. Structurally similar, but photochemically non-reactive, methyl ester **67** was included in this study to demonstrate that decarboxylation cannot occur via homolytic carbon-carbon bond cleavage.

A novel method of heterolytic carbon-carbon bond cleavage was introduced by Wan and Muralidharan.[26] Photo-retro-Aldol reactions occur from various β(*m*- and *p*-nitrophenyl)ethanols, such as **40**, which releases formaldehyde upon photolysis in aqueous solution (Equation 32). Extension of this type of photochemistry to nitrobiphenyl systems was demonstrated by the study of **59**.

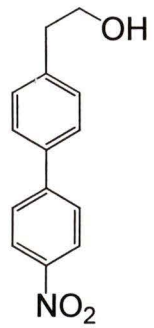

59

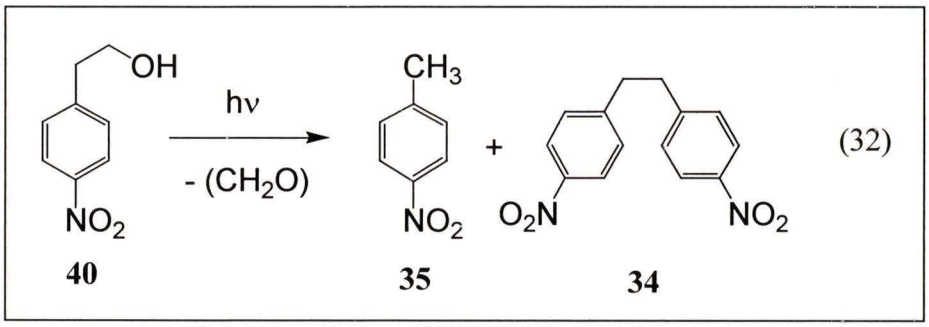

40 **35** **34** (32)

2.2 Synthesis

To minimize the total number of synthetic steps, 4-nitro-4'-methylbiphenyl (**68**) which is easily derivatized, was prepared by Suzuki coupling in this divergent synthesis of biphenyls **57** – **59** and **64** – **67** (Scheme 2.1). The yield of **68** was 84% in the palladium catalyzed coupling of 1-bromo-4-nitrobenzene with *p*-tolylboronic acid.

Bromination of **68** with one equivalent of N-bromosuccinimide gave the mono-brominated biphenyl **69a** in a mixture of other bromination products, which was used as

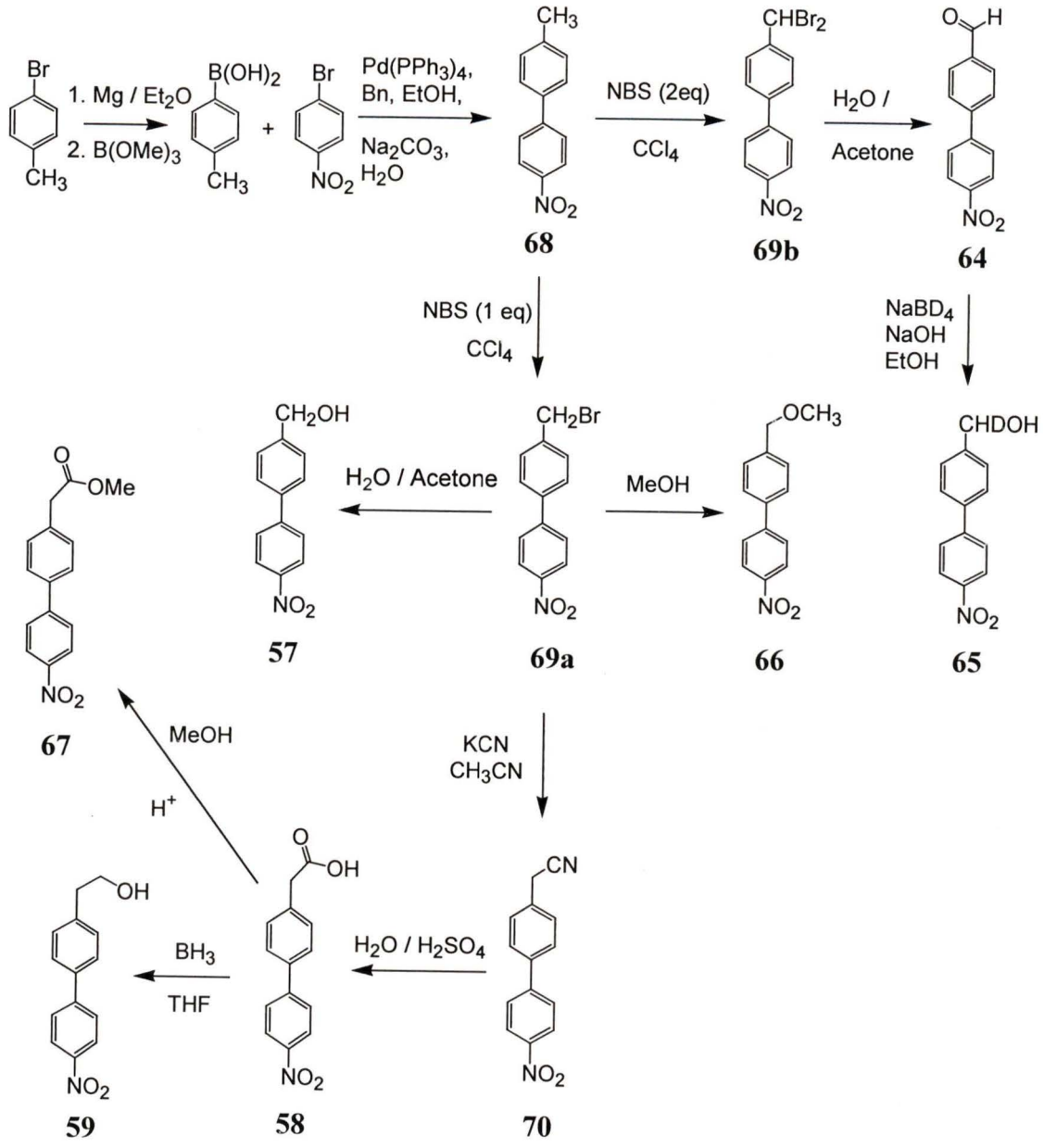

Scheme 2.1

such in the subsequent reactions. Reflux of **69a** in 50% aqueous acetone, followed by column chromatography and recrystallization from hot aqueous ethanol gave **57** in 48% yield (from **68**). Reflux of **69a** in methanol gave **66**, which was purified by column chromatography and recrystallization.

Reflux of **69a** with cyanide gave nitrile **70**, which upon hydrolysis in acidic conditions yielded carboxylic acid **58**. Precipitation of **58** from aqueous base by addition of H_2SO_4, followed by recrystallization from hot chloroform gave 36% yield of **58** (from **68**). Reduction of the carboxylic acid **58** to alcohol **59** was achieved via reaction with borane. The yield of **59** upon recrystallization from hot aqueous ethanol was 88%. Methyl ester **67** was also prepared from **58** via an acid catalyzed methanolysis, which, upon cooling of the reaction mixture yielded 81% yellow crystals of **67**.

Bromination of **68** with two equivalents of N-bromosuccinimide gave dibrominated biphenyl **69b** in a mixture of other bromination products, which was used as such in the subsequent reactions. Reflux of **69b** in 50% aqueous acetone gave **64**, which was purified by column chromatography and recrystallization from hot aqueous ethanol in 63% yield. Reduction of **64** with sodium borodeuteride gave mono-α-deuterated alcohol **65**.

Proof of structure was achieved by ^{1}H NMR, IR, and MS for all compounds, HRMS for **57-58**, and by X-ray crystallography for **59**. In the crystal structure of **59**, it can be seen that the asymmetric unit consists of 3 molecules of **59** lying head to tail, as is shown in the ORTEP diagram of Figure 2.1. Four asymmetric units were found to comprise a unit cell, which in turn comprised a primitive monoclinic crystal lattice. Interestingly, the torsion angle around the central biphenyl carbon-carbon bond is quite low for the right-most molecule and the central molecule (3° and 6°, respectively), while fairly twisted for the left-most molecule (25°), as would be expected due to steric reasons. The planar nature of the biphenyl rings in this crystal structure is suggested to be due to

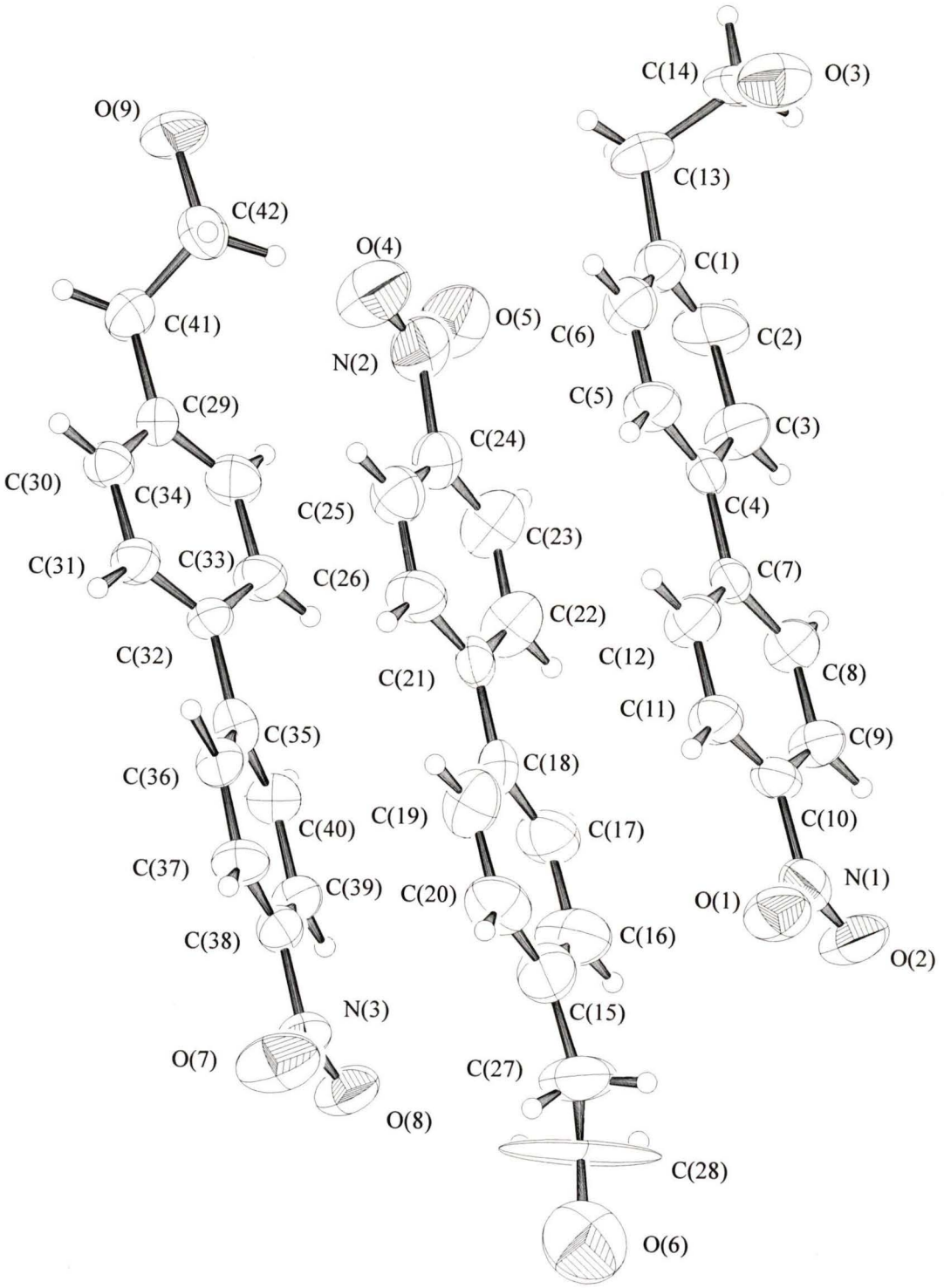

Figure 2.1 X-ray crystal structure of the asymmetric unit of **59** (ORTEP). Torsional angles about the central biphenyl bond: C(3), C(4), C(7), C(8) = 3.2°; C(17), C(18), C(21), C(22) = 6°; C(33), C(32), C(35), C(40) = 25°.

intermolecular π-stacking, and is not believed to reflect the ground state conformation of **59** in solution.

2.3 UV-Vis Studies

2.3.1 UV-Vis Studies in Neutral Aqueous Solution

For these experiments a mixture of 1:1 H_2O-CH_3CN was chosen. Water was chosen due to the requirement of a polar protic solvent for that was observed for the analogous nitrobenzyl systems, and acetonitrile for its superior spectroscopic properties and general lack of photochemical reactivity.

Initial studies were carried out using UV-Vis spectrophotometry to monitor for possible photochemistry. Photolysis of **57** and **58** in neutral aqueous solution (1:1 H_2O-CH_3CN; 10^{-5} **M**, argon purged prior to photolysis, Rayonet RPR 100 photochemical reactor, 300 nm lamps; 3.0 mL UV cuvettes, photolysis time 15 s - 6 min) resulted in significant UV-Vis spectral changes indicating photoreactivity of these compounds under these conditions (Figures 2.2 and 2.3). These spectral changes exhibit distinct isosbestic points, suggesting that the photochemical reactions are clean. Under similar conditions, alcohol **59** showed no observable changes in its UV-Vis absorption spectrum, indicative of a lack of photoreactivity.

2.3.2 UV-Vis Studies in Basic Aqueous Solution

As **59** appeared to be photoinert at pH 7 it was decided to probe its reactivity at high pH, where the parent compound **40** had been observed to be photoreactive.[23] At pH

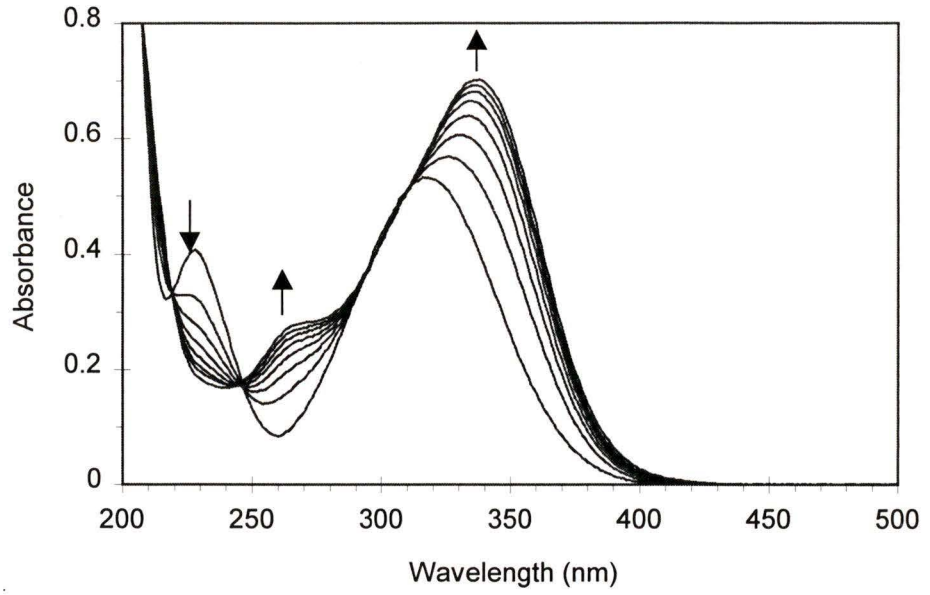

Figure 2.2 UV-Vis traces observed on photolysis of **57** in 1:1 H_2O-CH_3CN (pH 7). Each trace represents about 1 min photolysis at 300 nm.

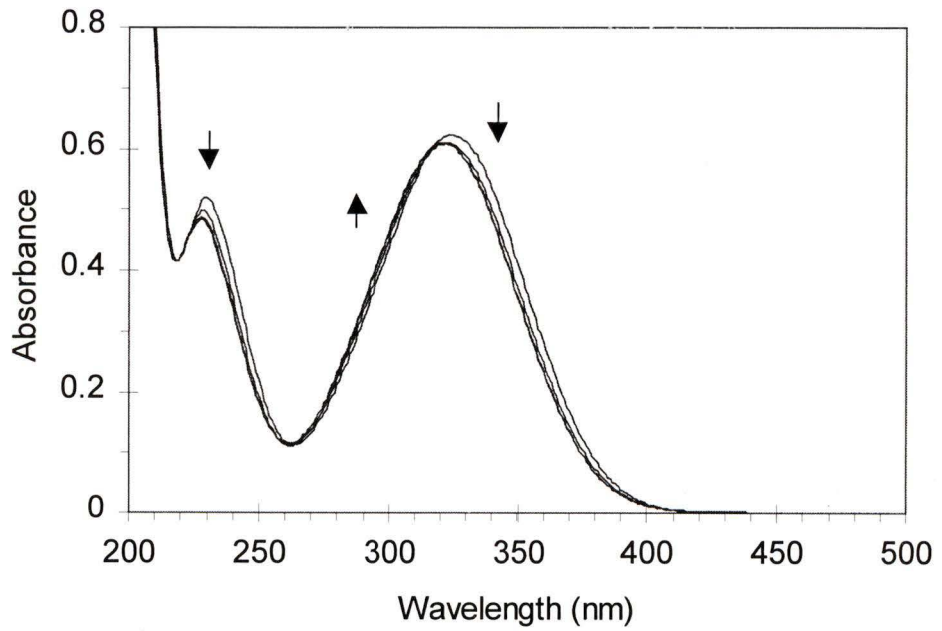

Figure 2.3 UV-Vis traces observed on photolysis of **58** in 1:1 H_2O-CH_3CN (pH 7). Each trace represents about 15 s photolysis at 300 nm.

13 (water portion) **59** showed significant spectral changes suggestive of a base-catalyzed photoreaction (Figure 2.4). These spectral changes are not as well behaved as those observed for **57** and **58** in neutral solution. As shown in Figure 2.4, the absorption spectrum tails out to 600 nm. This long tailing did not correspond to the UV-Vis spectra of any of the expected products of photo-retro-Aldol reaction. The pink colour persisted overnight and was stable to oxygen bubbling of the solution. Addition of a drop of concentrated H_2SO_4 had a dramatic effect, the solution in the cuvette immediately turned yellow. The spectrum of this acidified solution is shown as the dashed trace in Figure 2.4.

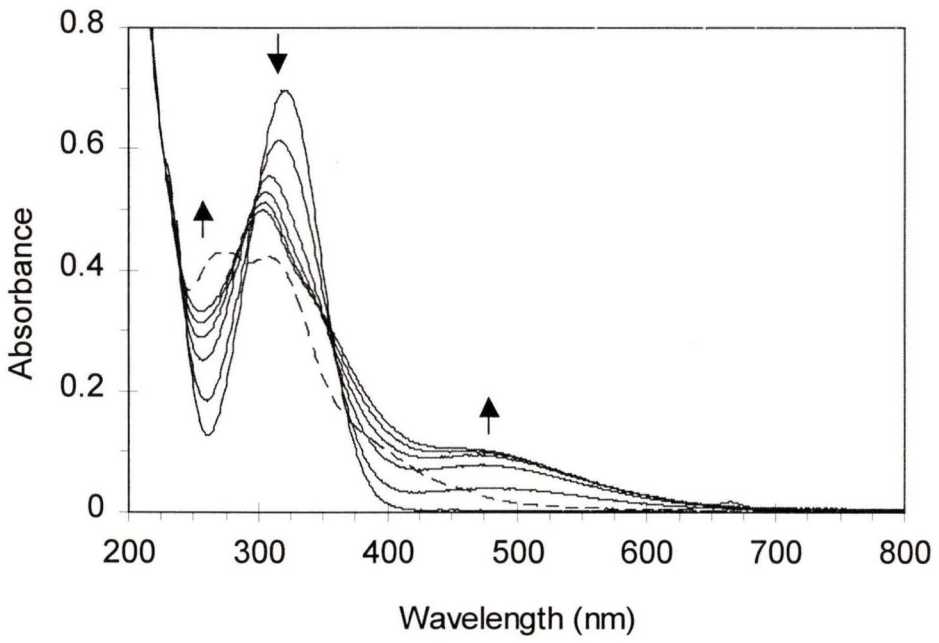

Figure 2.4 UV-Vis traces observed on photolysis of **59** in 1:1 H_2O-CH_3CN (pH 13, solid lines). Each trace represents about 1 min photolysis at 300 nm. Dashed line represents spectrum upon acidification.

Similar absorption spectra were generated upon photolysis of other biphenyls at pH 13, such as **57** and **58**, and **68**. The observed lack of clean isosbestic points and lack of distinct structure in these spectra suggest that the photochemistry of nitrobiphenyls in highly basic conditions is not straightforward, which was confirmed by preparative photolyses. For this reason the reactivity of nitrobiphenyls in basic solution has not been extensively probed in this study, with the exception of the investigation of the photoreactivity of **59**. While not proved conclusively, the photogeneration of highly coloured products in alkaline conditions is likely due to a photoreduction pathway available at high pH. Photoreduction of nitroaromatics in basic solution has been documented, and it is believed that hydroxide ion can act as an electron donor in the photoreduction of nitroaromatics.[1,3,4,38]

2.3.3 UV-Vis Studies in Acidic Aqueous Solution

Photoreactivity of **57** and **58** at pH 7 suggested the possibility of photoreactivity in acidic aqueous solution. While *m*-nitrobenzyl alcohol (**22**) had been found to undergo photoredox reaction at all pHs, *p*-nitrobenzyl alcohol (**18**) showed no photoreaction below pH 10. Photodecarboxylation of the *m*- and *p*- parent compounds, **29** and **30**, had not been observed at pH $\leq$ 2. Thus it was somewhat surprising that **57** and **58** both gave rise to spectral changes upon photolysis at pH 2 (Figures 2.5 and 2.6). Further, the spectral changes were significantly different from those observed at pH 7. This was indicative of a new reaction pathway in acid, which was not observed in either the *m*- or *p*- nitrobenzyl analogs of **57** and **58**. Unlike the photoreactions at high pH, these reactions exhibited clear isosbestic points and apparently had high quantum efficiency, as

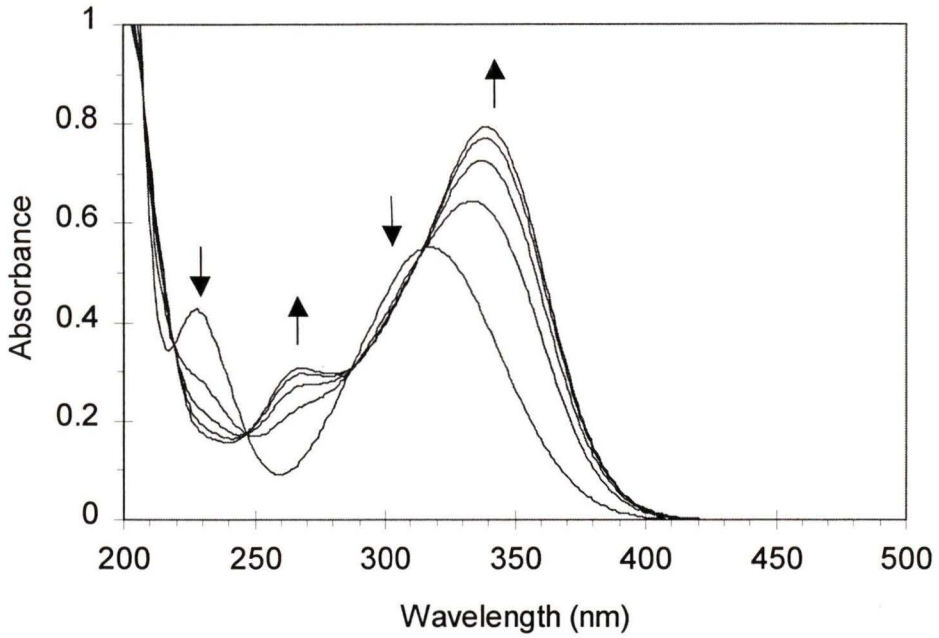

Figure 2.5 UV-Vis traces observed on photolysis of **57** in 1:1 H_2O-CH_3CN (pH 2). Each trace represents about 30 s photolysis at 300 nm.

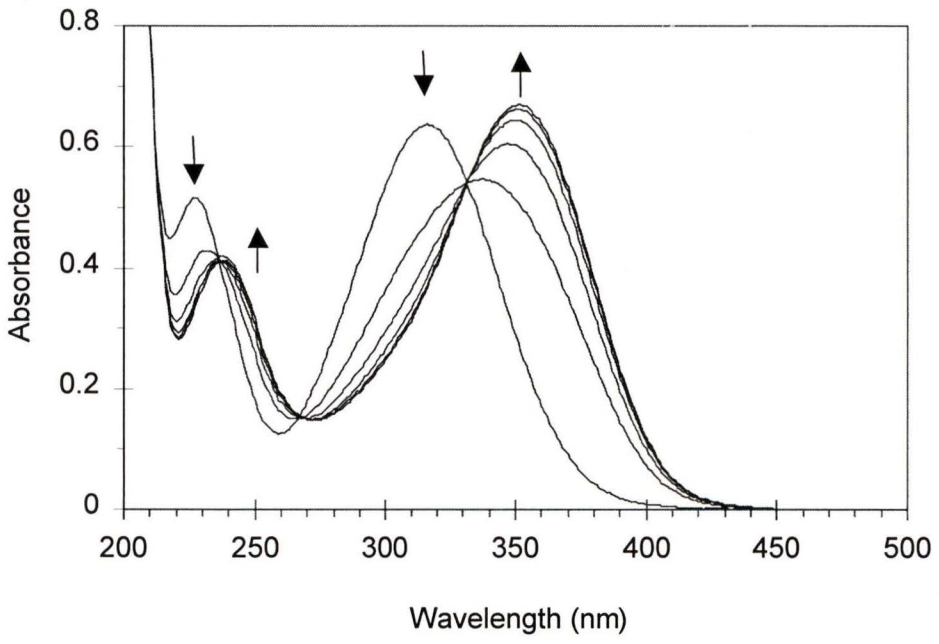

Figure 2.6 UV-Vis traces observed on photolysis of **58** in 1:1 H_2O-CH_3CN (pH 2). Each trace represents about 30 s photolysis at 300 nm.

suggested by the short photolysis times required to reach exhaustive conversion. For these reasons, and the novelty of these photoreactivities, **57** and **58** were subject to considerable study in acidic solution.

2.4 Products Studies

During the course of preparative photolysis experiments, dark control reactions were routinely carried out to monitor for possible thermal chemistry. No thermal chemistry was observed for the all compound studied in this work. Selected photolysis runs in other solvents (e.g., neat CH_3CN, neat and aqueous MeOH and THF) either resulted in no photochemistry or with substantially reduced yields compared to runs carried out in aqueous CH_3CN. This is consistent with the previously observed requirement for a polar protic solvent being essential for efficient photoredox, photodecarboxylation and photoretro-Aldol reactions of the *m*- and *p*-nitroaromatic compounds.[23-27]

2.4.1 Photolysis of 57 in Neutral Aqueous Solution

Preparatory photolysis of **57** (1:1 H_2O-CH_3CN, pH 7, 10^{-3} **M**, 300 or 350 nm lamps, argon purged before and during photolysis, < 15 °C, 5-60 min) gave *p*-(*p'*-nitrophenyl)benzaldehyde (**64**) and an unstable reduced product in a 3:1 ratio, confirming that photoredox chemistry occurs for **57** in a loosely similar fashion as **29** and **30** (Equation 33). The observed reduction product (tentatively assigned hydroxylamine, based on ^{1}H NMR chemical shifts) was found to transform to azoxy derivative **71** and an insoluble yellow-orange material within an hour. Interestingly, photolysis of **57** under

oxygen purging gave exclusively **64** in > 90% yield. The product ratio was independent of conversion at > 70% total conversion, suggesting that both products were primary photoproducts. This was further confirmed for the reduction product by the photolysis of a purified sample of **64**, which was found to be photoinert.

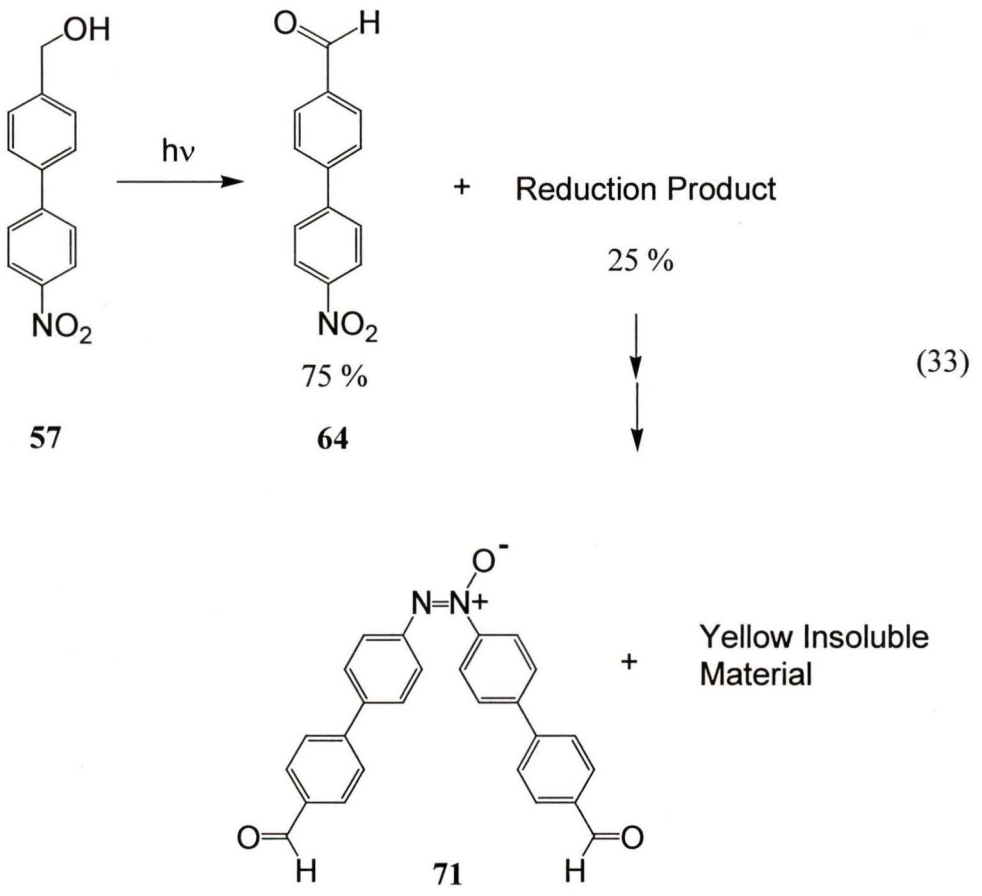

The observation of both oxidized and reduced products upon photolysis of **57** at pH 7 (Equation 33) is reminiscent of the observed photoredox chemistry of *m*-nitrobenzyl alcohol (**22**), where both *m*-nitrobenzaldehyde (**23**) and *m*-azoxybenzaldehyde (**24**) were observed in an apparently redox-unbalanced ratio (Section 1.1.5.3.2).[23] Since the reduction product does not arise via photolysis of **64**, another possible route is reduction of **64** via a dark reaction, if an electron source is available. If electrons are being

generated during the photoreaction of **57** this would explain how photolysis of **57** under oxygen purged conditions produces **64** as the exclusive product. To test this possibility reduction of **64** by a photogenerated electron was probed. Previous work by Muralidharan and Wan[27] using ESR and product studies has shown that photogenerated *m*- and *p*-nitrobenzyl carbanions (**32** and **31**, respectively) can act as electron sources, reducing other nitroaromatic compounds in solution, including substrate. For example, photogenerated *p*-nitrobenzyl carbanion (**31**) from photolysis of *p*-nitrophenyl acetic acid (**30**)(in aqueous CH_3CN) reduces added *m*-nitroacetophenone to *m*-azoxyacetophenone as well as *m*-aminoacetophenone.[27] This suggests that the reduction product might arise via reduction of **64** via a photogenerated "reducing" carbanion. To test this possibility, **64** was photolyzed in the presence of **30** (pH 7). In addition to products arising from **30** (viz., **34** and **35**), the reduction product was observed (7% yield from **64**). Therefore, this suggests that photolysis of **57** results in the formation of a transient carbanion **72**, which is subsequently reduced by additionally formed carbanions, to give the reduction product (Equation 34). This would be expected to yield a one to one ratio of **64** to the reduction product, thus there must be other reduced products which are not observed. One

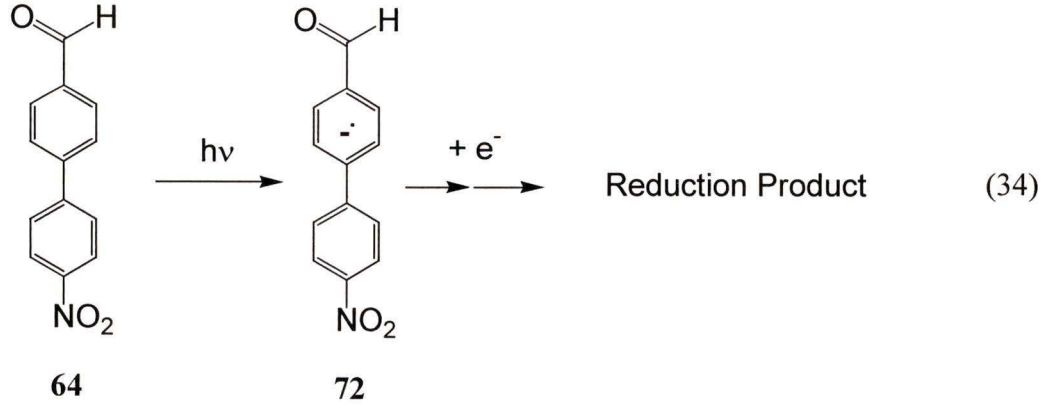

64 **72** (34)

explanation is that **72** is long lived such that it is oxidized by air (in the work up) to **64**. This scenario is corroborated by the observed efficient electron scavenging ability of oxygen for this reaction (when **57** is photolyzed in oxygen purged solution, *vide supra*).

2.4.2 Photolysis of 57 in Acidic Aqueous Solution

In acidic solution the photoreaction of **57** was redox balanced. Photolysis at pH 2 (aq. H_2SO_4) gave *p*-(*p'*-nitrosophenyl)benzaldehyde (**73**) exclusively, in yields > 90% (Equation 35). As mentioned above, the parent compounds (**18** and **22**) did not react to give novel products in acidic solution.

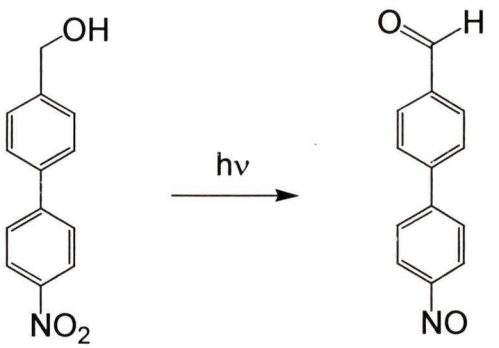

57 **73** (35)

2.4.3 Photolysis of 58 in Neutral Aqueous Solution

Efficient photodecarboxylation of **58** was observed at pH ≥3, producing primarily **68** (>95%) with small amounts of **74** (< 5%) at all conversions (Equation 36). These products are analogous to those observed for the parent compounds (**29** and **30**). Also, the photodecarboxylation efficiency was observed to decrease on decreasing the pH from 7 to 3. This is believed to reflect the photoinert nature of the protonated forms of **29** and **30**.[23,24]

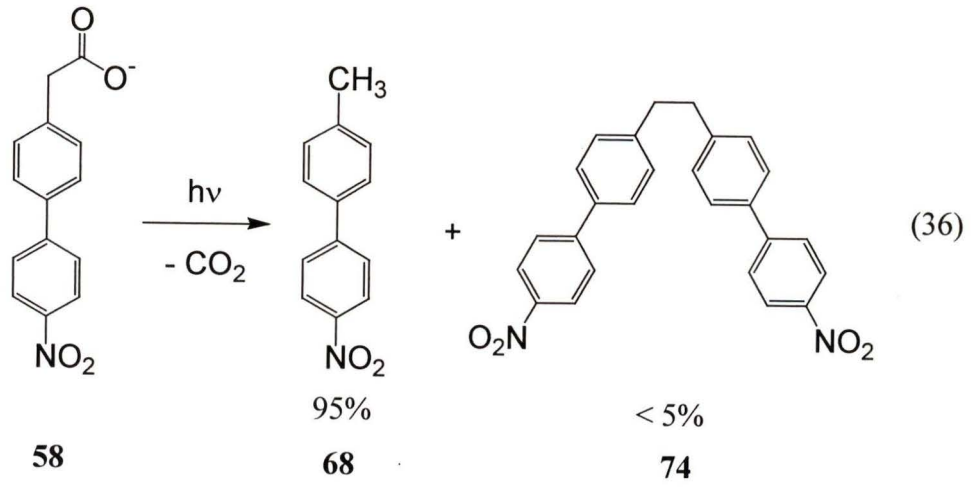

(36)

2.4.4 Photolysis of 58 in Acidic Aqueous Solution

The protonated form of **58** is not photoinert. Preparative photolysis of **58** at pH 2, where the substrate is fully protonated, allowed identification of a new product, *p*-(*p*'-nitrosophenyl)benzyl alcohol (**75**), which was formed exclusively (Equation 37). In light of this novel acid catalyzed pathway, the nature of the parent *p*-nitrophenylacetic acid (**30**) was probed in more acidic solution than has been previously reported[24,26] to establish whether or not **30** exhibits analogous photoreactivity. Photolysis of **30** in (5% (w/w) H_2SO_4/H_2O)-CH_3CN (pH ≈ 0) for extended periods of time did not result in photoreactivity, thus reconfirming the photoinert nature of this compound in acidic

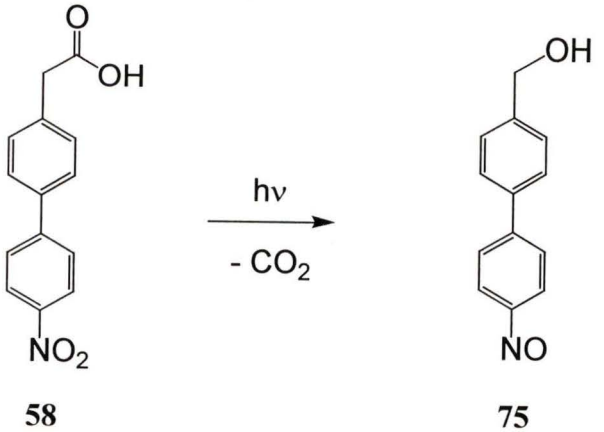

(37)

medium. It would appear, then, that **58** reacts via a different pathway in the acid form, one that involves both decarboxylation and an overall redox process.

2.4.5 Photolysis of 59 in Basic Aqueous Solution

To reconfirm UV-Vis results, **59** was photolyzed under conditions in neutral (1:1 H_2O-CH_3CN, pH 7), which resulted in complete recovery of substrate. Extended photolysis (1 h, 300 nm, 16 lamps) gave a trace yield of **68** (< 2 % conversion). However, photolysis under basic conditions (pH 13) gave **68** and **74** in the same relative yields as observed for **58** (Equation 38). Reaction of **59** to give **68** under basic conditions is suggestive of a retro-Aldol type reaction. In order to characterize the expected formaldehyde elimination product, photolyses were carried out in an NMR tube (pD 13, 1:1 D_2O-CD_3CN, λ_{ex} = 300 nm, 10 to 30 min). Photolysis resulted in growth of peaks assignable to **68** as well as a singlet at δ 4.8. This latter peak was assigned to formaldehyde hydrate, based on its similar chemical shift to 1,3-dioxane (δ 4.9) and 1,3,5-trioxane (δ 5.1). Enhanced reactivity of **59** at pH 13 is reminiscent of observations made previously for β(4-nitrophenyl)ethanol (**40**), where the retro-Aldol reaction was

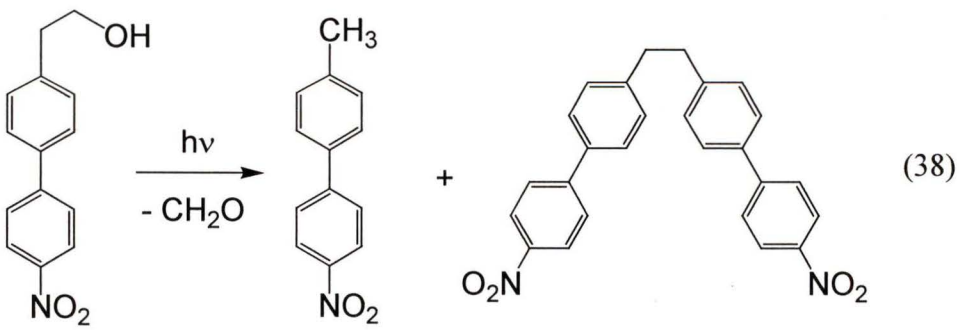

95% < 5% (38)

59 **68** **74**

shown to be base catalyzed.[26] It was suggested that hydroxide ion deprotonates the alcohol proton concerted with carbon-carbon bond heterolysis.

2.4.6 Photolysis of 65 in Neutral Aqueous Solution

Photoredox chemistry was also observed for **66**, which gave **64** and **71** in a 75% to 25% ratio, respectively, upon photolysis in 1:1 H_2O-CH_3CN, pH 7 (Equation 39). The quantum efficiency for photoredox reaction of **66** was approximately half that of **57**, however conversion could be extended to > 70 % in a manner analogous to that of **57**. To verify the release of methanol from **66**, photolysis was carried out in an NMR tube (1:1 D_2O-CD_3CN, λ_{ex} = 300 nm, 10 to 30 min), which allowed observation of the growth of peaks assignable to **64**, **71** and a peak at δ = 3.3. Addition of aliquots of authentic methanol via syringe verified the assignment of the latter peak to photoreleased methanol.

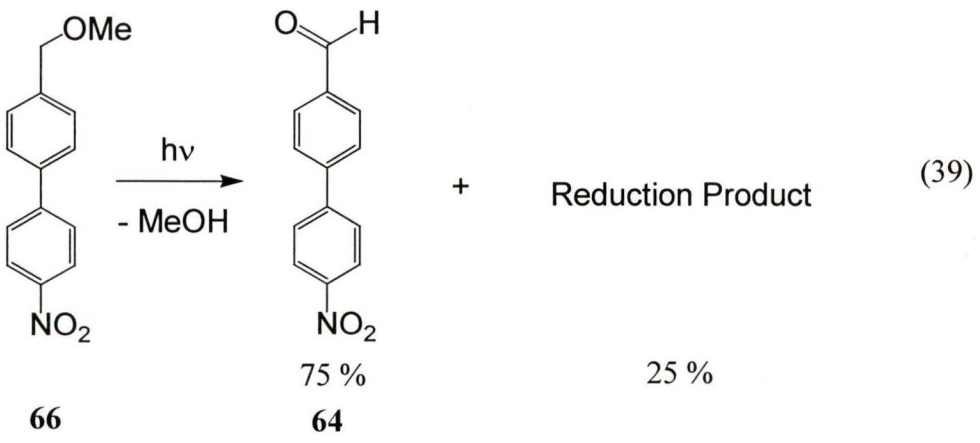

(39)

2.4.7 Photolysis of Non-Nitro Analogs 76, 77 and 78

Photolysis of the non-nitro analogs **76**, **77** and **78** sheds light on the role of the nitro group in the photochemistry of **57**, **58** and **59**. Photolysis of **76** (pH 7, 1:1 CH_3CN-

H_2O) for extended periods gave no observable photochemistry. Photolysis of **77** (pH 7) gave residual decarboxylation, to give *p*-methylbiphenyl and radical coupling product **79**, with an overall quantum efficiency that is about 50 times lower than for **58**. Photolysis of **78** (pH 13) also gave some retro-Aldol chemistry (viz., formation of *p*-methylbiphenyl), again in much lower quantum efficiency (about 20 fold less than for **10**). It is clear that the nitro group substantially enhances the reactivity of these biphenyl system, although the residual reactivity observed for both **77** and **78** suggests that the phenyl group itself (as a substituent) can act as an enhanced electron withdrawing group in the excited state, promoting decarboxylation and retro-Aldol reaction. This is not unexpected but the details of this effect remain to be explored further.

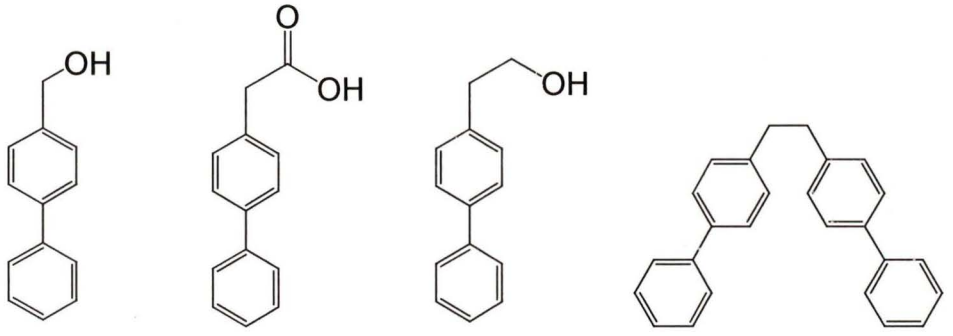

76 **77** **78** **79**

2.4.8 Deuterium Isotope Studies

The photochemistry observed for **58** (pH ≥ 3) and **59** is analogous to that reported for **30** (Equation 18) and **40** (Equation 22) where the *p*-nitrobenzyl carbanion **31** has been shown to be the reactive intermediate.[25] That a similar intermediate is operative in the photochemistry of **58** and **59** was demonstrated by the isolation of α-deuterated **80** when **58** was photolyzed in 1:1 D_2O-CH_3CN (pD 7). It was also observed that the relative

yield of **74** is much higher in 1:1 D_2O-CH_3CN (where 25% of the product mixture is **74**) than in 1:1 H_2O-CH_3CN (where < 5% of the product mixture is **74**). The implication of the relative yields of **74** will be adressed in Section 2.5.

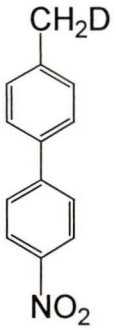

80

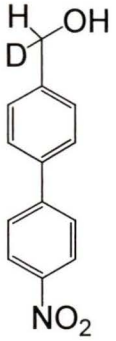

64

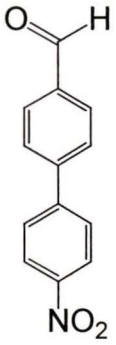

63

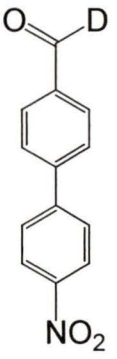

81

In order to gain insight into the photo-oxidation of **57** to **63**, photolysis of **64** was carried out (pH 7) to explore the possibility of an α-deuterium isotope effect on reaction efficiency. ^{1}H NMR analysis of the aldehyde products revealed formation of both **63** and **81** in 1:2 ratio (i.e., preference for removal of the proton from the benzylic position, as anticipated). This gives an isotope effect for quantum yield of formation of **81** vs **63**, $\Phi_H/\Phi_D = 1.9 \pm 0.2$.

2.4.9 Quantum Yields and pH Trends

Due to structural similarities, and to allow direct comparison with previous work, *p*-nitrophenyl acetic acid (**30**) was an obvious choice for secondary actinometer in the measurement of the quantum yields of **57-59**. In this study low conversion (< 30%) small scale preparatory photolysis with subsequent ^{1}H NMR analysis was used to measure the product quantum yields of product formation of **57** and **58** at pH 7,

Table 2.1 Comparison of Quantum Efficiencies of Reaction of Nitrobiphenyl and Nitrophenyl Systems.

Reaction Type	*p*-Nitrobiphenyl[a]	*m*-Nitrophenyl[b]	*p*-Nitrophenyl[c]
redox	0.13	0.055	< 0.01[d]
retro-Aldol	0.53[e]	0.039[e]	0.021[e]
decarboxylation	1	0.6	0.6

[a] Quantum Yields measured in this work for reaction of *p*-nitrobiphenyl derivatives **57**, **58** and **59** in the appropriate reaction type. In 1:1 H_2O-CH_3CN (pH 7) unless otherwise noted. Estimated error ± 10%.

[b] For reaction of **22**, **41**, and **29** from refs. 23 and 26.

[c] For reaction of **18**, **40** and **30** taken from refs. 23, 24 and 26.

[d] pH 14.

[e] pH 13.

and **59** at pH 13, summarized in Table 2.1. For each reaction type the quantum yield of nitrobiphenyl (**57-59**) is higher than the quantum yield of the *m*- and *p*-nitrophenyl counterparts (Table 2.1). In the case of **57** (pH 7) the quantum yield exceeds that of **18** (pH 14, does not react at pH 7) by more than an order of magnitude. Similarly the quantum efficiency of photo-retro-Aldol reaction of **59** is ten fold that of the *m*- and *p*-nitrophenyl counterparts (**41** and **40**). This highlights the overall enhanced efficiency of photoreaction of the nitrobiphenyl systems.

As already noted in the above product studies, the reaction pathway followed by alcohol **57** changes on going to acidic medium. Quantum yields for reaction vs pH were measured using small scale preparative photolyses in 1:1 H_2O-CH_3CN (Figure 2.7). While there is no effect on the quantum efficiency for formation of **64** and **71** from **57** between pH's 7 and 4, the quantum yield of reaction (to give **73**) is more than five fold higher at pH 2. Equally dramatic results were observed in the quantum yield vs pH plot for reaction of **58** (Figure 2.8). As the pH decreases from 7 to 3 the quantum efficiency for photodecarboxylation decreases in a similar manner as that observed previously for **30**.[24,26b] However, below pH 3, instead of progressively decreasing to zero, the quantum efficiency recovers to a plateau value of 0.43 at pH < 2. Note that below pH 2.8 the product is exclusively **75**. At pH 2.8 the product mixture consists of **75**, **68** and a trace of **74**.

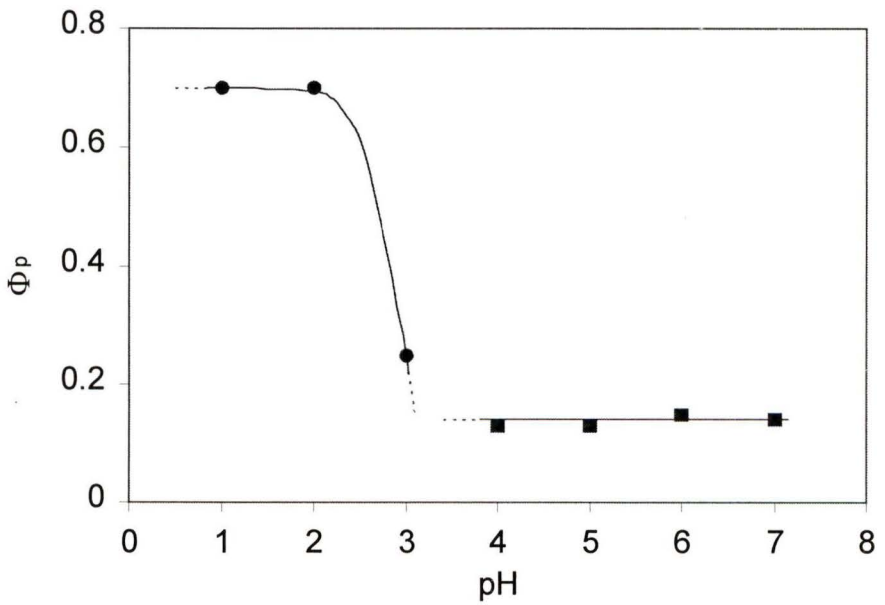

Figure 2.7 Plot of quantum yield for photoredox reaction of **57** vs pH (in 1:1 H_2O-CH_3CN, pH is of the aqueous portion). The filled circles show formation of **73**, filled squares formation of **64** and **71**.

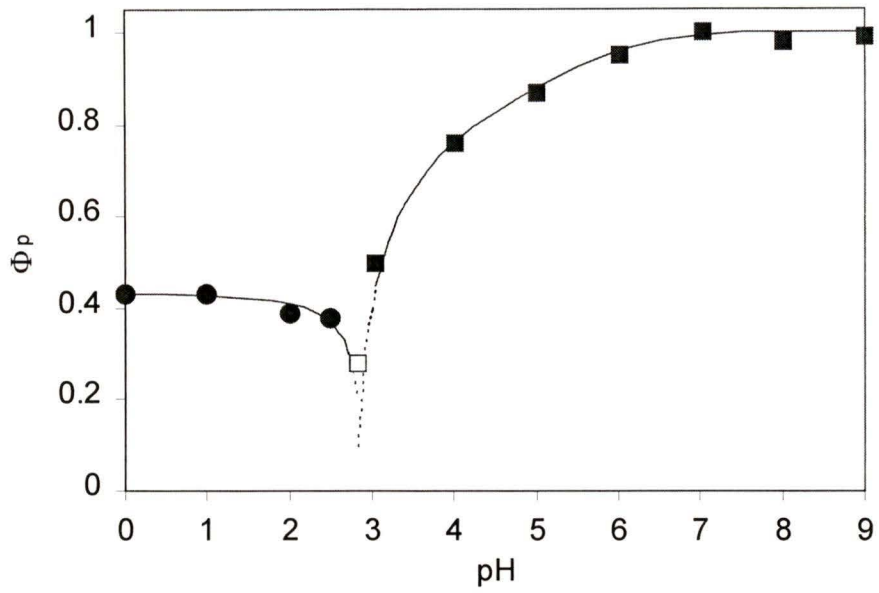

Figure 2.8 Plot of quantum yield for photodecarboxylation reaction of **58** vs pH (in 1:1 H_2O-CH_3CN, pH is of the aqueous portion). The filled circles show formation of **75**, filled squares formation of **68** and **74**. Open square represents mixture of 60% **75** and 40% **68** (and trace **74**).

2.4.10 Triplet Sensitization and Quenching

While the triplet state is responsible for many nitroaromatic photoreactions, by no means is it the exclusive reactive state.[1,2,3,4,18a] An assignment of a reactive triplet is best supported by both sensitization and quenching experiments. Triplet sensitization was carried out for **57** using sodium 2-benzoylbenzoate ($E_T \approx 69$ kcal mol^{-1}, based on the known triplet energy of benzophenone). Photolysis of **57** ($E_T \approx 60$ kcal mol^{-1})[3,4,18a] in the presence of excess sodium 2-benzoylbenzoate in 1:1 H_2O-CH_3CN ($\lambda_{ex} = 254$ nm; pH 7, argon purged) was carried out such that **57** absorbed ≈ 0.5 % of the light. This sensitized

run resulted in 41% conversion to product (**64** and **71**). The amount of product formed from direct absorption of light by the substrate was estimated by carrying out a second photolysis of **57** in absence of sensitizer in which conditions were identical except that photolysis time was shortened to reflect the amount of light **57** absorbed directly. This run gave only 3% conversion. These results indicate that the triplet state of **57** is reactive.

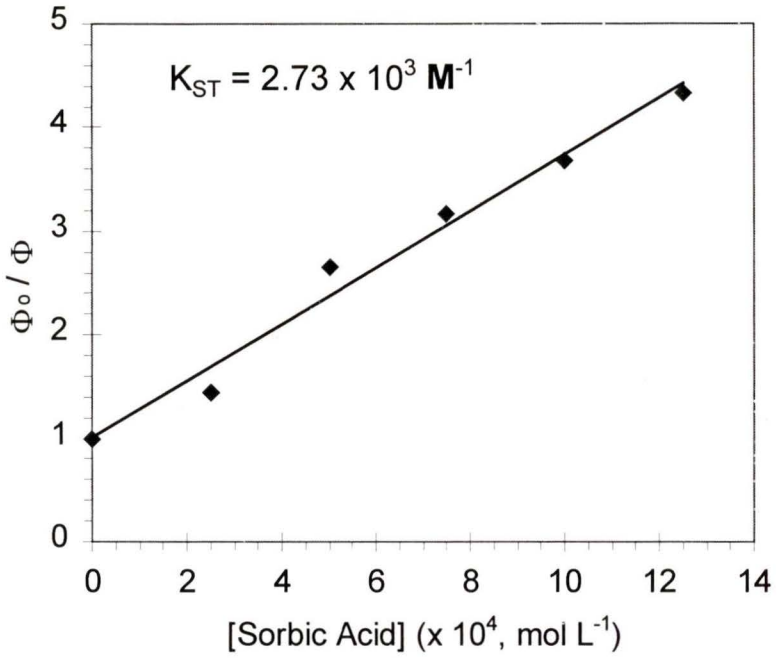

Figure 2.9 Stern-Volmer plot of the quenching of the photo-redox reaction of **57** by sorbic acid at pH 2 in 1:1 CH_3CN-H_2O.

Reactivity of the triplet state of **57** is also supported by triplet quenching experiments with sorbic acid (E_T = 57-59 kcal mol^{-1}, estimated based on piperylene).[39] Using small scale preparatory photolysis and ^1H NMR for conversion analysis, photolysis of **57** in presence of sorbic acid was carried out such that only **57** absorbed the excitation

light (λ_{ex} = 350 nm; pH 2, argon purged). Using this method a linear Stern-Volmer plot was attained with up to 75% quenching of **57** (Figure 2.9). Assuming a diffusion-controlled rate constant of 1 x 10^{10} M^{-1} s^{-1} for quenching, a lifetime of ≈ 300 ns was calculated for the reactive triplet state of **57** (at pH 2). Triplet sensitization and quenching experiments for **58** and **59** were more problematic. Compound **59** is reactive only at pH > 11. Reaction of hydroxide with the excited state sensitizers and interactions with the quencher makes such experiments more difficult to interpret. Separation of either sodium 2-benzoylbenzoate sensitizer or sodium sorbate quencher from **58** (itself a carboxylic acid) is often difficult to achieve quantitatively.

2.5 Laser Flash Photolysis (LFP) and Mechanisms of Reaction

Some prior LFP studies of transient absorption phenomena of nitrobiphenyls have been reported, especially those with both donor and acceptor groups ("push-pull" systems).[4,35,40] The triplet-triplet absorption spectrum of 4-nitrobiphenyl has been reported at 540 nm in benzene.[4] In the presence of an electron donating group such as amino (e.g., in *p*-amino-*p'*-nitrobiphenyl (**56**)), the triplet excited state becomes significantly polarized and is best characterized as a triplet charge transfer (CT) state. The absorption spectra of such triplet CT states (which are very broad and structureless) have been reported for *p*-amino-*p'*-nitrobiphenyl (**56**) and *p*-amino-*p'*-nitroterphenyl (λ_{max} = 700 and 900 nm, respectively).[40]

LFP (YAG laser, λ_{ex} = 355 nm, pulse width ≈ 20 ns, ≈ 20 mJ/pulse, 1:1 H_2O-CH_3CN) of 4-nitrobiphenyls **57**, **58**, **67** (photoinert) and **68** (photoinert) gave similar

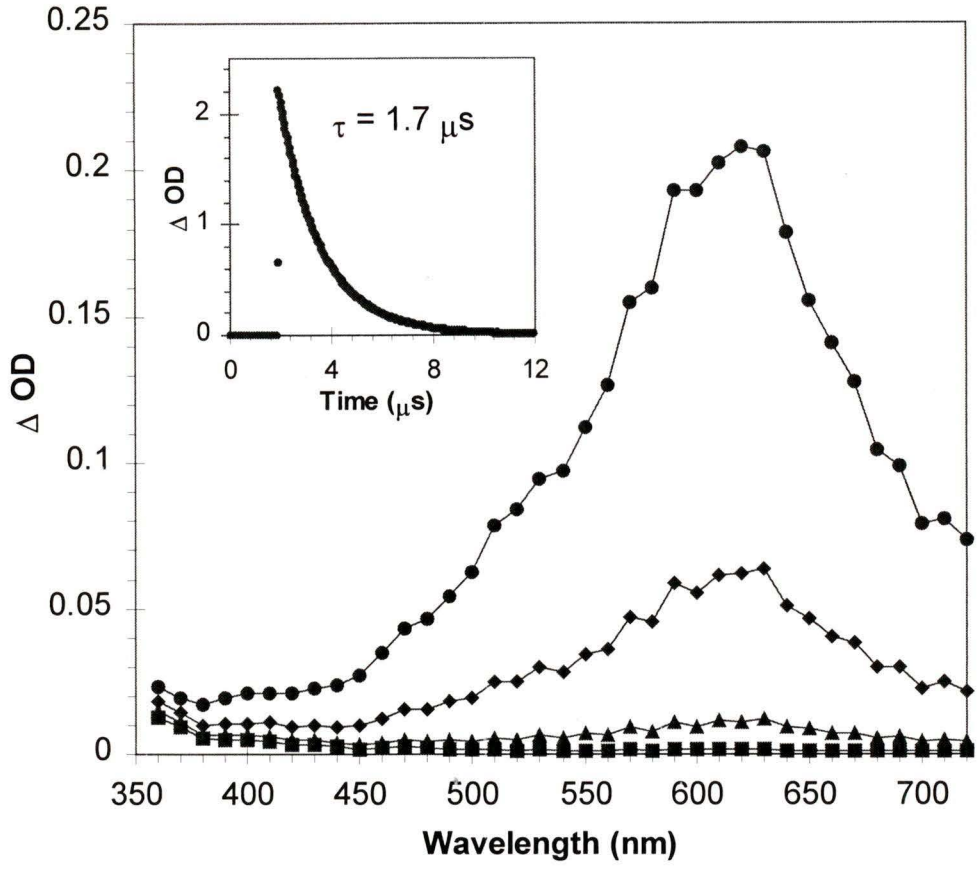

Figure 2.10 LFP traces for **67** in 1:1 CH_3CN-H_2O, pH 7, N_2 purged. Circles represent CT triplet state of **67** taken immediately after the laser pulse, diamonds and triangles represent spectra sampled during the decay to form substrate, squares represent decay back to baseline. Inset: Decay of CT triplet state of **67** ($k_{obs} \approx 5.9 \times 10^5\ s^{-1}$) at 620 nm.

strong broadly absorbing transients at 620 nm, all of which were formed within the laser pulse (Table 2.2, Figure 2.10). The lifetimes of these transients are significantly reduced in the presence of oxygen. LFP of **68** in dry CH_3CN also gave a strong broadly absorbing transient but blue-shifted to 580 nm. Water apparently is not required for formation of

Table 2.2 Summary of Observed Triplet Transients for **57**, **58**, **64**, **67**, and **68** in 1:1 H_2O-CH_3CN.[a]

Substrate	λ_{max} (nm)	N_2, τ (μs)	O_2, τ (μs)
57	620	2.2	0.24
58	620	1.1	0.33
64	540	1.3	0.27
67	620	1.7	0.24
68	620	5.2	0.22

[a] Lifetimes measured by LFP in 1:1 H_2O-CH_3CN (pH 7), N_2 or O_2 purged. All decays (monitored at λ_{max}) were first order; estimated error ± 5%.

these transients. With respect to structural similarities, all of **57**, **58**, **67** and **68** have an (electron donating) alkyl fragment as the other *para* substituent on the biphenyl ring system. As additional information useful for the assignment of the 620 nm transient, LFP of **64** (which has an electron withdrawing formyl group) gave a broadly absorbing transient at 540 nm (Table 2.2). These observations along with the above literature assignments are consistent with the 620 nm transients being assigned to a CT triplet state.

For the reactive compounds **57** and **58** and in 1:1 H_2O-CH_3CN (pH 7), in addition to the broad transient at 620 nm, additional transients were observed at 470 nm (narrow band) within the laser pulse (Figure 2.11, Table 2.3), which were quenchable by oxygen. The relative magnitude of Δ OD of these transients correlates directly with the quantum

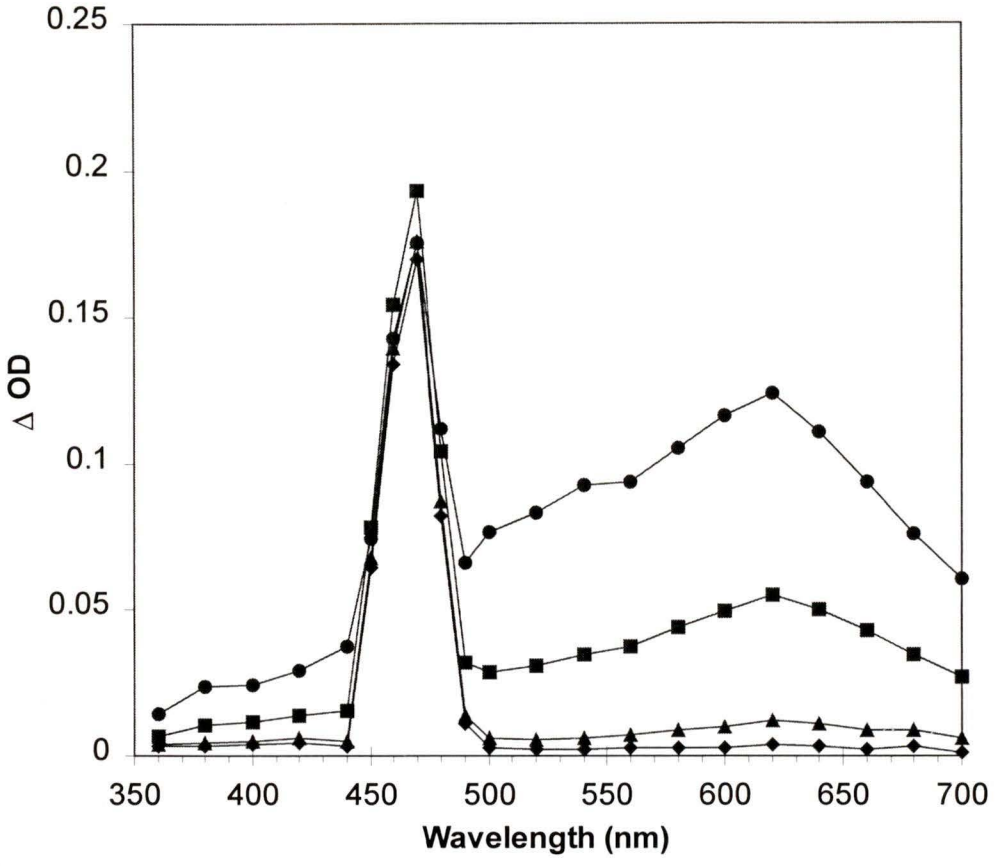

Figure 2.11 LFP traces for **58** in 1:1 CH_3CN-H_2O, pH 7, N_2 purged. Circles represent spectrum taken immediately after the laser pulse, which includes carbanion **82** at 470 nm and the CT triplet state of **58** at 620 nm. Squares and triangles represent the decay of the CT triplet state to background, represented by diamonds.

efficiencies of reaction of these substrate. That is, the signal observed for **58** ($\Phi \approx 1$) was intense (Δ OD = 0.2) while that observed for **57** ($\Phi = 0.13$) was much weaker (Δ OD = 0.02). This signal was not observed for **67** and **68** at pH 7 (conditions in which they have been found to be photoinert). As already demonstrated above, the photochemistry

displayed by **57-58** at pH 7 is very similar to that observed for the parent *p*-nitrobenzyl analogs **18** and **30** (and *m*-nitrophenyls **22** and **29**, however for sake of simplicity they are omitted from this discussion), with the added bonus of enhanced quantum efficiencies. It therefore seemed reasonable that the 470 nm transients observed for **57** and **58** could also be analogous to the previously proposed reactive intermediates for the parent compounds **18** and **30** (viz., *p*-nitrobenzyl carbanions **20** and **31**, respectively). Particularly well documented is the long-lived (in neutral water) *p*-nitrobenzyl carbanion **31** ($\tau > 10$ s; λ_{max} = 356 nm; narrow band) generated from **30** and **40**.[24,25] The decay of **31** exhibits unique kinetic behaviour: it is comprised of both first and second order components. These components have been assigned[25b] to, respectively, simple protonation from solvent water (to give **35**), and coupling of two molecules of **31**, to form a dianion which subsequently releases two electrons to starting material, to generate bibenzyl **34**. The yield of **34** provides a measure of the extent of the bimolecular decay pathway. It seems reasonable then that the 470 nm transients generated from **58** and **57** are assignable to the analogous *p*-(*p*-nitrophenyl)benzyl carbanion **82** and **83**, respectively (Schemes 2.2 and 2.3). The additional benzene ring of **82** and **83** (compared to **31** and **20**) would readily cause the required ca. 100 nm red shift. Additional supporting data came from LFP studies of **58** in 1:1 D_2O-CH_3CN (pD 7).

LFP of **58** in neutral 1:1 D_2O-CH_3CN gave the CT triplet at 620 nm and **82** (470 nm) with no observable loss in signal intensity (compared to runs in H_2O). The lifetime of the 620 nm transient was unchanged but the decay of the 470 nm transient was lengthened considerably with significant contribution of a second order component (Figure 2.12). The appearance of a second order component is consistent with the

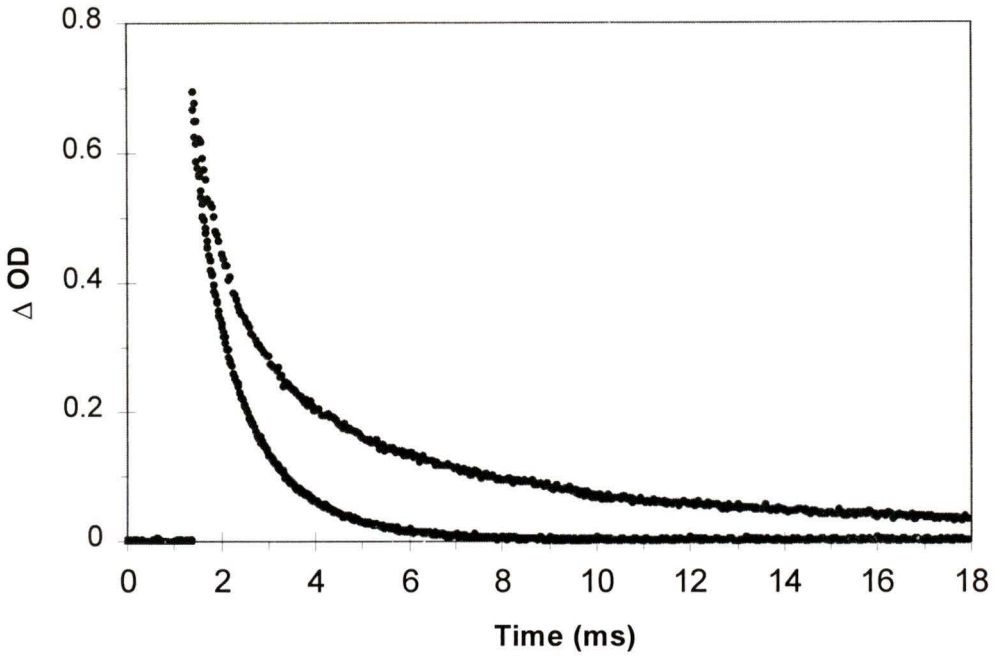

Figure 2.12 Decay traces of **82**, generated from **58** neutral 1:1 $H_2O(D_2O)$-CH_3CN (N_2 purged). Bottom trace is the decay of **82** in H_2O, which follows first order kinetics ($k_{obs} \approx 6.2 \times 10^2\ s^{-1}$). Top trace is the decay of **82** in D_2O, which cannot be fitted to a simple first order decay (but which decays to baseline).

observation (*vide supra*) of a significant increase in relative yield of **74**, which most likely arises via initial bimolecular coupling of **82** followed by loss of electrons, analogous to the mechanism of formation of **34** from **31**.[25b] The longer lifetime is also consistent with a primary kinetic solvent isotope effect for protonation of a carbanion.

It would be useful at this point of the discussion to summarize the proposed mechanisms for reaction of **57** and **58** at pHs > 4 (Schemes 2.2 and 2.3). Formation of **82** and **83** within the laser pulse suggests that the generation of these carbanions occurs from a precursor triplet state, which is supported by the sensitization experiment of **57**,

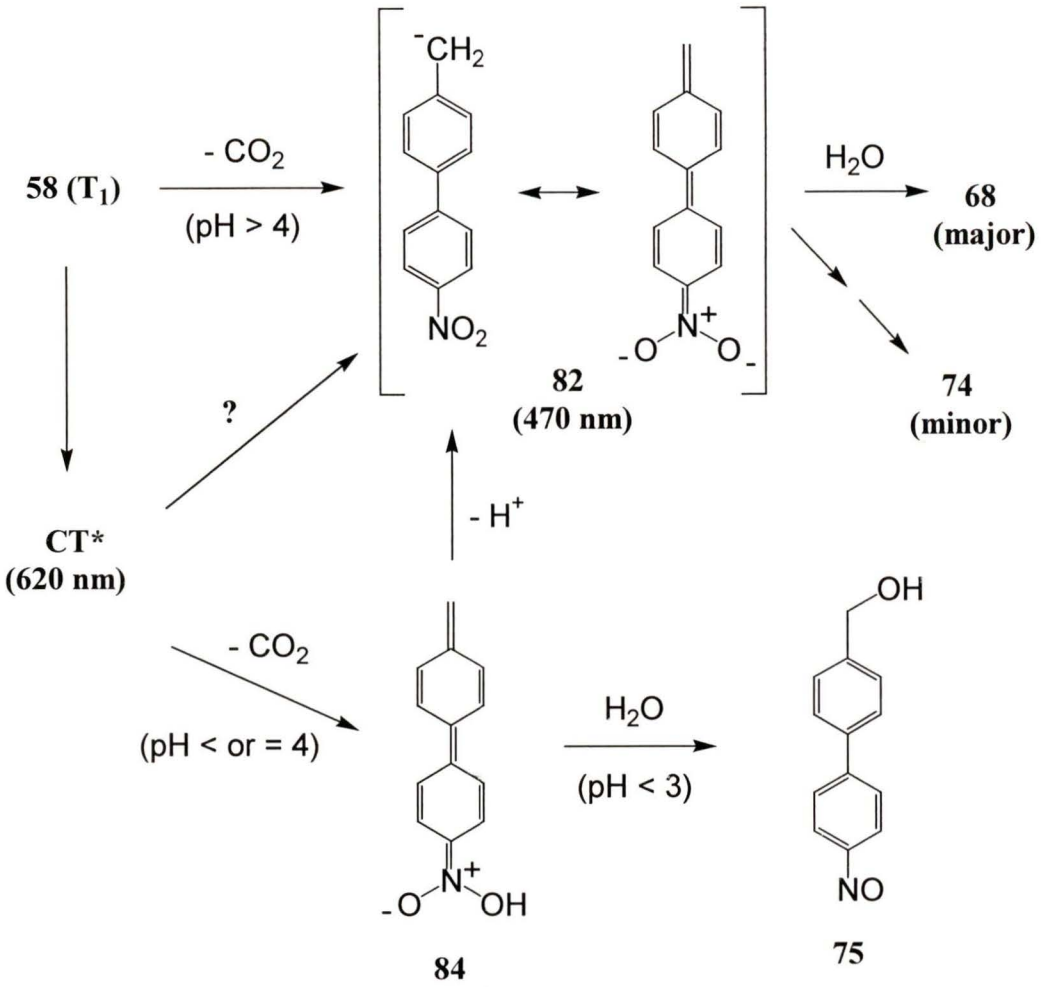

Scheme 2.2

although a reactive singlet state cannot be completely ruled out. The CT triplet state (CT*) cannot be the major precursor of **82** or **83** at pH 7 since the decay of CT* is complete within several microseconds, but results in no measurable enhancement of **82** and **83** (both of which are much longer lived). Although not studied by LFP, product studies of **59** indicate that it also forms **82** at pH 13, via a photo-retro-Aldol mechanism. Decay of **82** can occur via two pathways, both analogous to those of the parent carbanion **31**. The dominant pathway at pH 7 (or 13) is proton abstraction from water to form **68**. The minor pathway is dimerization of two molecules of **82**, with subsequent loss of

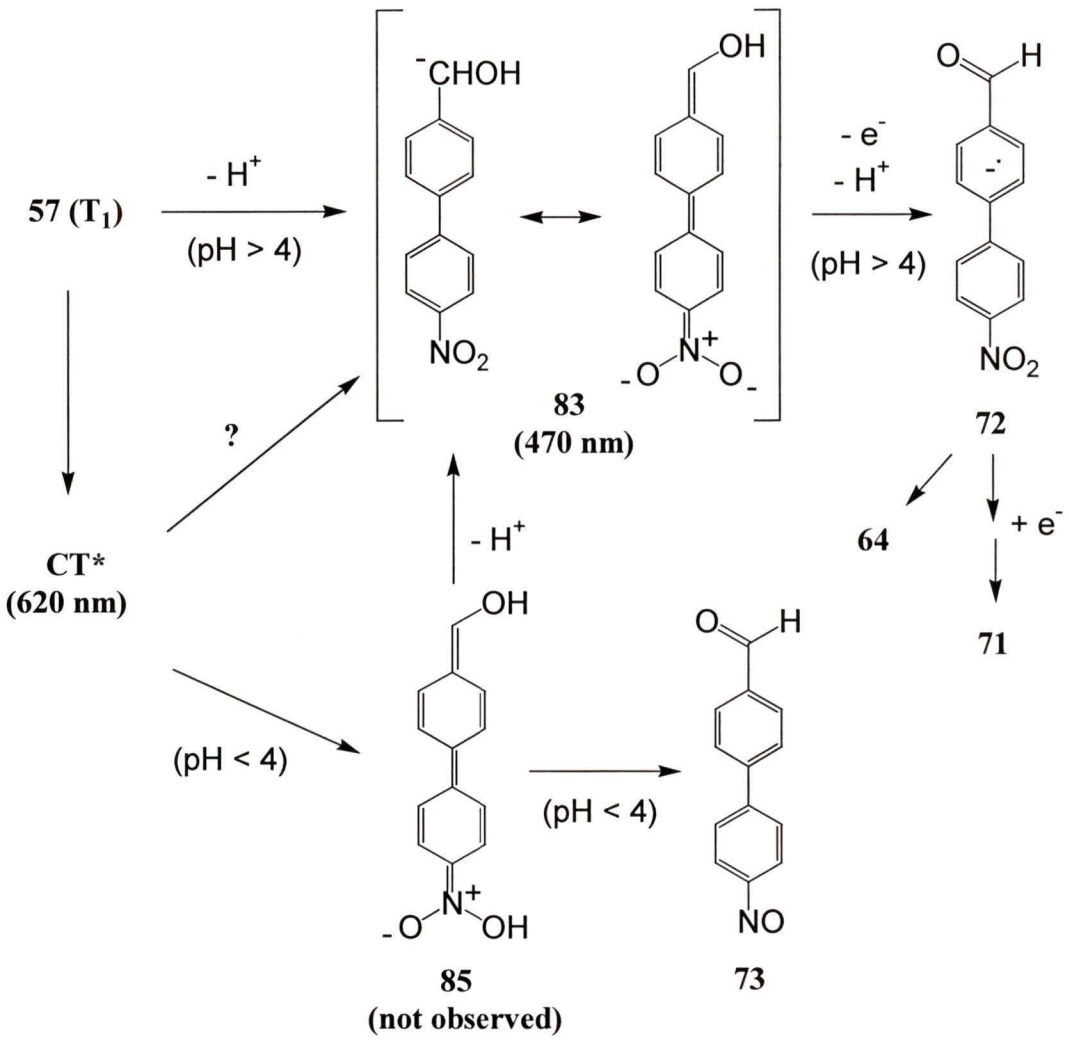

Scheme 2.3

electrons, to form **74**. This mechanism is analogous to that proposed for formation of **34**.[25b] Decay of **83** is more complex. A likely pathway for formation of **64** and **71** is deprotonation of the hydroxyl group and electron loss to generate *p*-(*p'*-nitrophenyl)benzaldehyde radical anion (**72**), which subsequently disproportionates to give the observed products. This mechanism is substantiated by the observation (*vide supra*) that reduction of **64** with photogenerated electrons indeed gives **71**. Additionally,

in the presence of oxygen, **71** was not observed upon photolysis of **57**, consistent with oxygen quenching of radical ion **72**, which would give only **64**.

LFP studies were also carried out at selected acidic pHs to probe the novel mechanisms of reaction observed in acidic solution for both **57** and **58**. LFP study of **58** was initially carried out at pH 4 (1:1 CH_3CN-H_2O)(Table 2.3). At this pH, the photochemical products are **68** and **74**, indicating that **82** should be the expected primary intermediate. This was confirmed by LFP detection of the 470 nm transient, and as expected its lifetime was shortened significantly (by a factor of 2 in comparison to its lifetime at pH 7, due to enhanced protonation by hydronium ion), further confirming its assignment as a carbanion. Surprisingly, given the observed "instantaneous" growth of **82** (formed within the laser pulse) at pH 7, it was possible to resolve the growth of the 470 nm transient from baseline at pH 4. Furthermore, the growth of **82** correlated directly with the decay of the CT triplet state at 620 nm (Table 2.3). At pH 6 approximately 50% of the signal of **82** was generated within the laser pulse and the remaining 50% of the signal growth was due to the above time resolvable growth. These observations show that at pHs 4 and 6, the CT triplet state (CT*, Scheme 2.2) reacts to generate **82**. At pH 4, it is the exclusive pathway. It is also important to note that at these acidic solutions, substrate **58** is partially, if not competely protonated (i.e., in the acid form), which is known to be unreactive with respect to photodecarboxylation, at least for the parent compound **30**. The operation of a completely new mechanism for photodecarboxylation at pH 4 is therefore not surprising. At this pH, the quantum yield for decarboxylation is actually significantly reduced compared to that at pH 7 (Figure

Table 2.3 Summary of LFP Data for Compounds **57**, **58** and **68**.[a]

Substrate	pH	λ_{max} = 620 nm CT State τ (μs)	λ_{max} = 470 nm Carbanion τ (μs)	(λ_{max} = 430) *aci*-Nitro τ (μs)
57	1.1	0.56	-	-
	2.0	1.1	-	-
	7.0	2.2	53	-
58	2.0	0.37	-	242 (0.37)[b]
	4.0	0.50	785 (0.51)[b]	-
	7.0	1.1	1600[c]	-
68	7.0	5.2	-	-
	13.0	1.3	> 1000[d] (1.1)[b]	-

[a] Lifetimes measured by LFP in 1:1 H_2O-CH_3CN (pH 7), N_2 purged. All decays were first order, estimated error ± 5%. Where there is no entry, no transient was observed. Although 59 is reactive, it was not studied by LFP in this work.

[b] Values in brackets are observed lifetimes of growth of the transient signal.

[c] Lifetime under oxygen was 280 μs.

[d] Lifetimes beyond the time scale of the pulsed lamp detection system (τ > 1 ms). Due to low Δ OD_{init} (< 0.1) values lifetimes were immeasureable without the pulser.

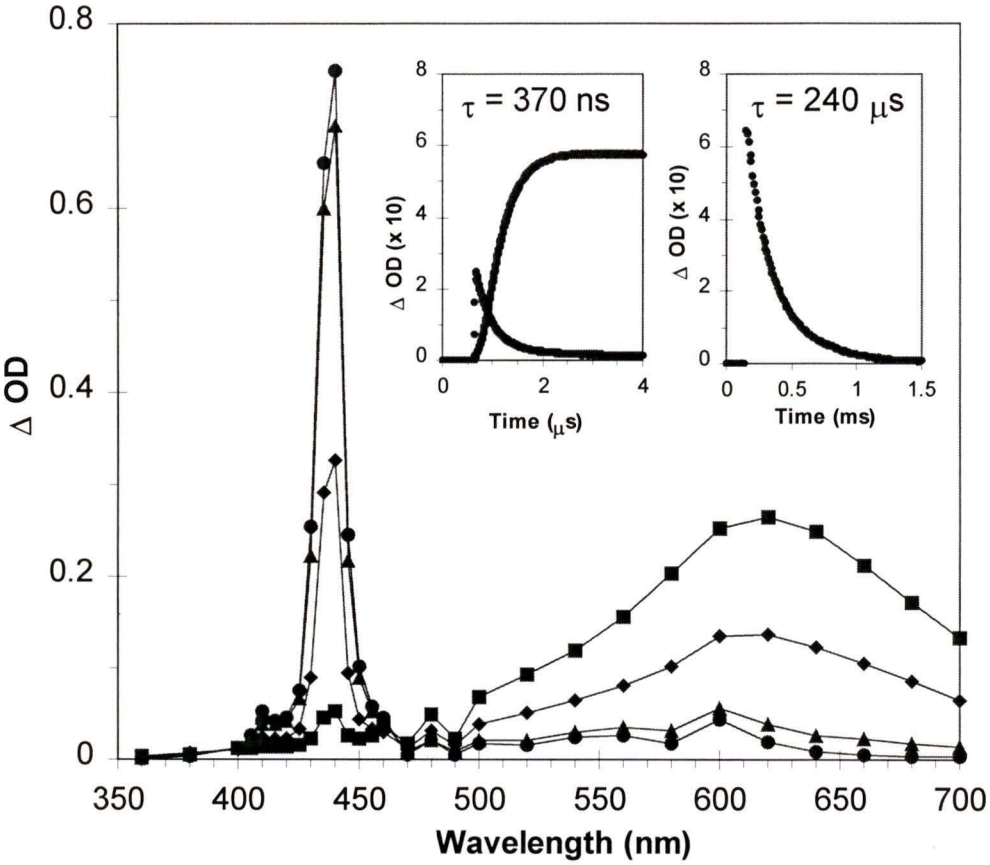

Figure 2.13 LFP traces for **58** in 1:1 CH_3CN-H_2O, pH 2, N_2 purged. Squares represent the spectrum of the CT triplet state of **58** at 620 nm, taken immediately after the laser pulse. Diamonds and triangles represent the decay of the CT triplet state to form *aci*-nitro **84** at 440 nm, which is fully represesented by the diamonds. Left inset: Decay trace represents disappearance of the CT triplet state of **58** at 620 nm, which coincides with the growth trace of *aci*-nitro **84** at 440 nm ($k_{obs} \approx 2.7 \times 10^6\ s^{-1}$). Right inset: Decay of *aci*-nitro **84** at 440 nm ($k_{obs} \approx 4.2 \times 10^3\ s^{-1}$).

2.8). A reasonable proposal for a reaction mechanism at pH 4 (Scheme 2.2) involves decarboxylation via the CT triplet state (CT*) concerted with proton transfer to one of the oxygens of the nitro group, to generate *aci*-nitro species **84**. At pH 4 and 6, this is readily deprotonated to give **82**. Alternatively the CT triplet could react directly to give **82**.

LFP of **58** at pH 2 provided confirming evidence for the formation of **84**. At this pH **75** was the exclusive product and the 470 nm transient was not observed. Instead, a transient with a sharp and strongly absorbing spectrum at 440 nm was observed (Figure 2.13, Table 2.3). The growth of this transient correlated with the decay of the CT triplet at 620 nm (CT*). The close spectral similarities of the 440 nm transient with the 470 nm absorption of **82** and that fact the product **75** must ultimately be formed strongly indicate that the 440 nm transient is due to *aci*-nitro species **84**. A 30 nm blue shift in λ_{max} has been observed on formation of the *aci*-nitro conjugate acid form of **31** in acidic solution.[25a]

LFP of **57** was studied at pHs 1 and 2 where formation of the redox product **73** occurs exclusively (Figure 2.7). At these pHs, the only observable transient was CT*, but with shorter lifetimes than at pH 7 (Table 2.3). Based on the mechanism presented in Scheme 2.3, it would seem reasonable that an analogous *aci*-nitro species **85** formed from CT* is responsible for the formation of the redox product **73**. Triplet quenching experiments of **57** by sorbic acid at pH 2 gave a linear plot with an estimate triplet lifetime of ≈ 300 ns (*vide supra*). Given that calculation of the triplet lifetime from these data involves an assumption of a diffusion controlled quenching rate and an estimation of the diffusion controlled rate constant in this solvent system, this calculated lifetime is reasonably close to the measured lifetime of CT* at pH 2 (1.1 μs, Table 2.3). This

suggests that the species quenched in the quenching experiment is the CT* state. The apparent shorter lifetime of **85** compared to **84** is consistent with a new mode of reaction available for the former, viz., overall dehydration via deprotonation of the vinyl alcohol and loss of the hydroxide from the nitrogen, to give **73** in a concerted step.

As an interesting observation it was noted during this work that LFP of **68** at pH 13 gave rise to a transient with matching absorption spectrum of **82** (Table 2.3). Growth of this transient at 470 nm was observed to occur simultaneously with decay of the 620 nm CT transient, in an analogous fashion as growth of **82** at pH 4 (from the CT of **58**). These data suggest that deprotonation of the benzylic position of **68** occurs from the CT state at pH 13. Given the highly photoreactive nature of some of the compounds in this project, this finding seems reasonable, however further evidence is required to support this finding (e.g., photolysis of **68** in D_2O, pD 13 is suggested).

2.6 Summary

In this project it has been shown that the *p*-nitrobiphenyl chromophore in suitably designed substrates is capable of inducing efficient photochemical reactions, some of which are directly analogous to those already reported for the parent nitrophenyl system. The overall enhancement of reaction efficiencies is consistent with the more polarizable biphenyl system, giving rise to more reactive polarized (or CT) triplet states. In neutral solution, the mechanisms of reaction proceed via photogenerated *p*-(*p*'-nitrophenyl)benzyl carbanions. In acidic solution, the new photochemical pathways observed are believed to proceed from the CT triplet state, to give *aci*-nitro species **84** and **85**, which are formally protonated (at oxygen) *p*-(*p*'-nitrophenyl)benzyl carbanions.

Chapter 3

Mechanisms of Photorelease of Carboxylic Acids from 1-Acyl-7-Nitroindolines in Aqueous Acetonitrile

3.1 Introduction

Photorelease compounds in general have a broad spectrum of applications. For a chemist a photorelease compound may act as a protecting group in a synthesis, which is easily removable under mild conditions in a controlled manner.[18] A biologist may use a photorelease compound as a means of introducing large concentrations of a biologically relevant molecule into a cell at will, allowing the study of the effect of that molecule.[31,41] In neurobiology there is a demand for photorelease compounds which can release specific amino acids under physiological conditions to allow kinetic studies of the effects of neurotransmitters.[31,41] For such a molecule it is desirable that it be activated by less harmful longer wavelength light (where tissue is transparent) and that the photorelease event be very fast.

As was mentioned in Chapter 1, the photorelease of carboxylic acids from 1-acyl-7-nitroindolines in aqueous conditions (pH 7) has been proven previously to be general. The release of a variety of compounds, such as L-glutamate, has been demonstrated.[31] This ability to release a broad spectrum of compounds, coupled with the apparent quick release time,[31] makes 1-acyl-7-nitroindolines an attractive release tool for biological studies. The practical application lends relevancy to the study of these molecules during the photorelease event as this time scale has not been accurately defined. Photoreactivity of 1-acyl-7-nitroindolines is also of interest due to the observed mechanistic differences

in organic solvent and in water, the origin of which is not immediately obvious. For these reasons the study reported here has been carried out.

3.2 Materials

The simple N-acetyl nitroindoline **60**, which would release acetic acid on photolysis, was chosen for this study as it contained all the required functionalities. The N-α-methoxyacetyl derivative **62** was included to further probe the mechanism, since the incipient α-methoxyacetate is a better leaving group than the parent acetate, with the intention that it would give insight to the study. It was anticipated that initial deprotonation at the 2-position is necessary for the eventual formation of **54**; thus **61** and **63** were also synthesized as additional probes into the reaction mechanism.

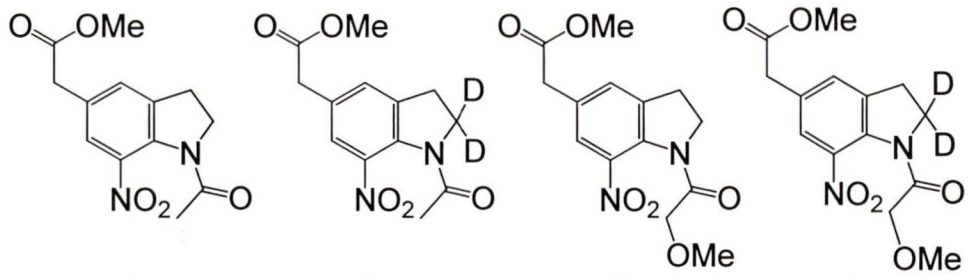

60 **61** **62** **63**

George Papageorgiou and John Corrie of the National Institute for Medical Research in London (UK), who were collaborators in this project, synthesized substrates **60** – **63** and **86**. All studies reported here were done at the University of Victoria by the author. Although previous studies of 1-acyl-7-nitroindolines have used a mixture of CH_2Cl_2-dioxane as the primary organic solvent system, in this study CH_3CN was used due to its superior spectroscopic properties and general lack of photochemical reactivity.

3.3 UV-Vis Studies

While previous studies were done on similar 1-acyl-7-nitroindolines (for example: **53**, R = $(CH_2)_3CO_2^-$, $(CH_2)_4PO_3^{2-}$, $(CH_2)_2CH(NH_3^+)CO_2^-$)[31] verification of analogous photochemistry for **60-63** was done initially by UV-Vis in quartz UV cuvettes. As shown in Figure 3.1, photolysis of 10^{-4} **M** solution of **60** (λ_{ex} = 350 nm, Rayonet photochemical reactor) in 100% water (pH $\approx$ 7) resulted in a smooth transformation to a product with λ_{max} = 413 nm, consistent with formation of **54**, by comparison with its authentic spectrum.[31] Photolysis in 99% CH_3CN-1% H_2O gave a final trace with λ_{max} = 434 nm (Figure 3.1), consistent with formation of **86**.[31] These results show that the reaction pathway followed by **60** is solvent dependent, as was observed for **53**. Photolysis of an authentic sample of **86** in 100% water for extended periods (up to 40 min) of time did not result in any spectral changes, demonstrating that N-substitution is required for photochemistry. Parallel UV-Vis studies with **61-63** gave similar results, except that **62** and **63** gave a mixture containing *both* **54** and **86** in 99% CH_3CN-1% H_2O. With respect to an isotope effect on relative quantum yields in 99% CH_3CN-1% H_2O, **60** and **61** reacted with equal efficiency (to give exclusively **86**). It was not possible to accurately determine (by UV-Vis) the relative reactivity of **62** vs. **63** in this solvent system. With respect to an isotope effect on relative quantum yields in 100% water, **60** reacted 30% more efficiently than **61**, whereas **62** and **63** showed similar reactivity.

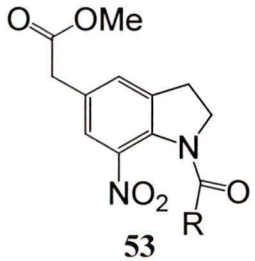

53

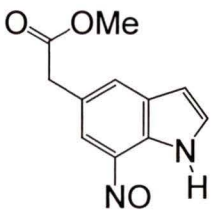

54

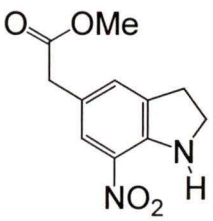

86

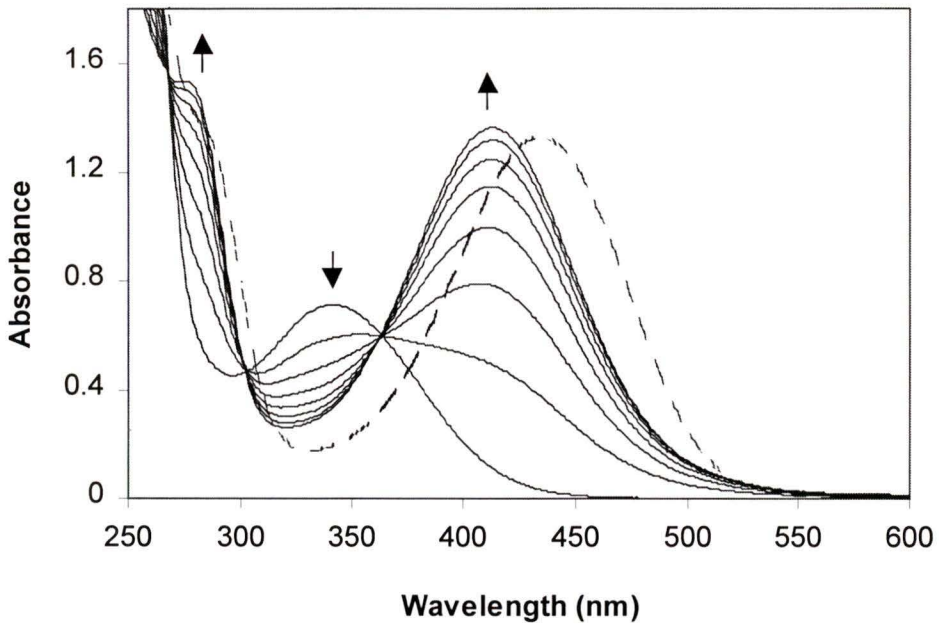

Figure 3.1 UV-Vis traces for the conversion of **60** to **54** on photolysis at 350 nm in 100% H_2O (solid traces, estimated 100% conversion). Each trace represents 8 min irradiation time. Exhaustive photolysis in 99% CH_3CN-1% H_2O gave a product with λ_{max} = 434 nm (**86**, dashed trace).

Relative efficiencies for reaction in 100% H_2O vs. 100% D_2O for **60** and **62** were measured by the above UV-Vis method. The reaction was about 10 ± 2% more efficient in D_2O for **60** (an *inverse* solvent isotope effect) whereas **62** showed no measurable solvent isotope effect on reaction efficiency. The possible implications of these results with respect to the mechanistic differences in the photochemistry of **60** and **62** in 100% water are discussed in Section 3.8.

3.4 Preparative Photolysis

Preparatory photolyses were carried out to prove structures of products and to confirm some of the relative reactivity results obtained by UV-Vis spectrophotometry above. Photolysis of **60** in 100% water ($\approx 10^{-3}$ **M**, Rayonet photochemical reactor, 300 nm lamps, 100 mL quartz vessels, argon purged continuously, $\approx 15^{o}$C, 1 to 20 min) yielded **54** (as identified by ^{1}H NMR) cleanly, even at > 95% conversion. The reaction efficiency was not noticeably affected by purging with oxygen (reduction in conversion by < 10%). Photolysis of **60** in 99% CH_3CN-1% H_2O gave **86** exclusively. Photolysis of **62** in 100% water also gave **54** exclusively but photolysis in 99% CH_3CN-1% H_2O gave both **54** and **86** in a 30% to 70% ratio, along with some unidentified products comprising about 30% of the product mixture. Formation of acetic acid from **60** was confirmed in photolyses run in NMR tubes (in 1:1 CD_3CN-D_2O), by matching the suspected acetic acid methyl peak in the spectrum with addition of small aliquots of authentic acetic acid.

The effect of water content (in CH_3CN) on the relative yields of **54** and **86** for both **60** and **62** was investigated. To avoid work-up, photolyses were carried out in NMR tubes ($\approx 10^{-2}$ **M**, CD_3CN-D_2O, < 20 ^{o}C by external cooling, 10-60 min) in solutions of < 80% (v/v) water content. Above 70% water content solubility problems necessitated the use of small scale preparatory photolyses. The results are shown in Figure 3.2 (plotted vs mole % water). In water-CH_3CN solutions of intermediate water content photolysis of **60** yielded both products **54** and **86**. The relative yields for these products give an apparent linear plot with respect to the mole fraction of water, indicative of the gradual nature in the change over from one mechanism to another. The relative yields of **54** and **86** from **62**

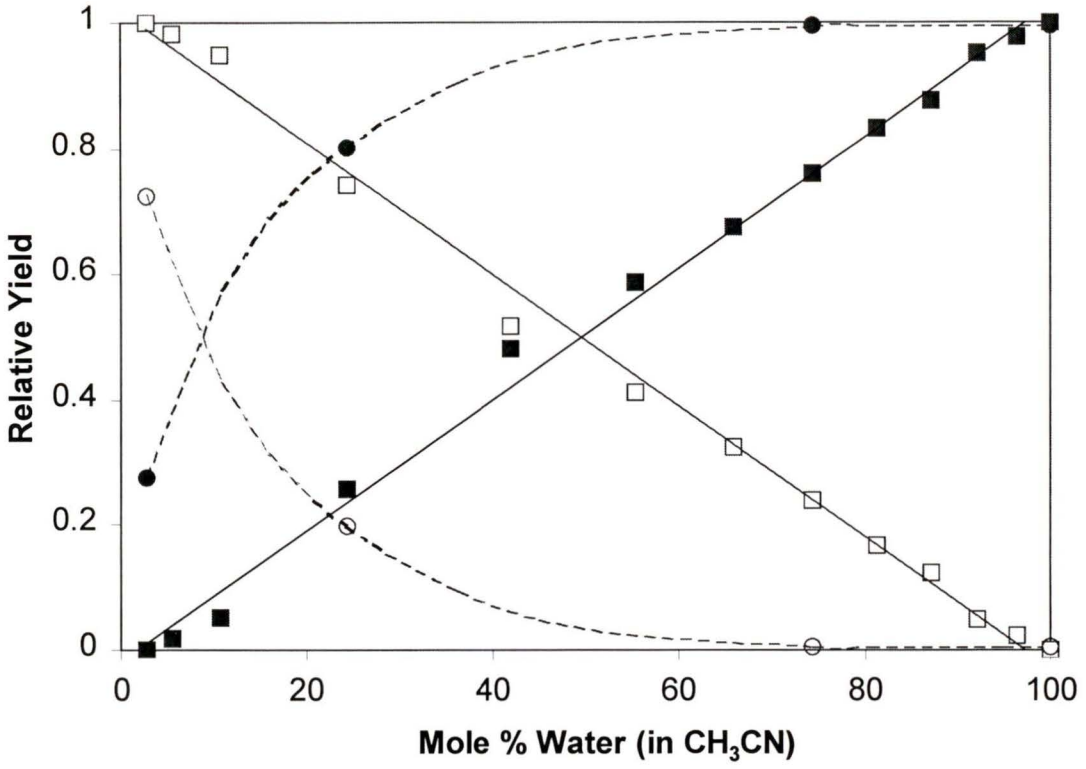

Figure 3.2 Plot of relative yields of photoproducts **54** and **86** from photolysis of **60** and **62** as a function of water content (in CH_3CN). Squares and circles denote products formed from photolysis of **60** and **62** respectively. Solid markers represent **54** and open markers represent **86**.

are more sensitive to the water content (apparent "exponential" behaviour), with formation of **54** dominating in most regions of the plot. This is presumably attributable to the better leaving group in α-methoxyacetate in **62** which is the required "leaving group" in order to form **54** (*vide infra*). The plot is consistent with the interpretation that the two products **54** and **86** arise via competing reactions from a common intermediate,

versus an interpretation in which there are two independent competing mechanisms from the excited state with opposite solvent effects that are fortuitously complementary.

Any mechanism explaining the formation of **54** (with its indole ring system) must necessarily include a step generating the new π–bond between carbons 2 and 3 in the indoline precursors **60-63**. An obvious route to the indole ring is via tautomerization of the 3*H*-indole **87** (Equation 40). Tautomerization of the parent 3*H*-indole (**88**) to 1*H*-indole (**89**) (Equation 41) has been studied by Gut and Wirz.[42] They reported that the dark tautomerization of photochemically generated **88** to **89** is acid and base catalyzed (general and specific).[42] Quick photolysis (30 s, Rayonet photochemical reactor, λ_{ex} = 254 nm) of **60** in pH 6 phosphate buffered solution (100% water) followed by immediate transfer of the photolyzed UV cuvette into a UV-Vis spectrophotometer allowed for the observation of a shift in the initially observed absorption spectrum, analogous to the observations made by Gut and Wirz[42] for the isomerization of **88**. The observed shift (pseudo first order, rate independent of wavelength) of the spectrum is to longer wavelength (Figure 3.3), which is consistent with extension of the π-network on going

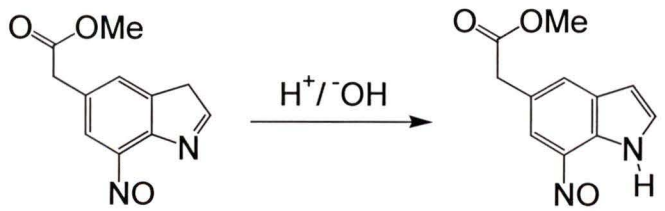

87 **54** (40)

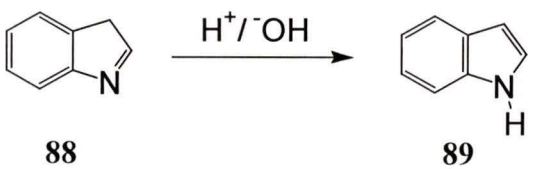

88 **89** (41)

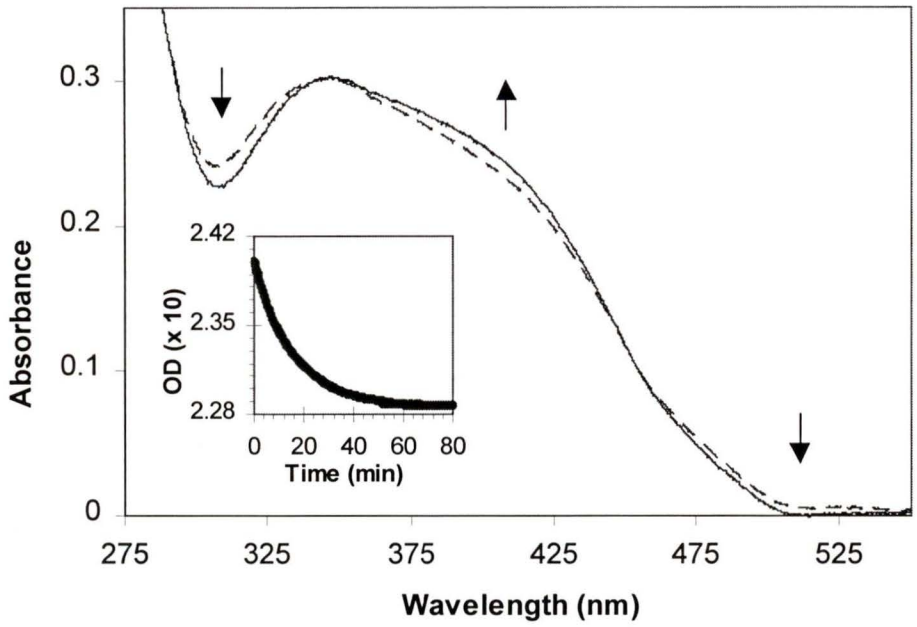

Figure 3.3 UV-Vis traces of tautomerization of photogenerated **87** to **54** at pH 6. Dashed line is the spectrum observed about 5 s after photolysis of **60**. Solid line is the spectrum observed after 90 min. Note that conversion < 30% and therefore, the absorption spectrum is dominated by that of starting material **60**. Inset shows decay of **87** to form **54** ($k_{obs} \approx 7.8 \times 10^{-2}$ min^{-1}) at 307 nm.

from **87** to **54**. A similar observation was made in the previously observed tautomerization of the parent indole system (Equation 41).[42] Note that in these experiments, the conversions were < 30% and therefore, the absorption spectrum is dominated by that of starting material **60**. Increasing the buffer concentration as well as increasing the pH from 6 to 7, or decreasing the pH to 5 resulted in faster rates of tautomerization. This indicates both general acid and base catalysis of reaction. The observed rates for tautomerization of **87** are significantly slower ($\tau_{1/2}$ = 13 min at pH 6)

than those reported for the parent system **88** ($\tau_{1/2} < 1$ s). This is consistent with the presence of a strongly electron withdrawing *ortho* nitroso group in **87** which would make protonation of the imino nitrogen less favourable in the acid catalyzed mechanism (which was observed to be the dominant pathway in the parent indole).[42] Since it has now been demonstrated that **87** is indeed photochemically generated from **60** which subsequently leads to **54**, the mechanistic problem is now reduced to deducing a pathway from **60** to **87**, which occurs on a much faster time scale.

3.5 Triplet Sensitization

Triplet sensitization experiments were carried out to determine whether the triplet state of **60** is reactive. Preparatory photolysis of **60** ($E_T \leq 60$ kcal mol^{-1})[4,18] in the presence of excess 2-benzoylbenzoate ($E_T \approx 69$ kcal mol^{-1}, based on the known triplet energy of benzophenone) in 1:1 H_2O-CH_3CN ($\lambda_{ex} = 300$ nm; pH 7, argon purged) was carried out such that **60** absorbed < 4% of the light. The sensitized run gave 81% conversion to **54** and **86** (with an identical ratio as that observed on direct photolysis) whereas **60** gave 9% conversion when exposed to an equivalent amount of light in the absence of the triplet sensitizer (under otherwise identical conditions). These data indicate that the triplet state of **60** is reactive, to form **54** and **86**. Although triplet quenching experiments would be required to definitively prove that the triplet state is wholly responsible for reaction, these experiments are problematic for **60** since LFP studies (*vide infra*) indicate that the triplet state (if formed) has a lifetime of < 20 ns. Such short-lived triplets would require the use of high concentrations of triplet quenchers which is problematic for these studies in aqueous solution.

3.6 Quantum Yields

The quantum yield for formation of **54** from **53** (R = $(CH_2)_2CH(NH_3^+)CO_2^-$) in water has been previously reported to be 0.043.[31] In this study low conversion (< 10%) small scale preparatory photolysis (λ_{ex} = 300 nm, Ar purged, 5 min) was used to measure the product quantum yield for formation of **54** from **60**. *p*-Nitrophenylacetic acid (**30**) was used as a secondary actinometer. Using this method the quantum yield for formation of **54** from **60** was determined to be 0.06 ± 0.01 in 100% water. The quantum yield for reaction of **86** in 99% CH_3CN-1% H_2O was determined to be about twice that in 100% water, which is similar to observations made for the photoreactivity of **53** (R = $(CH_2)_3CO_2H$) in 100% water vs CH_2Cl_2-dioxane-H_2O (2:3:0.05).[31] The quantum yield of total product formation (**54** and **86**) was observed to decrease gradually as the water content was increased from 1% to 100% H_2O (in CH_3CN).

Relative quantum yields were measured using small scale preparatory photolysis for **60** vs **61** and **62** vs **63** in 100% water, to probe the effect of dideutero substitution at the 2-position, which gave Φ_H/Φ_D = 1.30 ± 0.05 and 1.10 ± 0.10, respectively, consistent with the observations made using UV-Vis spectrometry (*vide supra*). This suggests that proton abstraction is involved in the product determining step for the formation of **54** from **60** and **61**, but not from **62** and **63**. In 99% CH_3CN-1% H_2O the relative quantum yields of production of **86** from **60** and **61** were identical, consistent with the lack of involvement of the protons/deuterons at the 2-position.

3.7 Laser Flash Photolysis (LFP)

Nanosecond LFP studies provided additional valuable information as to the mechanistic details of photorelease from **60** and **62**. LFP of **60** in 99% CH_3CN-1% H_2O allowed for the observation of an initially formed transient (within the laser pulse) at $\lambda_{max} \approx 420$ nm (Figure 3.4). This transient was observed to undergo a first order decay over several microseconds ($k_{obs} \approx 1.4 \times 10^5\ s^{-1}$) to a species ($\Delta OD \approx 0.01$, $\lambda_{max} \approx 420$ nm) that does not decay within the time frame of the detection system (> 3 ms), but was shown to transform to a spectrum identical to product **86** ($\lambda_{max} = 434$ nm) over timescales of > 10 ms (by standard UV-Vis spectrophotometry). LFP of **86** did not generate any observable transients, which shows that the formation of the above transient requires N-substitution. This suggests that the transients observed are assignable to species in which the acetyl group (of **60**) has already been transferred (to give **90**) since it is unlikely that the transfer of the acetyl group itself would have been resolvable within the timescale of our nanosecond laser system.[2,43] Recent LFP studies by Schwörer and Wirz[2] have shown that the lifetime of *aci*-nitro anion **91** is pH dependent, with very long lifetimes ($\tau \approx 1$ s) in neutral water. Although **92** would be expected to be more reactive than **91**, it is anticipated that any reasonable increase in its reactivity would still not allow observation

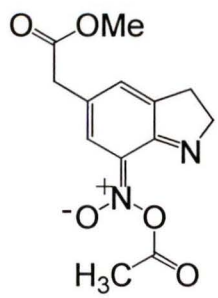

90

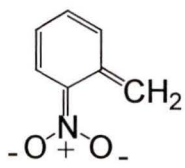

91

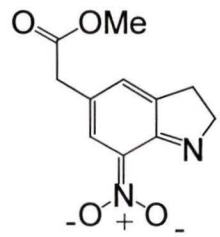

92

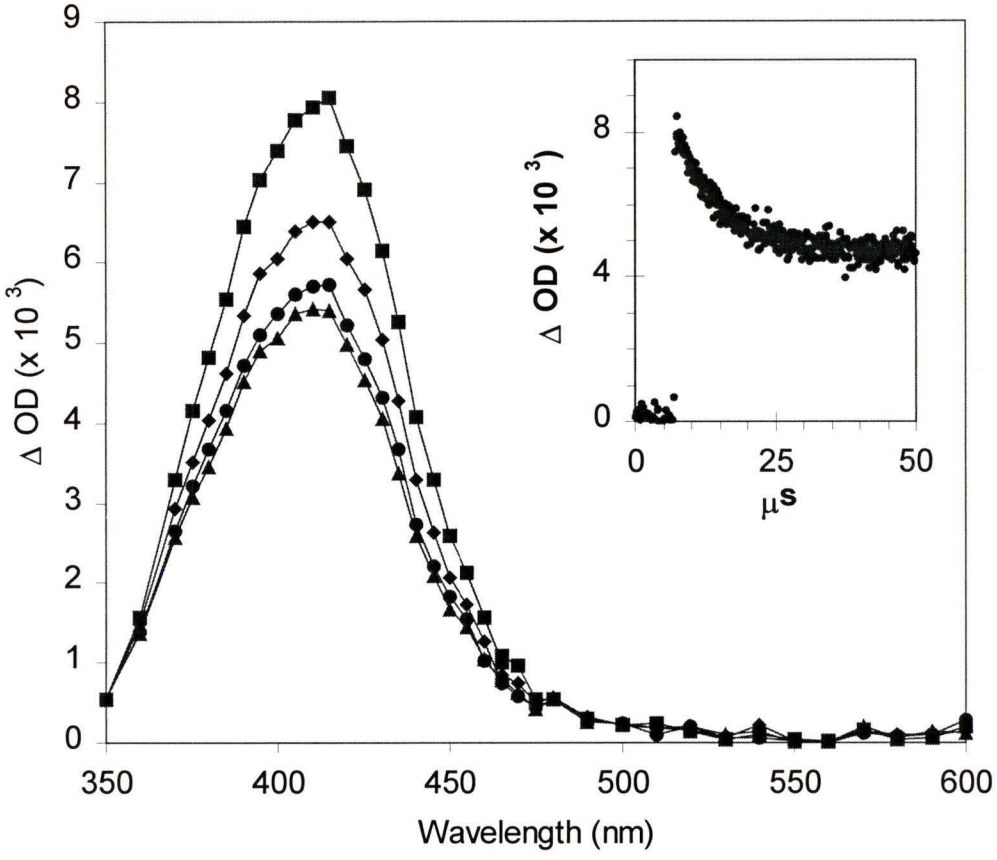

Figure 3.4 LFP traces for **60** in 99% CH_3CN-1% H_2O. Squares represent spectrum of **90** taken immediately after the laser pulse, diamonds and circles represent spectra sampled during the decay to form **92**, represented by the triangles. Inset: Decay of **90** to form **92** ($k_{obs} \approx 1.4 \times 10^5\ s^{-1}$) at 410 nm.

of its decay with the present LFP system ($\tau > 3$ ms). Therefore, the long-lived transient at 420 nm is assigned to **92**. Its precursor, also absorbing at 420 nm ($k_{obs} \approx 1.4 \times 10^5\ s^{-1}$) is assigned to **90**.

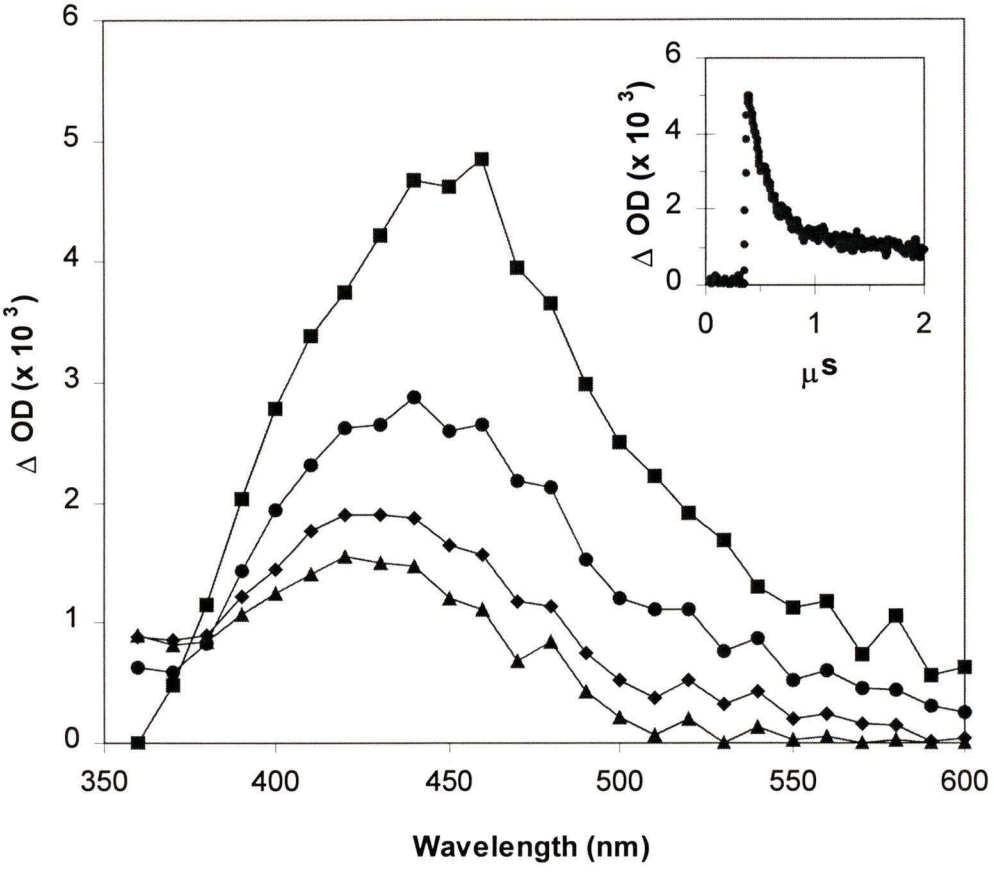

Figure 3.5 LFP traces for **60** in 100% water. Squares represent spectrum of **90** taken immediately after the laser pulse, circles and diamonds represent spectra sampled during the decay to form **87**, represented by the triangles. Inset: Decay trace of **90** to form **87** ($k_{obs} \approx 5 \times 10^6\ s^{-1}$) at 450 nm.

LFP of **60** and **62** was more extensively studied in 100% water since understanding the dynamics of the release in this solvent is relevant for potential biological applications. LFP of **60** gave a broadly absorbing transient with $\lambda_{max} \approx 450$ nm within the pulse (Figure 3.5). The observed first order decay of this transient ($k_{obs} \approx 5 \times 10^6\ s^{-1}$) was found to have a small (normal) deuterium isotope effect for decay (measured by LFP of **61**), to

give $k_H/k_D = 1.2 \pm 0.1$, demonstrating that abstraction of a proton (or deuteron) from position 2 (of **60** and **61**) is involved in the decay of this transient. This is consistent with the observed relative quantum yields of **60** and **61** (*vide supra*) which suggest that proton abstraction is involved in the product determining step. Release of acetate is likely to be in the product determining step due to its irreversibility. Hence it is proposed that deprotonation at the 2-position and acetate release are likely concerted. Therefore, the initially observed transient at 450 nm is assigned to **90** which decays by formation of acetic acid, giving isoindole **87** (Equation 42). Note that the λ_{max} of **90** is red shifted by 30 nm relative to the assigned spectrum in 99% CH_3CN-1% H_2O, which is entirely consistent with the change in solvent polarity. The resulting spectrum ($\lambda_{max} \approx 420$ nm) did not exhibit any changes within the longest time scale available (≈ 3 ms), consistent with it being the isoindole **87**, which was observed to tautomerize to **54** over the course of minutes (*vide supra*). These results suggest that the release of acetic acids from these 1-acyl-7-nitroindolines is on the order of 10^{-6} s in water.

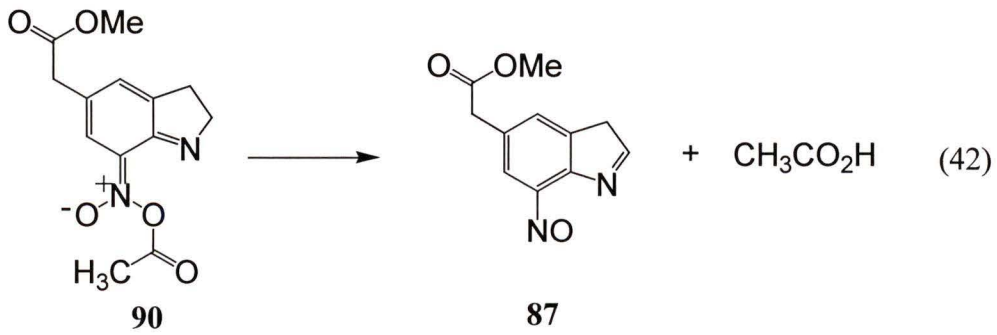

(42)

To further substantiate the above LFP assignments, compound **62** with its better leaving group in α-methoxyacetate was studied. LFP of **62** in water gave a broadly absorbing transient at 450 nm similar to that observed for **60** (Figure 3.6). However, its

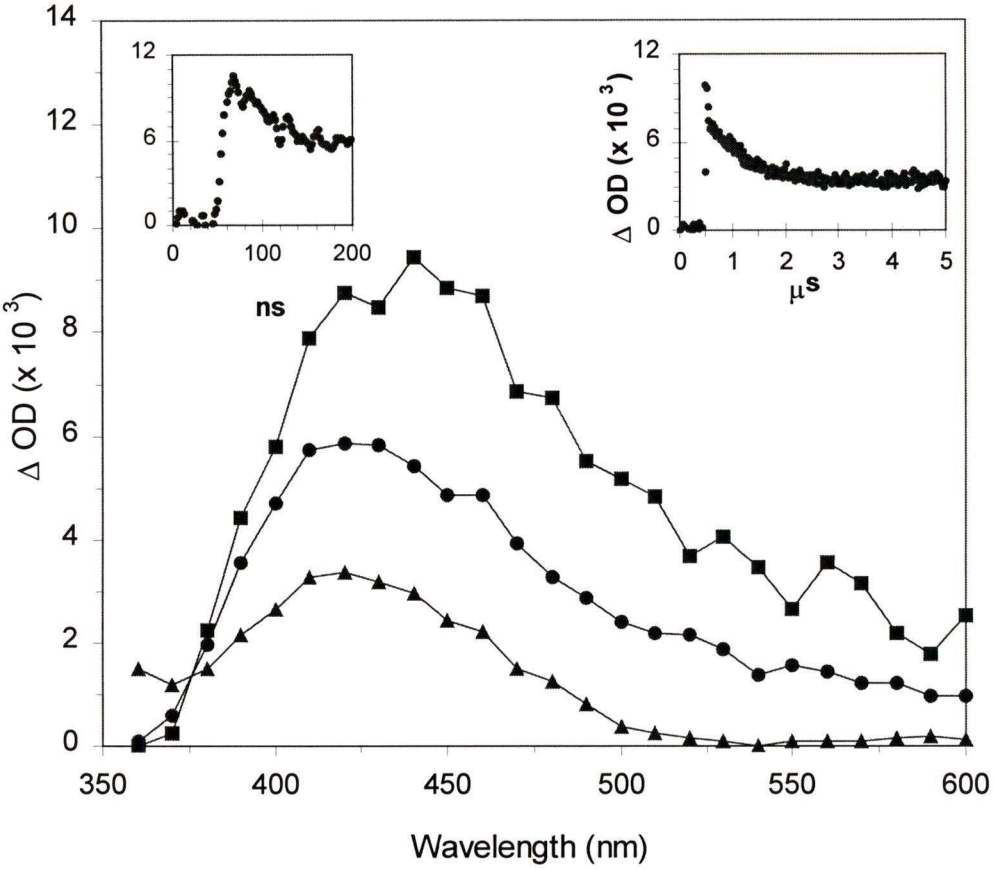

Figure 3.6 LFP traces for **62** in 100% water. Squares represent spectrum of **93** taken immediately after the laser pulse, which releases α-methoxyacetate to generate the observed **94,** represented by circles, which on deprotonation gives **87** (represented by triangles). Left inset: initial decay of **93** to **94** ($k_{obs} \approx 2 \times 10^7\ s^{-1}$) at 450 nm. Right inset: slower decay of **94** to **87** ($k_{obs} \approx 1.5 \times 10^6\ s^{-1}$) at 420 nm.

decay was found to be biphasic. The initial first order decay ($k_{obs} \approx 2 \times 10^7\ s^{-1}$) gave another broadly absorbing transient at 425 nm, which subsequently undergoes another first order decay ($k_{obs} \approx 1.5 \times 10^6\ s^{-1}$) to a spectrum with λ_{max} = 420 nm essentially identical to that assigned to **87** above. The initially formed 450 nm transient is assigned

to **93** based on similar arguments used for assigning **90** (Equation 43). LFP of **63** provided key kinetic data that allowed us to assign the 425 nm transient. For example, the initial 450 nm transient observed for both **62** and **63** showed no observable differences in decay rate, consistent with lack of deprotonation at the 2-position in this step (contrary to what was observed for **60** and **61**). On the other hand, use of **63** resulted in a slower decay (compared to that observed from **62**) of the 425 nm transient, resulting in a normal isotope effect for the rates of decay, $k_H/k_D = 1.2 \pm 0.05$. These observations are consistent with a reaction mechanism in which the first step of reaction from **93** is unimolecular departure of α-methoxyacetate, to generate an arylnitrenium ion intermediate **94** (assigned as the 425 nm transient), which subsequently decays via deprotonation to give **87** (and hence observation of the small normal isotope effect). Several such nitrenium ions have been generated in this fragmentation manner, and have been observed to have similar lifetimes.[44]

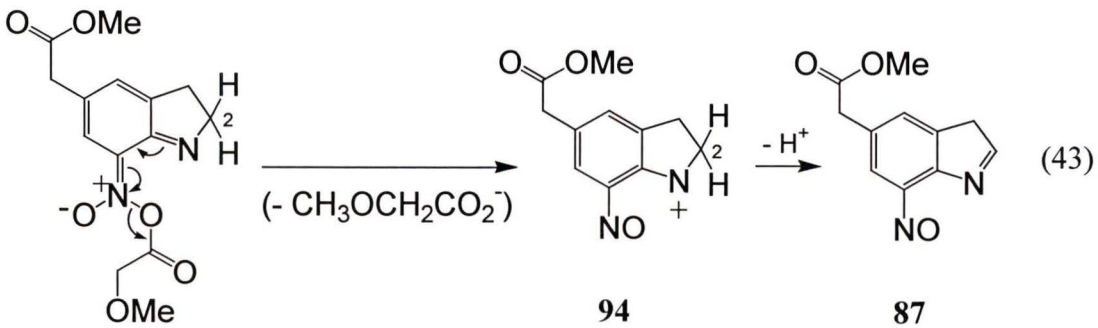

93 **94** **87** (43)

3.8 Mechanisms of Reaction

This study has shown that the pathway of reaction resulting in the release of protected carboxylic acids from 1-acyl-7-nitroindolines is sensitive to the water content in the solvent as well as the leaving group ability in the carboxylate, making it a rich system for mechanistic studies. This is unlike the photochemical behaviour of *o*-nitrobenzyl systems, discussed in Chapter 1, that have been used extensively in photodeprotection applications. The mechanistic fate of the nitroindoline moiety of **60** and **62** depends on the water content of the solvent (see Scheme 3.1 for the proposed mechanism for **60**). In CH_3CN-H_2O solutions of high water content, the main pathway is an overall intramolecular redox reaction, to give nitrosoindole **54**. In wet CH_3CN (99% CH_3CN-1% H_2O), the main pathway is an overall simple hydrolysis of the amide giving nitroindoline **86**. Both mechanisms are operative in solutions covering a wide range of water content suggesting that there is a common intermediate. The initially observed transient in LFP experiments in 99% CH_3CN-1% H_2O and in 100% water (420 and 450 nm, respectively) appear to be the same species (assigned to **90** or **93**) except for the expected solvent-induced shift in its λ_{max} in water. Based on this assignment, the rate of release of acetate from photoexcited **60** is 5×10^6 s^{-1}. This corresponds to a time scale of 200 ns for the release of the protected acetate, which is the fastest reported to date for these types of compounds.

Quantum yields of reaction for **60** were two fold higher in 99% CH_3CN-1% H_2O ($\Phi = 0.12$) compared to that in 100% water ($\Phi = 0.06$). The initially observed ODs at λ_{max} in these two solvent systems in LFP experiments also differ by a factor of two (in favor of the run in 99% CH_3CN-1% H_2O). This lends support for the above assignment

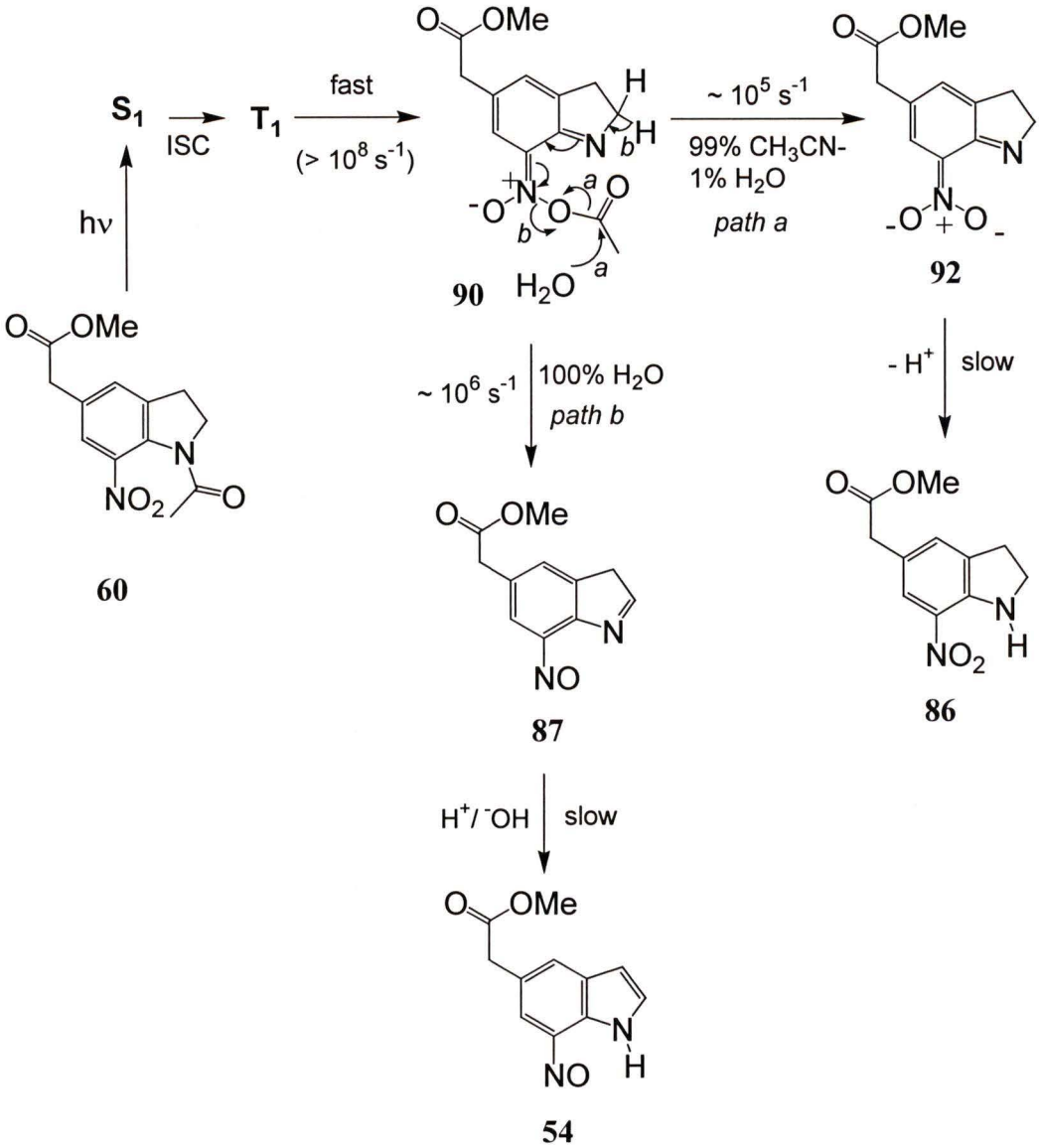

Scheme 3.1

in which the initially observed transients in both 99% CH_3CN-1% H_2O and in 100% water are due to the same species, assigned as **90**. Therefore, a reasonable explanation for the lower quantum yield in 100% water is due to the lower efficiency in which the acetyl group (of **60**) is transferred to the nitro group, resulting in reduced yield of **90**. Increased hydrogen bonding from water to the amide oxygen and nitro group of **60** with

increasing water content would be expected to retard the transfer of the acetyl group. Once transferred, there are two pathways for reaction of this *aci*-nitroester **90**, viz., via the standard nucleophilic attack of water at the ester carbonyl followed by elimination of the aci-nitro species **92** (which protonates to give nitroindoline **86**) or an S_N1-type reaction involving cleavage of the N-O bond with deprotonation at the 2-position (to give **87**). The deprotonation at the 2-position is believed to be in concert with loss of acetate for **60** but step-wise for **62** (via the arylnitrenium ion **94**). S_N1-type reactions are favored in solvents of high ionizing power and hence the higher contribution of this pathway in CH_3CN-H_2O solutions of higher water content, as observed in Figure 3.2. Quantum yields for reaction of **60** (to form **54**) were 10% higher in runs carried out in 100% D_2O vs 100% H_2O (*vide supra*). If this difference is attributed to a kinetic solvent isotope effect for the reaction of **90**, then it would imply that the departure of the acetate is specific acid catalyzed, as D_3O^+ in D_2O is a stronger acid than H_3O^+ in H_2O. The details of this and other steps of the overall reaction remain topics for further studies.

Chapter 4

Experimental

4.1 General Procedures and Instrumentation

^{1}H NMR spectra were recorded using a Bruker AC 250 (250 MHz), a Bruker AC300 (300MHz) or a Bruker AM 360 (360 MHz) instrument using $CDCl_3$ CD_3CN, D_2O, DMSO-d_6 or acetone-d_6 as solvents. Chemical shifts were reported in ppm downfield from 0 (determined from the residual solvent signal). Spectra run in a mixed solvent systems of CD_3CN-D_2O were treated as CD_3CN solvent samples; the instrument locked on the solvent residual peak of CD_3CN. Splitting patterns were reported as s (singlet), d (doublet), t (triplet), q (quartet). UV-Vis spectra and kinetic experiments were run on a Varian Cary 50 Bio instrument. IR spectra were done using a Perkin Elmer Spectrum 1000 instrument as KBr disks. Mass spectra were determined on a Finnegan 3300 (CI) or a Kratos Concept 1H (EI and HRMS). Melting points were taken on a Gallenkamp apparatus and are uncorrected. pH was measured with a Corning 140 pH meter. Preparatory photolyses were carried out using a Rayonet RPR 100 photochemical reactor using 254, 300, or 350 nm lamps. Transient UV-Vis and kinetic measurements were recorded using nanosecond LFP with excitation by a Nd:YAG laser (Spectra Physics Quanta-Ray, GCR-12) with an excitation wavelength of 355 nm.

4.2 Materials

4.2.1 Common Laboratory Reagents and Solvents

HPLC grade acetonitrile was freshly distilled over CaH_2 for use in LFP studies and preparatory photolyses when the solvent was 100% CH_3CN. HPLC grade

acetonitrile was used for all other photolyses where a mixture of CH_3CN-H_2O was the solvent system. Reagent grade dichloromethane was distilled before use. Anhydrous THF and diethyl ether for synthesis were distilled over sodium benzophenone indicator prior to use. Solutions of specific pH were made up with aqueous NaOH, aqueous H_2SO_4, or potassium phosphate buffers (≤ 0.01**M**). For mixed solvent systems, the reported pH is that of the aqueous solution prior to addition of substrate or acetonitrile. The only exception is in the cases where the desired pH was 7 and the substrate contained a carboxylic acid. In this case the aqueous acetonitrile solution containing substrate was made neutral with the addition of 1 **M** NaOH solution.

4.2.2 Synthesis

p-Nitrobiphenyls **57-59** and **63-68** were readily synthesized by initial Suzuki cross-coupling of *p*-tolyl boronic acid with *p*-bromonitrobenzene, to give 4-nitro-4'-methylbiphenyl (**68**). Subsequent bromination with NBS (1 eq) gave 4-nitro-4'-(bromomethyl)biphenyl (**69a**), which was converted to **57-59**, **66** and **67** via standard functional group manipulations. Bromination of **68** with 2 eq of NBS gave 4-nitro-4'-(dibromomethyl)biphenyl (**69b**), which was converted to **64** and **65** via standard functional group manipulations.

4-Nitro-4'-Methylbiphenyl (68)

A two neck 500 mL round bottom flask was charged with 18.7 g 1-bromo-4-nitrobenzene (93 mmol), 1.1 g tetrakis(triphenylphosphine)palladium (0.93 mmol), 200 mL benzene, 100 mL 2 **M** aqueous Na_2CO_3 and 13.9 g *p*-tolylboronic acid (102 mmol)

dissolved in 50 mL ethanol. The mixture was stirred vigorously and refluxed for 10 h. Upon cooling to room temperature 5 mL of 30% H_2O_2 was added to the mixture, which was then stirred for 1 h. The mixture was extracted with diethyl ether, and the combined organic layers were washed with saturated aqueous NaCl, dried over anhydrous $MgSO_4$, and evaporated to solid. Recrystallization from hot 95% ethanol gave 16.6 g light yellow crystals of **68** (78 mmol): mp 135 °C (lit.[46] 140-141 °C, lit.[47] 143.5-144.5 °C); yield 84%, lit.[46] 98%) ^{1}H NMR ($CDCl_3$) δ 2.41 (s, 3 H), 7.29 (d, J = 8.1 Hz, 2H), 7.51 (d, J = 8.1 Hz, 2H), 7.70 (d, J = 8.8 Hz, 2H), 8.26 (d, J = 8.8 Hz, 2H); IR, 1594, 1513, 1339 cm^{-1}; mass spectrum (EI) *m/z* 213 (M^+).

4'-Nitro-[1,1'-Biphenyl]-4-Methanol (57)

A 500 mL round bottom flask was charged with 7.8 g **68** (37 mmol), 6.5 g NBS (37 mmol), 250 mL CCl_4 and 100 mg benzoyl peroxide (0.4 mmol). After a 24 h reflux a precipitate formed on cooling which was removed by filtration, and the filtrate was concentrated to an orange oil. To this oil 200 mL of 50% aqueous acetone was added, and the solution was refluxed for 6 h. Upon cooling the solution was extracted with CH_2Cl_2, the combined organic layers were evaporated to a yellow solid. This crude product mixture contained approximately 75% **57**, 11% **64** and 14% **68**, as determined by ^{1}H NMR. Silica gel column chromatography (CH_2Cl_2 as eluent) allowed separation of **57** (R_f = 0.1). Recrystallization from hot aqueous ethanol afforded 4.1 g yellow crystals of **57** (18 mmol). mp 161 °C (lit.[47] 165-167 °C,), yield (48%), ^{1}H NMR ($CDCl_3$) δ 1.73 (t, J = 5.9 Hz, exchangeable with D_2O, 1H), 4.77 (d, J = 5.1 Hz, 2H), 7.49 (d, J= 8.1 Hz, 2H), 7.61 (d, J = 8.1 Hz, 2H), 7.72 (d, J = 8.8 Hz, 2H), 8.28 (d, J = 8.8 Hz, 2H); IR, 3506,

1593, 1500, 1336 cm^{-1}; mass spectrum (EI) *m/z* 229 (M^+). HRMS (EI) Calc. for $C_{13}H_{11}NO_3$: 229.0755, found: 229.0735.

4'-Nitro-[1,1'-Biphenyl]-4-Acetic Acid (58)

To a 500 mL round bottom flask 10.0 g **68** (47 mmol), 8.4 g NBS (47 mmol), 300 mL CCl_4 and 100 mg benzoyl peroxide (0.4 mmol) were added and refluxed for 24 h. Upon cooling the precipitate formed was removed by filtration and the filtrate was concentrated to an orange oil. A solution of this oil with 2.98 g NaCN and 300 mL CH_3CN was refluxed for 24 h. Upon cooling to room temperature the brown mixture was filtered, and the filtrate was evaporated to a brown solid. This brown solid mostly dissolved in 100 mL dry $CHCl_3$. The insoluble portion was removed by filtration, and the filtrate was concentrated to an orange oil. To the oil 80 mL 50% aqueous H_2SO_4 was carefully added drop-wise, and the mixture was refluxed for 30 min. In the cooled flask a brown precipitate settled out, allowing most of the clear aqueous acid to be decanted off. Base extraction of the precipitate dissolved in diethyl ether, followed by acidification of the aqueous layers yielded a light yellow precipitate. Recrystallization from hot $CHCl_3$ gave 4.4 g yellow crystals of **58** (17 mmol). mp 181 °C, yield 36%, ^1H NMR ($CDCl_3$) δ 2.8 (br, exchangeable with D_2O), 3.69 (s, 2H), 7.41 (d, J = 8.1 Hz, 2H), 7.59 (d, J = 8.1 Hz, 2H), 7.71 (d, J = 8.8 Hz, 2H), 8.28 (d, J = 8.8 Hz, 2H); IR, 1712, 1596, 1509, 1340 cm^{-1}; HRMS (EI) Calc. for $C_{14}H_{11}NO_4$: 257.0688, found: 257.0692.

4'-Nitro-[1,1'-Biphenyl]-4-(β)-Ethanol (59)

An oven dried three-neck 250 mL round bottom flask was charged with 1.0 g **58** (4.5 mmol) and 100 mL freshly distilled THF and purged with nitrogen. The flask was

sealed with a rubber septum and kept on ice while 6 mL of 1 **M** BH_3-THF (0.6 mmol) was added slowly via syringe through the septum. After stirring for 30 min the remaining borane was quenched by adding 10 mL water carefully to the flask. An additional 90 mL of water was added, clearly causing two layers to form. A CH_2Cl_2 extraction followed, with the combined organic layers being dried over anhydrous $MgSO_4$ and evaporated to a yellow solid. Recrystallization from hot aqueous ethanol gave 970 mg yellow crystals of **59** (3.9 mmol). mp 89 °C, yield (88%), ^{1}H NMR ($CDCl_3$) δ 1.4 (t, J = 5.9 Hz, exchangeable with D_2O, 1H), 2.93 (t, J = 6.6 Hz, 2H), 3.93 (q, J = 6.5 Hz, 2H), 7.35 (d, J = 8.1 Hz, 2H), 7.57 (d, J = 8.1 Hz, 2H), 7.71 (d, J = 8.8 Hz, 2H), 8.27 (d, J = 8.8 Hz, 2H); IR, 3400, 1594, 1507, 1339 cm^{-1}; mass spectrum (CI) *m/z* 244 (M^+ + 1). HRMS (EI) Calc. for $C_{14}H_{13}NO_3$: 243.0896, found: 243.0896.

4'-Nitro-[1,1'-Biphenyl]-4-Aldehyde (64)

A 250 mL round bottom flask was charged with 1.0 g **68** (4.7 mmol), 1.7 g NBS (9.4 mmol), 100 mL CCl_4 and 50 mg benzoyl peroxide (0.2 mmol). After a 23 h reflux, a precipitate which had formed was removed by filtration once the flask cooled to room temperature, leaving an orange solution, which was concentrated to an orange oil. To this oil 50 mL 1:1 aqueous acetone was added and the solution was refluxed in for 10h. Upon cooling the solution was extracted into 100 mL CH_2Cl_2 and washed with 10^{-2} **M** pH 7 phosphate buffer. The organic layer was evaporated to an orange solid. By column chromatography (silica gel/CH_2Cl_2) **64** (R_f = 0.45) was isolated in high purity (0.67 g, 3.0 mmol). Recrystallization from hot aqueous ethanol gave yellow crystals of **64**. mp 125 °C, yield 0.67 g (63%), ^{1}H NMR ($CDCl_3$) δ 7.77 (d, J = 8.8 Hz, 4H), 8.00 (d, J = 8.8 Hz,

2H), 8.33 (d, J = 8.8 Hz, 2H), 10.08 (s, 1H); IR, 1702, 1604, 1508, 1343 cm^{-1}; mass spectrum (EI) *m/z* 227 (M^+).

4'-Nitro-[1,1'-Biphenyl]-4-Acetic Acid Methyl Ester (67)

A solution comprised of 2.0 g **68** (7.8 mmol) dissolved in 100 mL methanol with 3 mL concentrated sulfuric acid was refluxed for 3 h. The volume of solution was reduced such that 1.7 g light yellow crystals of **67** formed upon cooling: mp 126 °C, yield (81%), ^1H NMR ($CDCl_3$) δ 3.69 (s, 2H), 3.71 (s, 3H), 7.40 (d, J = 8.1 Hz, 2H), 7.58 (d, J = 8.1 Hz, 2H), 7.71 (d, J = 8.8 Hz, 2H), 8.28 (s, J = 8.8 Hz, 2H); IR, 1735, 1594, 1508, 1342 cm^{-1}; mass spectrum (CI) 272 *m/z* ($M^+ + 1$).

4'-Nitro-[1,1'-Biphenyl]-4-Methanol-α-D (65)

A solution of 5 mg $NaBD_4$ (0.1 mmol) in 1 mL 0.5 **M** NaOH a solution of 70 mg **64** (0.3 mmol) in 20 mL ethanol was added. After the solution was allowed to stir for 12 h 20 mL of 3% aqueous HCl solution was added, which caused an instantaneous milky yellow precipitate to form. After 20 min stirring the mixture was extracted with 60 mL CH_2Cl_2, at which time the precipitate dissolved. The combined organic layers were dried with anhydrous $MgSO_4$, and evaporated to a yellow solid. Recrystallization from hot ethanol/ water gave 60 mg of yellow crystals of **65** (0.27 mmol, 85% yield): mp 161 °C, ^1H NMR ($CDCl_3$) δ 4.77 (s, 1H), 7.49 (d, J= 8.1 Hz, 2H), 7.61 (d, J = 8.1 Hz, 2H), 7.72 (d, J = 8.8 Hz, 2H), 8.28 (d, J = 8.8 Hz, 2H); IR, 3506, 1594, 1500, 1336 cm^{-1}; mass spectrum (EI) *m/z* 230 (M^+).

4'-Nitro-[1,1'-Biphenyl]-4-(α-Methoxy)-Methane (66)

A 250 mL round bottom flask was charged with 4.0 g **68** (19 mmol), 3.3 g NBS (19 mmol), 100 mL CCl_4 and 50 mg benzoyl peroxide (0.2 mmol). After a 24 h reflux a precipitate formed on cooling which was removed by filtration, and the filtrate was concentrated to an orange oil. To this oil 100 mL of methanol was added, and the solution was refluxed for 4 h. Upon cooling the solution was extracted with CH_2Cl_2, the combined organic layers were evaporated to a yellow solid. This crude product mixture contained approximately 74% **66**, 12 %**64** and 14% **68**, as determined by ^{1}H NMR. Pure **66** was obtained by silica gel column chromatography using 3 to 1 hexanes / ethyl acetate as eluent. Recrystallization from hot aqueous ethanol afforded 1.7 g yellow crystals of **66** (7 mmol). mp 106 °C, yield (37%), ^{1}H NMR ($CDCl_3$) δ 3.42 (s, 3H), 4.51 (s, 2H), 7.45 (d, J = 8.1 Hz, 2H), 7.60 (d, J = 8.1 Hz, 2H), 7.72 (d, J = 8.8 Hz, 2H), 8.28 (d, J = 8.8 Hz, 2H); IR, 1597, 1508, 1335 cm^{-1}; mass spectrum (EI) 243 *m/z* (M^+).

4.3 UV-Vis Studies

UV-Vis studies were carried out by direct photolysis in cuvettes. A stock solution was made by dissolving 20 mg of substrate in 1 mL CH_3CN. Aliquots (typically 1 to 20 μL) of the stock solution were added to the quartz cuvette containing 3 mL of the appropriate mixture of H_2O-CH_3CN. Once an appropriate concentration of substrate in the cuvette had been attained samples were purged for 5 min with argon and sealed tightly with a Teflon cap. This sample was suspended in a rotating carousel and irradiated at 300 or 350 nm immediately following argon purging. An internal fan was

deemed to be sufficient to cool the instrument during photolysis as no noticeable heating of the cuvettes was observed. UV-Vis spectra were run immediately after photolysis with a cuvette containing the appropriate H_2O-CH_3CN mixture used for baseline correction. Quick photolysis was used when the study of dark reactions of photogenerated intermediates was desired. To allow for maximum conversion in a short period the brighter 254 nm lamps were used with a cuvette suspended in the centre of the photoreactor by a wire cage for maximize exposure. Transfer time to the spectrophotometer was about 5 s.

4.4 Product Studies

4.4.1 Preparative Photolysis

All preparative photolyses were carried out in a Rayonet RPR 100 photochemical reactor (254, 300 or 350 nm) using 200 mL quartz photolysis tubes with a coldfinger (ca. 14 °C) inserted. Solutions were purged with a steady stream of Ar > 15 min prior to and during photolysis, except in certain cases where oxygen was used. Work up involved extraction of the photolysate with 100 mL distilled CH_2Cl_2, addition of $MgSO_4$ drying agent to the combined organic layers, filtration and evaporation of the solvent using rotovaporation and reduced pressure on a standard vacuum line. For nitrobiphenyls conversion was calculated using methyl, methylene or aldehyde proton integrations from ^{1}H NMR spectra. Products **64** and **68** were identified by comparison with the ^{1}H NMR signals of the authentic samples. Product **74** precipitated from the photolysate solution, product **75** was isolated by extraction, while all other products were isolated by

preparative tlc (silica/CH_2Cl_2). The purification steps used for these products are described below. All nitrobiphenyl products were fully characterized by standard techniques where possible. Nitroindoline products **54** and **86** were identified by match of the ^{1}H NMR signals with those reported previously.[31] Full characterization of **54** and **86** has been given elsewhere,[31] so thus was not included in this work.

Photolysis of 57 in 1:1 H_2O-CH_3CN (pH 7)

Photolysis of 50 mg of **57** in 100 mL 1:1 H_2O-CH_3CN (Ar purged) at 300 nm (16 lamps) for 30 min resulted followed by immediate workup and ^{1}H NMR analysis allowed observation of 54% conversion of **57** to two products, **64** (75% relative yield) and a species with the following ^{1}H NMR signals (25% relative yield, based on integration of aldehyde signal): δ 7.08 (d, J = 8.8 Hz, 2H), 7.57 (d, J = 8.1 Hz, 2H), 7.71 (d, J = 8.1 Hz, 2H), 7.91 (d, J = 8.8 Hz, 2H), 10.02 (s, 1H) ($CDCl_3$). The product ratio was independent of conversion. Over the course of tens of minutes (in solution or as a powder) the formation of a highly coloured insoluble (in all common solvents available) solid was observed, simultaneous to the disappearance of the minor photoproduct (as observed by ^{1}H NMR). Silica gel proved to accelerate the decomposition of the minor product, such that tlc was not feasible for isolation of the minor product. Combined preparative photolysates in which the orange precipitate had already formed with was extracted with CH_2Cl_2, affording some of the corresponding azoxy species **71**. The amount of **71** recovered suggested that it accounted for approximately a third of the original reduction product obseved. The structure of **71** was assigned from the following data: decomposes at 125 °C, ^{1}H NMR δ 7.80 (m, 8H), 7.98 (m, 4H), 8.33 (d, J = 8.7 Hz, 2H), 8.44 (d, J =

8.8 Hz, 2H), 10.07 (s, 1H), 10.08 (s, 1H); IR (cm^{-1}) 2925 (m), 1686 (s), 1606 (s), 1458 (s); HRMS (EI) calc. for $C_{26}H_{18}N_2O_3$: 406.1318, found: 406.1316. The ^1H NMR data of the primary minor photoproduct, which shows an aldehyde proton signal and corresponding aromatic proton signals characteristic of a 4,4'-substituted biphenyl, is also consistent with a species in which the nitrogen atom has been reduced relative to substrate.

Photolysis of 58 in 1:1 H_2O-CH_3CN (pH 7)

In 5 mL CH_3CN and 25 H_2O 20 mg of **58** was dissolved and neutralized to pH 7 with a small amount (< 1 mL) of 1 **M** NaOH. Additional CH_3CN and H_2O was added to make a 100 mL solution of **58** in 1:1 H_2O-CH_3CN, which was photolyzed (Ar purged) at 300 nm (4 lamps) for 1 min, resulting in 30% conversion to **68** and **74** (relative yields: 95% and 5%, respectively). In a separate photolysis (50 mg **58** in 100 mL 1-1 D_2O-CH_3CN, pD 7, Ar purged, 16 x 300 nm, 5 min) a yellow precipitate formed during photolysis which upon isolation proved to be highly pure 4,4'-(*p*-nitrophenyl)-bibenzyl (**74**): decomposes at 220 °C, ^1H NMR ($CDCl_3$) δ 3.02 (s, 4H), 7.30 (d, J = 8.1 Hz, 4H), 7.55 (d, J = 8.1 Hz, 4H), 7.71 (d, J = 8.8 4H), 8.27 (d, J = 8.8 Hz, 4H); IR, 1592, 1507, 1336 cm^{-1}; HRMS (EI) calc. for $C_{26}H_{20}N_2O_4$: 424.1424, found: 424.1423.

Photolysis of 59 in 1:1 H_2O-CH_3CN (pH 7)

Photolysis of 20 mg of **59** in 50 mL CH_3CN and 50 mL pH 13.0 NaOH solution (Ar purged) at 300 nm (16 lamps) for 1 min resulted in 13% conversion to **68** and **74** (identified by comparison to ^1H NMR peaks of authentic **74**, isolated above).

Photolysis of 57 in 1:1 H_2O-CH_3CN (pH 2)

A solution of 20 mg of **57** in 100 mL 1:1 H_2O-CH_3CN (pH 2, H_2SO_4) was photolyzed (Ar purged) at 300 nm (8 lamps) for 1 min resulting in 33% conversion to **73**. Preparatory tlc (silica / CH_2Cl_2, R_f (**73**) = 0.7) allowed isolation of highly pure 4'-nitroso-[1,1'-biphenyl]-4-aldehyde (**73**): decomposes at 115 °C, ^{1}H NMR ($CDCl_3$) δ 7.77 (d, J = 8.8 Hz, 2H), 7.85 (m, 2H), 8.00 (d, J = 8.1 Hz, 2H), 8.32 (d, J = 9.6 Hz, 2H), 10.08 (s, 1H) ; IR 2819, 2723, 1698, 1598, 1510, 1343 cm^{-1}; HRMS (EI) calc. for $C_{13}H_9NO_2$: 211.0670, found: 211.0641.

Photolysis of 58 in 1:1 H_2O-CH_3CN (pH 2)

A solution of 14 mg of **58** in 100 mL 1:1 H_2O-CH_3CN (pH 2, H_2SO_4) was photolyzed (Ar purged) at 300 nm (4 lamps) for 3 min resulting in 50% conversion to **75**. The mixture of **58** and **75** was dissolved in 50 mL CH_2Cl_2 and extracted with pH 12 aqueous solution. Evaporation of the organic layer yielded highly pure 4'-nitroso-[1,1'-biphenyl]-4-methanol (**75**): decomposes at 105 °C, ^{1}H NMR ($CDCl_3$) δ 4.77 (s, 2H), 7.49 (d, J = 8.1 Hz, 2H), 7.66 (d, J = 8.1 Hz, 2H), 7.81 (d, J = 8.8 Hz, 2H), 7.96 (d, J = 8.8 Hz, 2H) ; IR 3380, 1594, 1517, 1343 cm^{-1}; HRMS (EI) Calc. $C_{13}H_{11}NO_2$: 213.0806, found: 213.0800.

Photolysis of 31 in Presence of 64 (pH 7)

A solution of 200 mg **31** and 20 mg **64** in 100 mL 1:1 H_2O-CH_3CN (pH 7) was photolyzed for 15 min (300 nm, 16 lamps, Ar purged). Following work up ^{1}H NMR showed 7% conversion to **71** (by match of the ^{1}H NMR signals with authentic **71**),

whereas photolysis of **64** for 30 min (otherwise similar conditions) did not result in photoreaction.

Photolysis of 60 in 100% H_2O

A solution of 5.0 mg **60** in 100 mL neat distilled water was transferred to a quartz photolysis tube and purged for 15 min prior to and during the 5 min photolysis (16 lamps). The resulting yellow solution was extracted with 100 mL CH_2Cl_2. The organic layer was dried over anhydrous $MgSO_4$, and evaporated to solid. Product **54** was identified by the match of the new signals in the ^{1}H NMR spectrum (δ 10.20 (br, 1 H), 9.11 (s, 1 H), 7.97 (s, 1 H), 7.26 (m, 1H), 6.56 (m, 1 H), 4.00 (s, 2 H), 3.76 (s, 3 H)) to those reported previously for **54**.[31] The conversion was 87.3%, calculated by integration of the aromatic signals of **60** (δ 7.52 (s, 1 H), 7.30 (s, 1 H)) and those distinguishable of **54** (δ 9.11 (s, 1 H), 7.97 (s, 1 H), 6.56 (s, 1 H)). The signal at δ 7.26 of **54** was overlapped by the solvent residual signal.

Photolysis of 60 in 99% CH_3CN-1% H_2O

A solution of 5.0 mg **60** in 99 mL CH_3CN and 1 mL distilled water was transferred to a quartz photolysis tube and purged for 15 min prior to and during the 5 min photolysis (2 lamps). The resulting golden yellow solution was dried over anhydrous $MgSO_4$, and evaporated to solid. The product **86** was identified by the match of the new signals in the ^{1}H NMR spectrum (δ 7.64 (s, 1 H), 7.16 (s, 1 H), 6.71 (br, 1 H), 3.87 (t, 2 H), 3.69 (s, 3 H), 3.51 (s, 2 H), 3.15 (t, 2 H)) to those of authentic **86**. The percent conversion was 87.3%, calculated using integration values of the aromatic signals of **60** (δ = 7.52 (s, 1 H), δ = 7.30 (s, 1 H)) and those of **86** (δ = 7.64 (s, 1 H), δ = 7.16 (s, 1 H)).

Photolysis of 60 in 80% CH_3CN-20% H_2O

A solution of 11.3 mg **60** in 20 mL CH_3CN and 80 mL distilled water was transferred to a quartz photolysis tube and purged with argon for 15 min prior to and during the ten minute photolysis (16 lamps). The resulting golden yellow solution was extracted with 60 mL distilled CH_2Cl_2. The organic layer was dried with anhydrous $MgSO_4$ and evaporated to solid. The products **54** and **86** were identified by the match of the new signals in the ^1H NMR ($CDCl_3$) spectrum (δ 10.20 (br, 1 H), 9.11 (s, 1 H), 7.97 (s, 1 H), 7.26 (m, 1H), 6.56 (m, 1 H), 4.00 (s, 2 H), 3.76 (s, 3 H), and δ 7.64 (s, 1 H), 7.16 (s, 1 H), 6.71 (br, 1 H), 3.87 (t, 2 H), 3.69 (s, 3 H), 3.51 (s, 2 H), 3.15 (t, 2 H), for **54** and **86**, respectively) to those reported previously for **54,**[31] and to those of authentic **86**. The conversion was 97%, calculated using integration values of the aromatic signals of **60** (δ 7.52 (s, 1 H), 7.30 (s, 1 H)) and those of the two observed products **54** (δ 9.11 (s, 1 H), 7.97 (s, 1 H), 6.56 (s, 1 H)) and **86** (δ 7.64 (s, 1 H), 7.16 (s, 1 H). The product distribution was 95% **54** and 5% **86**, calculated using the ^1H NMR aromatic signal integration method described above.

4.4.2 Analytical Photolysis in NMR tubes

Analytical runs in NMR tubes were carried out by direct photolysis of samples in NMR tubes. A solution was made by dissolving 60 mg substrate in 600 μL of the appropriate ratio of D_2O-CD_3CN and transferred to an NMR tube. This NMR tube was suspended in a 2 L Pyrex beaker of cool (≈ 14 °C) tap water inside the Rayonet RPR 100 photochemical reactor and irradiated at 300 nm. An internal fan was used to cool the

instrument during photolysis such that the temperature of the tap water in the beaker did not exceed 25 °C. Photolysis times ranged from 10 to 60 min, depending on the number of lamps used, the conversion desired, and the efficiency of the reaction. ^{1}H NMR spectra were taken directly after the photolysis without further treatment.

2-Dideutero Isotope Effects of 60 and 61

A solution of 5.0 mg **60** in 250 μL CH_3CN and 100 mL distilled water was transferred to a quartz photolysis tube and purged with argon for 15 min prior to and during the 5 min photolysis (300 nm, 4 lamps). The resulting yellow solution was extracted with 60 mL distilled CH_2Cl_2, dried with anhydrous $MgSO_4$, and evaporated to solid. By ^{1}H NMR ($CDCl_3$) it was shown that **54** was the exclusive product. The conversion of 22.3% was determined by integration of the aromatic peaks (**60** (δ 7.52 (s, 1 H), 7.30 (s, 1 H)), and those characteristic (and distinguishable) of **54** (δ 9.11 (s, 1 H), 7.97 (s, 1 H), 6.56 (s, 1 H)). Immediately following this experiment the same procedure was repeated for **61** (using the same photolysis tube and photoreactor). The conversion of **61** to **54-2D** (deuterated at the 2 position) was 17.1% by ^{1}H NMR ($CDCl_3$, for **61** signals used were δ 7.52 (s, 1 H), 7.30 (s, 1 H), for **54-2D** signals used were δ 9.11 (s, 1 H), 7.97 (s, 1 H), 6.56 (s, 1 H)). The observed deuterium isotope effect (Φ_H/Φ_D) in this run was 1.30. The experiment was repeated three times to calculate the average deuterium isotope effect.

4.4.3 Dark Reactions

Substrates **57-59** dissolved in 1:1 H_2O-CH_3CN at pH 1 - 13 (no purging) were allowed to sit in the dark for several hours. Following normal work up, no reaction was observed for any of these substrates.

4.4.4 Deuterium Isotope Effects by Preparative Photolysis

Deuterium isotope effects were determined by preparative photolysis, as described above in Section 4.3.2.

2,2-Dideutero Isotope Effects of 60 and 61

A solution of 5.0 mg **60** in 250 μL CH_3CN and 100 mL distilled water was transferred to a quartz photolysis tube and purged with argon for 15 min prior to and during the 5 min photolysis (4 lamps). The resulting yellow solution was extracted with 60 mL distilled CH_2Cl_2, dried with anhydrous $MgSO_4$, and evaporated to solid. By ^1H NMR ($CDCL_3$) it was shown that **54** was the exclusive product. Product **54** was identified by the match of the new signals in the ^1H NMR spectrum (δ 10.20 (br, 1 H), 9.11 (s, 1 H), 7.97 (s, 1 H), 7.26 (m, 1H), 6.56 (m, 1 H), 4.00 (s, 2 H), 3.76 (s, 3 H)) to those reported previously for **54**.[31] The conversion of 22.3% was determined by integration of the aromatic signals of **60** (δ 7.52 (s, 1 H), 7.30 (s, 1 H)) and those distinguishable of **54** (δ 9.11 (s, 1 H), 7.97 (s, 1 H), 6.56 (s, 1 H)). To minimize error caused by changes in lamp intensity, photolysis of **61** was done immediately following the photolysis **60**, using the same photolysis tube, photoreactor, mass of sample and procedure as above. The methyl 2-deutero-7-nitrosoindole-5-acetate product (**54-2D**)

was identified by the match of the new signals in the ^{1}H NMR ($CDCl_3$) spectrum (δ 10.20 (br, 1 H), 9.11 (s, 1 H), 7.97 (s, 1 H), 6.56 (s, 1 H), 4.00 (s, 2 H), 3.76 (s, 3 H)) to those observed for **54**, except the signal associated with the 2 position was absent, as was expected. The conversion was 17.1%, calculated using the integration of the observed aromatic signals of **61** (δ 7.52 (s, 1 H), 7.30) and methyl 2-deutero-7-nitrosoindole-5-acetate (δ 9.11 (s, 1 H), 7.97 (s, 1 H), 6.56 (s, 1 H)). The observed deuterium isotope effect (Φ_H/Φ_D) in this run was 1.30. The average of three separate runs was used in this measurement of the deuterium isotope effect.

4.4.5 Quantum Yields and pH Effects

Quantum yields were measured by preparative photolysis and ^{1}H NMR using *p*-nitrophenyl acetic acid (**31**) as a secondary actinometer ($\Phi = 0.6$).[24] In conditions where all the light passing into the photolysis was absorbed, photolysis of **31** (15 - 20 mg, 100 mL 100% pH 7 10^{-2} **M** phosphate buffer, 254 nm, 4 lamps, 1 min, Ar purged) was alternated with photolysis of **57** (pH 7), **58** (pH 7), **59** (pH 13) and **60** (pH 7) using the same lamps and photolysis tube and approximate mass of substrate (15 -20 mg). Photolysis time was adjusted, depending on the substrate, such that conversion was between 10 to 30%: **57** (4 min), **58** (1 min), **59** (1 min) and **60** (8 min). These runs were repeated a total of three times, and the average value was taken. The quantum yields established for **57** and **58** using at pH 7 were used to measure the relative quantum yields at different pH. In a similar manner as above, small scale preparative photolysis of **57** or

58 at pH 7 was compared to photolysis at different pHs, with photolysis times adjusted accordingly such that conversion was between 10 and 30%.

4.4.6 Triplet Sensitization

Triplet states of **57** and **60** were sensitized using 2-benzoylbenzoate ($E_T \approx 69$ kcal mol^{-1}, based on the known triplet energy of benzophenone) in 1:1 CH_3CN-H_2O (pH 7). A detailed description of these sensitizations is given below.

Sensitization of 60 with 2-Benzoylbenzoate

A solution of 500 mg 2-benzoyl benzoic acid was dissolved in 50 mL H_2O and brought to pH 7 by addition of small amounts of 1 **M** NaOH. A second solution of 10.0 mg **60** dissolved in 50 mL CH_3CN was added, and the entire solution was transferred to a quartz tube. The solution was photolyzed for 15 min (Ar purged, 300 nm). Standard workup (CH_2Cl_2) at pH 7 with an additional washing of the combined organic layer with 150 mL 10^{-2} **M** pH 7 phosphate buffer ensured removal of the sensitizer. ^1H NMR ($CDCl_3$) showed the total conversion from **60** to **54** and **86** was 81% (using aromatic signal integrations). A second photolysis of **60** (under the same conditions but in absence of sensitizer) was done to quantify the amount of product that was produced by direct photolysis of **60**. To determine the appropriate photolysis time it was estimated how much light **60** absorbed directly in the sensitized photolysis experiment. The molar absorptivities of 2-benzoylbenzoate and **60** at 300 nm were estimated to be 960 M^{-1} cm^{-1} and 2200 M^{-1} cm^{-1} (respectively) by measuring the absorbances of dilute solutions of known concentration in 1:1 pH 7 CH_3CN-H_2O. Using these values it was calculated that

60 absorbed less than 4% of the light during the sensitzed photolysis experiment. Accordingly, a solution of 10.0 mg of **60** in 100 mL 1:1 CH_3CN-H_2O was photolyzed in the same photolysis tube as above under the same conditions as above. ^1H NMR ($CDCl_3$) showed the total conversion from **60** to the products **54** and **86** was 8.9%

Triplet Sensitization of 57 with 2-benzoylbenzoate

Triplet sensitization of 10 mg **57** was achieved using 500 mg sodium benzophenone-2-carboxylic acid, all dissolved in 100 mL 1:1 H_2O-CH_3CN, with the pH adjusted to 7 with small amounts of 1 **M** NaOH. Under these conditions the sensitizer absorbed 99.5% of the light at 254 nm (based on similar arguments as for **60**). Photolysis of this solution (Ar purged) at 254 nm for 30 min, followed by standard work up (*vide supra*) at pH 7. ^1H NMR analysis of the product mixture revealed 41% conversion to **64** and **71**. Conversion due to direct absorption of light was approximated in a photolysis containing 10 mg **57** dissolved in 100 mL 1:1 H_2O-CH_3CN, pH 7. Photolysis for 15 s (> 0.5% of 30 min) under the same conditions as above resulted in 2.9 % conversion to **64** and **71**, as observed by ^1H NMR.

4.4.7 Triplet Quenching

Triplet Quenching of 57 at pH 2

Aliquots (0 to 2500 μL) of a 0.05 M sorbic acid solution (in CH_3CN) were added to solutions of 10 mg **57** in 100 mL 1:1 H_2O-CH_3CN, where the aqueous portion had previously been made pH 2 with H_2SO_4. After photolysis at 350 nm (where it is estimated $\epsilon < 1$ $\mathbf{M}^{-1}$ cm^{-1} for sorbic acid) for 1 min the solution was neutralized using 0.1

M phosphate buffer (pH 7). Normal work up (*vide supra*) ensued. Conversion to **73** was determined using ^{1}H NMR.

4.5 Laser Flash Photolysis (LFP) Studies

LFP studies were conducted at the University of Victoria LFP Facility. All transient spectra and kinetic measurements were obtained using a Nd:YAG laser (Spectra Physics Quanta-Ray, GCR-12) with pulse width of ~ 10 ns and excitation wavelength of 355 nm. Pulse energies were adjusted to < 25 mJ/pulse to avoid possible multiphoton effects. The monitering light source was an Osram lamp Model XBO 150W-1 with Oriel housing Model 66057, which was pulsed at 150 W with a PTI power supply LPS-220. For the measurement of the decay of long lived transients ($\tau > 10$ μs) with strong signals ($\Delta OD_{init} > 0.1$) the pulser was turned off to allow observation of the transient decay. The monitoring lamp and detection equipment was kept at 90° to the laser beam to minimize interference from the laser. Detection instruments used were a CVI Digikrom 240 monochromator, a Hamamatsu R446 (5 dynodes) photomultiplier tube (PMT). Measurement of Δ OD values occurs as follows. Upon pulsing of the monitoring lamp, and prior to the laser pulse, the signal measured by the PMT is held in the baseline compensation unit as the background intensity. Upon firing of the laser the signal measured by the PMT is sent to the Tektronix TDS 520 digital oscilloscope, where the signal is recorded and sent to the computer. In cases where the time scale observed exceeded 2 μs/div the pulse decay of the monitoring lamp required the use of a baseline correction, which compensated for the lamp profile. In cases where the monitoring lamp

pulser was turned off baseline compensation was unnecessary. The software used in these LFP studies was Labview 5.01, which was run on a MacIntosh G3.

In experiments with the monitoring lamp pulser turned on, P_o values were maintained at –0.2 V ± 15% by the Labview program, which adjusted the PMT voltage and monochromator slit width accordingly. In experiments where the monitoring lamp pulser was turned off, the P_o values were maintained at –0.2 V ± 15% by manually controlling the PMT voltage and monochromator slit width.

Flow cells were used for the measurement of transient spectra and kinetics of their decay. Flow cells were attached to a solution reservoir by rubber tubing, which ran through a mechanical pump which allowed control of the flow rate. The solution reservoir was purged from 15 min before and during the experiment, with either nitrogen or oxygen gas. To ensure an adequate flow of substrate solution, ΔOD_{init} repetitive measurements at one wavelength were monitored and the flow was adjusted such that the $\Delta\ OD_{init}$ was stable over several shots.

Static cells were used for measurement of transient decay in D_2O and H_2O. Each cell was purged individually for 5 min prior to photolysis and capped with a rubber septum during the photolysis. Flow cells were used for a maximum of 12 shots of the laser.

Substrate solutions were prepared such that optical densities at the laser wavelength (355 nm) were 0.3 in the 7 mm path length of the flow cell and static cell. LFP solutions were prepared from a stock solution (typically containing 10 – 20 mg substrate in 1 – 2 mL dry acetonitrile) immediately prior to the experiment. The optical

density of substrate in 3 mL of the solution of interest (prepared quantitatively, OD ≈ 0.3 at 355 nm) was measured accurately in a standard 10 mm x 10 mm quartz cuvette. Equation 44 below was used to determine the volume of stock solution required to make a predetermined volume (typically 80 mL) of substrate solution.

$$SV = (0.3\ \mathbf{S} / Abs)\ (10 / 7)\ (\mathbf{x} / (3 + s)) \qquad (44)$$

Where: SV = Spike volume (in μL) required to give an OD of 0.3 in **x** mL

S = Volume of spike (in μL) used to give OD ≈ 0.3 in the 3 mL cuvette

Abs = Actual accurately measured OD (≈ 0.3) in the 3 mL cuvette

x = Volume of solvent required for the substrate solution of predetermined volume (typically 80 mL)

s = Volume of spike (in mL) (same as **S**, but in mL)

10 / 7 = ratio of path lengths for the cuvette and flow cell (or static cell)

Transient spectra were a compilation of Δ OD measurements at different monitoring wavelengths. Typically, at each wavelength, 8 to 12 laser shots and the subsequent time resolved Δ OD measurements were taken. The monitoring window was divided into four smaller windows, each typically spanning a portion of the transient signal decay (or growth). Decay and growths of transient signals were fit using FitVic (a Labview program written for the University of Victoria LFP Facility).

4.6 X-Ray Crystallography

The X-ray crystal structure of **57** was solved by Dr. B. Chak, Department of Chemistry, University of Victoria using a Nonius CAD-4 diffractometer with Cu-Kα radiation. Crystal data is summarized in Table 4.1.

Table 4.1 Crystal data for **59** (Figure 2.1).

Empirical Formula	$C_{42}H_{39}O_9$
Formula Weight	727.78
Crystal Color	yellow
Crystal Dimensions (mm)	0.20 x 0.20 x 0.20
Crystal System	monoclinic
Lattice Type	Primitive
Lattice Parameters	
a (Å)	7.9183(6)
b (Å)	33.605(4)
c (Å)	14.087(2)
β (Å)	102.933(9)
V (Å)	3653.5(7)
Space Group	$P2_1/c$ (#14)
Z value	4
D_{calc}	1.327 g/cm^3
$D_{measured}$	1.325 g/cm^3
F_{000}	1536.00
μ(CuKα)	7.74 cm^{-1}
R, R_w	0.097, 0.059
No. of Observations	2473
No. of Variables	488
Radiation	CuKα (λ = 1.54178 Å)

References

1. Döpp, D. In *CRC Handbook of Organic Photochemistry and Photobiology*, Horspool, W. M., Song, P.-S. (eds.), CRC Press; Boca Raton: **1995**, Chapter 81.
2. Schwörer, M., Wirz, J. *Helv. Chim. Acta* **2001**, *84*, 1441.
3. Morrison, H. A. In *The Chemistry of Nitro and Nitroso Groups*, Feuer, H., Ed.; Wiley: New York, **1969**, Chapter 4.
4. Döpp, D. *Top. Curr. Chem.* **1975**, *55*, 49.
5. (a) Charlton, J. L., de Mayo, P. *Can. J. Chem.*, **1968**, *46*, 1041. (b) Charlton, J. L., Liao, C. C., de Mayo, P. *J. Am. Chem. Soc.*, **1971**, *93*, 2463.
6. Okada, K., Saito, Y., Matsuura, T. *J. Chem. Soc., Chem. Commun.*, **1992**, 1731.
7. Hurley, R., Testa, A.C. *J. Am. Chem. Soc.*, **1966**, *88*, 4330.
8. Jagannadham, V., Steenken, S. *J. Am. Chem. Soc.*, **1984**, *106*, 6452.
9. Wubbels, G. G., Jordan, J. W., Mills, N.S. *J. Am. Chem. Soc.*, **1973**, *95*, 1281.
10. (a) Letsinger, R. L., Wubbels, G. G. *J. Am. Chem. Soc.*, **1966**, *88*, 5041. (b) Wubbels, G. G., Letsinger, R. L. *J. Am. Chem. Soc.*, **1974**, *96*, 6698.
11. Kronenberg, M. E., van der Heyden, A., Havinga, E. *Rec. Trav. Chim.*, **1967**, *86*, 254.
12. Letsinger, R. L., McCain. J. H. *J. Am. Chem. Soc.*, **1966**, *88*, 2884.

13. Fleming, I. In *Frontier Orbitals and Organic Chemical Reactions*, Wiley: New York, 1967.

14. Yokoyama, K., Nakagaki, R. *Bull. Chem. Soc. Jpn.*, **1980**, *53*, 2472.

15. Wubbels, G. G., Halverson, A. M., Oxman, J. D., De Druyn, V. H. *J. Org. Chem.*, **1985**, *50*, 4499.

16. (a) Nakagaki, K., Hiramatsu, R., Mutai, M., Nagakura, S. *Chem. Phys. Lett.*, **1985**, *121*, 262. (b) Nakagaki, R., Hiramatsu, M., Mutai, K., Tanimoto, Y., Nagakura, S. *Chem. Phys. Lett.*, **1987**, *134*, 171. (c) Nakagaki, R., Mutai, K., Hiramatsu, M., Tukada, H., Nagakura, S. *Can. J. Chem.*, **1988**, *66*, 1989.

17. (a) George, M. V., Scaiano, J. C. *J. Phys. Chem.*, **1980**, *84*, 492. (b) Yip, R. W., Sharma, D. K. *Res. Chem. Intermed.*, **1989**, *11*, 109.

18. (a) Chow, Y. L. In *The Chemistry of Functional Groups, Supplement F (The Chemistry of Amino, Nitroso and Nitro Compounds and Their Derivatives)*, Patai, S. Ed., Wiley: New York, **1982**, chap. 6. (b) Binkley, R. W., Flechtner, T. W. In *Synthetic Organic Photochemistry*, Horspool, W. M., Ed., Plenum: New York, **1984**, 375.

19. Givens, R. S., Kueper, L. W. *Chem. Rev.* **1993**, *93*, 55.

20. (a) Wubbels, G. G., Hautala, R. R., Letsinger, R. L. *Tetrahedron Lett.*, **1970**, 1689. (b) Wubbels, G. G., Kalhorn, T. F., Johnson, D. E., Campbell, D. *J. Org. Chem.*, **1982**, *47*, 4664.

21. Görner, H. *J. Photochem. Photobiol. A: Chem.*, **1998**, *112*, 155.

22. Görner, H., Currell, L. J., Kuhn, H. J. *J. Phys. Chem.*, **1991**, *95*, 5518.

23. (a) Wan, P., Yates, K. *J. Chem. Soc., Chem. Commun.*, **1982**, 275. (b) Wan, P., Yates, K. *Can. J. Chem.* **1986**, *64*, 2076.

24. Margerum, J. D., Petrusis, C. T. *J. Am. Chem. Soc.*, **1969**, *91*, 2467.

25. (a) Craig, B. B., Weiss, R. G., Atherton, S. J. *J. Phys. Chem.*, **1987**, *91*, 5906. (b) Craig, B. B., Atherton, S. J. *J. Chem. Soc., Perkin Trans. II*, **1988**, 1929.

26. (a) Wan, P., Muralidharan, S. *Can. J. Chem.* **1986**, *64*, 1949. (b) Wan, P., Muralidharan, S. *J. Am. Chem. Soc.*, **1988**, *110*, 4336; see also: Wan, P., Muralidharan, S. *J. Am. Chem. Soc.*, **1990**, *112*, 4611, for error correction.

27. Muralidharan, S, Wan, P. *J. Photochem. Photobiol. A: Chem.*, **1991**, *57*, 191.

28. Amit, B., Ben-Efraim, D. A., Patchornik, A. *J. Am. Chem. Soc.*, **1976**, *98*, 843.

29. Pass, Sh., Amit, B., Patchornik, A. *J. Am. Chem. Soc.*, **1981**, *103*, 7674.

30. Nicolaou, K. C., Safina, B. S., Winsinger, N. *Synlett.*, **2001**, 900.

31. Papageorgiou, G.; Ogden, D. C.; Bath, A.; Corrie, J. E. T. *J. Am. Chem. Soc.* **1999**, *121*, 6503.

32. Amit, B., Ben-Efraim, D. A., Patchornik, A. *J. C. S. Perkin Trans. 1*, **1976**, 57.

33. Papageorgiou, G., Corrie, J. E. T. *Tetrahedron*, **2000**, *56*, 8197.

34. (a) T. C. Werner, In *Modern Fluorescence Spectroscopy*, Vol. 2, E. Wehry (ed.), Plenum Press, New York, **1976**. (b) Berlman, I. *J. Chem. Phys.*, **1970**, *74*, 3085. (c) Zimmerman, H. E., Crumrine, D. S. *J. Am. Chem. Soc.*, **1972**, *94*, 498. (d) Mislow, K., Gordon, A. J. *J. Am. Chem. Soc.*, **1963**, *85*, 3521. (e) Huang, C., -G., Beveridge K., Wan, P. *J. Am. Chem. Soc.*, **1991**, *113*, 7676.

35. (a) Maus, M., Rettig, W., Bonafoux, D., Lapouyade, R. *J. Phys. Chem. A*, **1999**, *103*, 3388. (b) Delmond, S., Létard, J.-F., Lapouyade, R., Rettig, W. *J. Photochem. Photobiol. A*, **1997**, *105*, 135.

36. (a) Lippert, E. *Z. Electrochem.*, **1957**, *61*, 962. (b) O'Conner, D. B., Scott, G. W., Tran, K., Coulter, D. R., Miskowski, V. M., Stiegman, A. E., Wnek, G. E. *J. Phys. Chem.*, **1992**, *97*, 4018. (c) Paddon-Row, M. N., Oliver, A. M., Warman, J. M., Smit, K. J., de Haas, M. P., Oevering, H., Verhoeven, J. W. *J. Phys. Chem.*, **1988**, *92*, 6958.

37. (a) Naito, I., Uryu, T., Sasaki, H., Ishikawa, T., Kobayashi, S., Kamata, I., Oku, A. *J. Photochem. Photobiol. A*, **2001**, *140*, 33. (b) Lee, C. W., Pan, D. H., Shoute, L.C. T., Phillips, D. L. *Res. Chem. Int.* **2001**, *27*, 485. (c) Park, S. K. *J. Photochem. Photobiol. A*, **2000**, *135*, 135.

38. (a) El'tsov, A. V., Kuznetsova, N. A., Frolov, A. N., *Zh. Org. Khim.*, **1971**, *7*, 817. (b) Frolov, A. N., Kuznetsova, N. A., El'tsov, A. V., Rtishev, N. I., *Zh. Org. Khim.*, **1973**, *9*, 963. (c) Frolov, A. N.,

Kuznetsova, N. A., Rtishev, N. I., El'tsov, A. V., *Zh. Fiz. Khim.*, **1975**, *49*, 115.

39. Murov, S. L., Carmichael, I., Hug, G. L., In *Handbook of Photochemistry*, 2nd ed., M. Dekker, New York, **1993**.

40. Schatz, T. R., Kobetic, R., Piotrowiak, P., *J. Photochem. Photobiol. A*, **1996**, *105*, 249.

41. Corrie, J. E. T., Trentham, D. R. In *Biorganic Photochemistry*, Morrison, H. Ed., Wiley: New York, **1993**, Vol. 2. 243.

42. Gut, I. G., Wirz, J., *Angew. Chem. Int. Engl.* **1994**, *33*, 1153.

43. Yip, R. W., Sharma, D. K., Giasson, R., Gravel, D. *J. Chem. Phys.* **1984**, *88*, 5770.

44. Falvey, D. E. In *Molecular and Supramolecular Photochemistry*, Vol. 6, Ramamurthy, V.; Schanze, K. S. (eds.), Marcel Dekker; New York: **2000**, Chapter 6.

45. Miller, R. B., Duger, S., *Organometallics*, **1984**, *3*, 1261.

46. Shudo, K., Ohta, T., Okamoto, T., *J. Am. Chem. Soc.*, **1981**, *103*, 645.

47. Bly, R. S., Tse, K. K., Bly, R. K., *Journal of Organometallic Chemistry*, **1976**, *117*, 35.

VITA

Surname: Morrison

Given Names: James Patrick

Place of Birth: Victoria, Canada

Date of Birth: February 21, 1975

Educational Institutions Attended

University of Victoria 1993-1999

Degrees Awarded:

B.Sc. (Co-op) University of Victoria 1999

Publications:

1. James Morrison, Hans Osthoff, and Peter Wan, Photoredox, Enhanced Photoreactivity of the Nitrobiphenyl Chromophore, *Photochem. Photobiol. Sci.*, **2002**, *1*, 22.
2. James Morrison, John E.T. Corrie, George Papageorgiou, and Peter Wan, Mechanisms of Photorelease of Carboxylic Acids from 1-Acyl-7-Nitroindolines in Aqueous Acetonitrile, *J. Am. Chem. Soc.*, Submitted (**2002**).
3. James Morrison, Hans Osthoff, and Peter Wan, Photoredox, Photodecarboxylation, and Photo-Retro-Aldol Chemistry of 4-Nitrobiphenyls, *Photochem. Photobiol. Sci.*, In Preparation.

Conference Presentations:

1. James Morrison, John E.T. Corrie, George Papageorgiou, and Peter Wan, Mechanistic Studies of the Photorelease of Carboxylic Acids from 1-Acyl-7-Nitroindolines in Aqueous Solution, *84th CSC Conference*, Montreal, QC, May 26-31, 2001.
2. James Morrison, Hans Osthoff, and Peter Wan, Photochemistry Induced by the Nitro Group in Biphenyls, *18th IUPAC Symposium on Photochemistry*, Dresden, Germany, July 22-27, 2000.
3. James Morrison, Hans Osthoff, and Peter Wan, Photochemistry Induced by the Nitro Group in Biphenyls, *83rd CSC Conference*, Calgary, AB, May 27-31, 2000.

Partial Copyright License

I hereby grant the right to lend my thesis (or dissertation) to users of the University of Victoria Library, and to make single copies only for such users or in response to a request from the Library of any other university, or similar institution, on behalf or for one of its users. I further agree that permission for extensive copying of this thesis for scholarly purposes may be granted by me or a member of the University designated by me. It is understood that copying or publication of this thesis for financial gain shall not be allowed without my written permission.

Title of Thesis: Mechanistic Studies of the Photochemistry of 4-Nitrobiphenyls and 1-Acyl-7-Nitroindolines

Author 

James Patrick Morrison

November 30, 2001